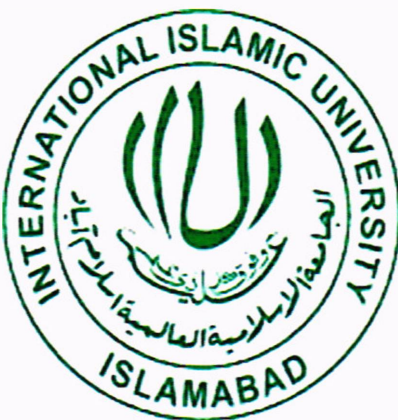


Different Computational Approaches to Explore Protein Ligand Interaction of Cholinesterase Inhibitor for Alzheimer's Disease



Supervisor

Dr. Naveeda Riaz

Assistant Professor

Co-Supervisor

Mrs. Saima Kalsoom

PhD. Scholar (QAU)

Candidate

Sumra Wajid Abbasi

30-FBAS/MSBI/F09

**Department of Environmental Sciences
Faculty of Basic & Applied Sciences
International Islamic University Islamabad
2012**

Accession No. TH-8538

MS

362-196831

SUD

1 Alzheimer's disease Patients; care

DATA ENTERED

Amz 8
27/9/13

checked for Tl:

- Abdullah
28-05-2013

Different Computational Approaches to Explore Protein Ligand Interaction of Cholinesterase Inhibitor for Alzheimer's Disease



By

Sumra Wajid Abbasi

**Department of Environmental Sciences
Faculty of Basic & Applied Sciences
International Islamic University Islamabad**

2012



بِسْمِ اللّٰهِ الرَّحْمٰنِ الرَّحِيْمِ

**Department of Environmental Sciences
International Islamic University Islamabad**

Dated: 08-02-2012

FINAL APPROVAL

It is certificate that we have read the thesis submitted by Ms. Sumra Wajid Abbasi and it is our judgment that this project is of sufficient standard to warrant its acceptance by the International Islamic University, Islamabad for the M.S Degree in Bioinformatics.

COMMITTEE

External Examiner

Dr. Naeem Zafar Azeemi

Director Center for Advance studies in Telecommunication (CAST)

COMSATS Institute of Information Technology, Islamabad



Internal Examiner

Dr. Sobia Tabassum

Assistant Professor

Dept. Environmental Sciences

International Islamic University, Islamabad



Supervisor

Dr. Naveeda Riaz

Assistant Professor

Dept. Environmental Sciences

International Islamic University, Islamabad



Co-Supervisor

Mrs. Saima Kulsoom

PhD Scholar

Quaid-e- Azam University, Islamabad



Dean, FBAS

Dr. Irfan Khan

International Islamic University, Islamabad



A thesis submitted to Department of Environmental Sciences,
International Islamic University, Islamabad as a partial
fulfillment of requirement for the award of the
degree of Ms. Bioinformatics

CONTENTS

Acknowledgements	(i)
Abbreviations	(iii)
List of Figures	(v)
List of Tables	(viii)
Abstract	(x)
Chapter 1	(2-4)
1 Introduction	2
Chapter 2	(6-34)
2 Literature Review	6
Chapter 3	(36-49)
3 Methodology	36
3.1 Protocol for Insilco drug designing	36
3.2 Disease Selection	37
3.3 Protein Target	38
3.4 Data Set Formation	38
3.5 Compounds Drawing	39
3.6 2D and 3D Pharmacophore Generation	43
3.7 Molecular Docking	44
3.7.1 Steps for Molecular Docking	44
3.7.2 Ligand-Protein Interaction	46
3.7.3 Lead Identification	46
3.7.4 Analogue Designing	47
3.8 Quantitative Structure Activity Relationship	46

Chapter 4	(51-116)
4.1 Rule of Five	51
4.2 Pharmacophore Modeling	55
4.2.2 Pharmacophoric Triangle	65
4.3 Molecular Docking	66
4.3.1 Active Site of Cholinesterase	66
4.3.2 Docking of Standard Drugs	72
4.3.3 Docking of Inactive Compound	73
4.3.4 Interactions of Ligand and Target Protein	73
4.4 Lead Compound Identification	90
4.5 Analogues Designing	96
4.6 Docking and Interactions of Analogues with Target Protein	99
4.7 Quantitative Structure Activity Relationship	107
Conclusion	(118-119)
Future Enhancement	(121-121)
References	(123-141)

ACKNOWLEDGEMENTS

In the name of Allah, the Most Gracious and the Most Merciful
Praise and Gratitude be to **Allah** Almighty for the strengths and His blessing in
completing this thesis. His compassion and mercifulness allow me in finalizing this
thesis. Peace and blessing be upon Prophet **Muhammad SAW**., his family, his relatives
and all his followers.

Special appreciation goes to my co-supervisor, **Mrs. Saima Kalsoom**, PhD
Scholar, Quaid-e-Azam University Islamabad, who put forth this idea and her invaluable
help of constructive comments and suggestions throughout thesis work have contributed
to the success of this research. Her support and knowledge regarding my topic really
proved helpful number of times. She supported me at each and every step of hurdle I
faced during my thesis either academic or non-academic. This is because of her that my
research competency is enhanced.

Not forgotten, my appreciation to my supervisor, **Dr.Naveeda Riaz**, Assistant
Professor, International Islamic University Islamabad who taught us to face the up-
coming challenges open heartedly and guided me to complete the manuscript in time.

I highly appreciate the contributions of my Senior **Pakeeza Akram**, who shared a
lot of knowledge and opinions during the thesis work.

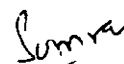
I would like to express my appreciation to the Dean of Faculty, **Dr. Irfan Khan**
Professor Dept BI & BT and my Head of Department **Dr. Shaheen Shahzed**, Assistant
Professor, Dept of Biotechnology and Bioinformatics, International Islamic University
Islamabad for their support and help towards my Postgraduate affairs.

Sincere thanks to all my friends and fellows especially **Asma Abro, Zoya, Sheema , Uzma Malik, Aruba, Madeeha, Javaria, Mehrin , Yusra , Ambreen, Zuhra , Fatima, Arshia, Saba, Uzma** and others for their kindness and moral support during my study. The work could not have been completed without the constant support of my dearest friend **Asma Abro** who offered both practical and emotional support throughout the writing of this thesis and has remained very supportive and encouraging over the last few years. She has given me the most support when she herself didn't realize that I needed it. She is thanked for her earnest desire to see me attain my goal. Thanks for the friendship and memories.

Last but not least, my deepest gratitude goes to my beloved parents; **Mr. Wajid Ali Abbasi and Mrs. Tasneem Wajid** and also to my brother **Hyder Wajid Abbasi** for their endless love, prayers and encouragement.

I would like also to acknowledge the support offered by my PIMS Colleague **Mr. Muhammad Arshad**. My acknowledgement also goes to our lab attendant **Fozia** for her co-operation.

To those who indirectly contributed in this research, your kindness means a lot to me. Thank you very much.



Sumra Wajid Abbasi, February 2012.

ABBREVIATIONS

AD	Alzheimer's disease
ChEIs	Cholinesterase Inhibitors
ChAT	Choline Acetyl Transferase
ChEs	Cholinesterases
AChE	Acetylcholinesterase
BChE	Butyrylcholinesterase
Ach	Acetylcholine
PDB	Protein Data Bank
FDA	Food and Drug Administration
CADD	Computer-Aided Drug Designing
CAMD	Computer Aided Molecular Design
CAMM	Computer Aided Molecular Modeling
COMFA	Comparative Molecular Field Analysis
COMSIA	Comparative Molecular Similarity Indices Analysis
QASR	Quantitative Structure Activity Relationship
SS_R	Sum of squares due to regression
SS_E	Sum of squares due to error
SS_T	Total sum of squares
RSQ	r^2 , square of co-relation coefficient
2D	Two Dimensional
3D	Three Dimensional
Å	Angstrom
HBA	Hydrogen Bond Acceptor

HBD	Hydrogen Bond Donor
HOMO	Highest Occupied Molecular Orbital
LUMO	Lowest Unoccupied Molecular Orbital
IC₅₀	Half Maximal Inhibitory Constant
LogP	Partition Coefficient
MR	Molar Refractivity
CV	Critical Volume
HF	Heat of formation
TE	Total Energy

LIST OF FIGURES

Figure 2.1	Comparison of Normal Brain verses Alzheimer's Patient Brain	10
Figure 2.2	Ribbon Diagram of Human BChE from PDB entry 1P0I	14
Figure 2.3	Active site of BChE	14
Figure 2.4	Pathogenesis of Alzheimer's disease	17
Figure 2.5	Computer Aided Drug Designing flow chart	23
Figure 2.6	Different Softwares for Molecular Docking	29
Figure 3.1	Protocol for Insilco drug design and development	36
Figure 4.1	Bar chart showing detailed analysis of Rule of Five in percentage form	53
Figure 4.2a	Feature Pattern, best Conformations, Cluster ID and Pharmacophore Fit for Selected Datas	57
Figure 4.2b	Pharmacophore Models generated for Selected Dataset	57
Figure 4.3a	Feature Pattern, best Conformations, Cluster ID and Pharmacophore Fit for Selected Dataset	58
Figure 4.4	2D Pharmacophore Models of Selected Data along with Standard	

Drugs	60
Figure 4.5 3D Pharmacophore Models of Selected Data along with Standard Drug	60
Figure 4.6a Merged Pharmacophore of selected ligands, Donepezil and Rivastigmine generated by LigandScout	62
Figure 4.6b Merged Pharmacophore showing 2 Hydrogen Bond Acceptors, 1 Hydrogen Bond Donor and 2 Hydrophobic/ Aromatic and 1 Positive ionizable	62
Figure 4.7a Shared Pharmacophore of selected ligands, Donepezil and Rivastigmine generated by LigandScout	63
Figure 4.7b Shared Pharmacophore showing 1 Hydrogen Bond Acceptor, 1 Hydrogen Bond Donor, 1 aromatic ring, 1 hydrophobic volume and 1 Positive Ionizable	63
Figure 4.8 Three featured Pharmacophoric Triangle of BChE inhibitor	65
Figure 4.9 Binding interactions of SW8 with 1P0I	75
Figure 4.10 Binding interactions of SW16 with 1P0I	75
Figure 4.11 Binding interactions of Donepezil with 1P0I	76

Figure 4.12 Binding interactions of Rivastigmine with 1P0I	76
Figure 4.13 Binding interactions SW18 (Inactive compound) with 1P0I	77
Figure 4.14 Binding interactions SW19 (Lead compound) with 1P0I	92
Figure 4.15 Analogues of Lead compound and their IUPAC Names	98
Figure 4.16 Binding Interactions of 1 st Analogue with 1P0I	103
Figure 4.17 Binding Interactions of 2 nd Analogue with 1P0I	103
Figure 4.18 Binding Interactions of 3 rd Analogue with 1P0I	104
Figure 4.19 Binding Interactions of 4 th Analogue with 1P0I	104
Figure 4.20 QSAR Equation	110
Figure 4.21 Percentage Contribution of Descriptors	113
Figure 4.22 Plot of Actual Values verses Predicted Values	116

LIST OF TABLES

Table 2.1	List of Drugs Approved by FDA	12
Table 2.2	Similarities and Differences between BChE and AChE	18
Table 2.3	The costs incurring in each step in overall drug development process	21
Table 3.1	2D view of Selected Compounds and their IC ₅₀ values	40
Table 3.2	Chemical structures and IC ₅₀ values of Compounds for QSAR studies	48
Table 4.1	Lipinski's rule (Rule of Five) applied to data set	52
Table 4.2	Pharmacophoric Features of Data set	61
Table 4.3	Amino Acids within 5Å of the target Protein where + and – signs indicates the presence and absence of amino acids	68
Table 4.4a	Energies of Ligands and Inhibition Concentration	78
Table 4.4b	Amino Acids within 5Å of the target Protein	80
Table 4.5	Active Ligands their interactions, IC ₅₀ values and Binding Affinity	91
Table 4.6	Binding Interactions of Analogues with target Protein	105
Table 4.7	QSAR descriptors of Ligands	108

Table 4.8 Statistics of Analysis	112
Table 4.9a Correlation of Descriptors with Activity (IC50)	112
Table 4.9b Correlation among Descriptors	112
Table 4.10 Actual values and Predicted Values	115

ABSTRACT

With the advent of Computer-aided drug designing and discovery, bioinformatics become the major tool for designing and discovering most potent leads against different targets. A Pharmacophore is built from knowledge of the structure of the novel drugs. Ligand-based Pharmacophore modeling was carried out on a set of 10 compounds using Ligand Scout. All of the compounds shared six common features. The Merged feature model : 2 Hydrogen Bond Acceptors, 1 Hydrogen Bond Donor, 1 aromatic ring, 2 hydrophobic volumes, 1 Positive ionizable and 30 exclusion features whereas a shared feature model contains: 1 Hydrogen Bond Acceptor, 1 Hydrogen Bond Donor, 1 aromatic ring, 1 hydrophobic volume and 1 Positive ionizable respectively . *In-silico* approaches have been used to determine the Pharmacophore triangle.

Molecular docking was the test vector for the current studies. Docking studies were carried out in order to identify the lead compound among the selected Butyrylcholinesterase inhibitors. AutoDock Vina was used for docking studies. The binding interactions of the active conformations of the ligands and the target protein have been identified by using VMD. Lead compound showed strong ligand-protein interaction which includes 3 ionic interactions and 15 hydrophobic interactions and IC_{50} value 0.011 μM and Binding energy is -10.1Kcal/mol. Four analogues of the lead compound were made. They were also docked in order to predict their bioactivity.

Quantitative structure-activity relationship was established to find dependency trend in Cholinesterase Inhibitors and various molecular descriptors. Molecular descriptors were calculated and plotted against the IC_{50} for predicting the biological activities of selected dataset.

On the base of extensive computational studies some active compounds were identified that were involved in the considerable number of binding interactions and showed lower binding affinities. Analogues were designed from the potential lead compound and Molecular Docking studies of analogues were carried out in order to suggest the most appropriate compound that has the potential to act as potent Butyrylcholinesterase inhibitors.

CHAPTER 1

INTRODUCTION

1. INTRODUCTION

About 100 years ago, Alzheimer's disease (AD) was identified. Since its identification the global fight for a world without Alzheimer's disease has been launched by researchers. AD is being the main focal point for many researchers. Many different Alzheimer's Associations, Alzheimer's disease Education and Referral (ADEAR) Center and Alzheimer societies has been established for helping people affected by AD. Still more efforts are required in order to prevent AD from developing. According to *Facts and Figures, an annual report released by the Alzheimer's Association in 2011* an estimated 5.4 million people are victims of AD. Among people of different ages, AD is the sixth-leading cause of death while it is the fifth-leading cause of death for those aged 65 and older in United States (Minino et al, 2010). In *World Alzheimer Report 2009, Alzheimer's disease International reported* that in 2010 35.6 million people living with dementia worldwide. This number will be increasing to 65.7 million by 2030 and 115.4 million by 2050. Among the estimated AD patients nearly two-thirds live in low and middle income countries, where the sharpest increases in numbers are set to occur.

Among the developing nations 4.6% of population is facing mental retardation issues (Gadit et al., 1998). In Pakistan the conditions are equally bleak where the percentage of mental disorders depicts a gloomy image. 6% of population is suffering from depression, 1.5% from schizophrenia, 1 – 2% from epilepsy and 1% from Alzheimer's disease (Gadit et al., 1999).

The main reason for selecting Cholinesterase Inhibitors as a drug target for current study is that ChEIs are the only *therapeutic agents reported so far that* consistently proven to be effective in treatment of AD but currently available drugs for treating AD only mask the symptoms of Alzheimer's, but do not treat the underlying cause of disease. In addition that's drugs cause severe hepatic complications and cholinergic side effects. Although The U.S. Food and Drug Administration (FDA) has approved four ChEIs for treatment of AD, there is still a need of Alzheimer's drug that would not only overcome the sever hepatic complications but would also treat the underlying disease and stop or delay the cell damage that eventually leads to the worsening of symptoms.

Using *in-silico* drug designing techniques it is promised that novel drug and effective drug for the treatment of Alzheimer's disease will be developed in short time span.

During this study a Pharmacophore model is generated using the information derived from data set, as yet there is not a single confined Pharmacophore model identified for the AD Cholinesterase inhibitors. Therefore it will contribute positively towards more accurate treatment of AD.

Secondly, a protocol is designed that will help in the *in-silico* drug development. This protocol incorporates Pharmacophore modeling, molecular docking and quantitative structure-activity relationship (QSAR). This investigation resulted in identification of

lead compound and its analogue formation having tendency to be next potential drug candidate.

2D QSAR Multiple linear Regression Analysis was also observed in which molecular descriptors were calculated and correlation was determined which resulted in finding biological activities of ligands and providing insight of which relevant and consistent chemical properties are important relationship for the biological activity of selected compounds

Effectiveness of work states: Lead compound was identified that enhance the therapeutic ability and will help to cure Alzheimer's disease by increasing the binding interactions and its bioavailability.

CHAPTER 2

LITERATURE REVIEW

2. LITERATURE REVIEW

Alzheimer's disease (AD) is the most common cause of dementia among the older people. AD is characterized by progressive and long-lasting loss and declines in memory, everyday tasks performance, communication proficiency and language, conceptual thinking and ability to learn and carry out mathematical calculations. Other symptoms of AD include personality changes and destruction of judgments (Caroline, 1997). Dementia is because of different diseases and conditions that are responsible for damaged brain cells or links between brain cells (William Thies and Laura Bleiler, 2011). The history of AD begins about 100 years ago when AD's first case was reported by Alois Alzheimer on November 3, 1906, in Tubingen, Germany. Alois presented that case on the 37th meeting of the Society of Southwest German Psychiatrists (Godert *et al.*, 2006).

The pathogenic grounds of the disease are not recognized so far, but the obvious neuro-pathological alterations like neurofibrillary tangles and amyloid plaques are reported in the Alzheimer's patient brain. Similarly, there are neuro-chemical and biochemical variations which are also linked with AD. In case of AD, the decrease in the choline acetyltransferase (ChAT) enzyme activity has been reported as the major biochemical change. The decrease in ChAT enzyme activity occurs in the major regions of basal forebrain cholinergic neurons, particularly in the neocortex (Rossor *et al.*, 1982). As a result, this decrease reported intense breakdown of cholinergic neurons (Whitehouse *et al.*, 1981). Moreover, it has been reported that the decrease in ChAT activity in the cerebral cortex is associated to the severity of the dementia (Perry *et al.*, 1978). Different

Alzheimer's patients show different signs and symptoms, but the most common symptom starts with steadily increasing difficulty in remembering new information. Such condition occurs because of the interruption of brain cell function in those regions which are mainly involved in forming new memories. With the increase of damage, persons face other complications including loss of memory, poor judgment and change in personality, difficulties in scheduling or resolving issues and trouble in completing known tasks, confusion with time or place, difficulty in understanding visual images and spatial relationships, speaking or writing issues, and misplacing things and difficulty in retracing (William Thies and Laura Bleiler, 2011).

Alzheimer's disease is of both types, sporadic as well as familial. Majority of Alzheimer's disease cases are sporadic but to some extent the disease is inherited by an autosomal dominant mechanism of inheritance. Four different gene mutations have been reported for the familial form of the disease (M-M Mesulam, 1993).

The etiology of the AD is not well-known. Many studies are carried out and documented possible risk and protective factors responsible for AD. The most obvious and undisputed factor amongst the risk factors associated with AD is age. AD being the most common type of dementia accounts for 50 % to 60% of all cases. Dementia shows a direct relation with age. It accounts for less than 1% in persons aged 60 to 64 years, but in persons aged 85 years or so the rate is between 24% and 33% in the Western world (Ferri *et al.*, 2005). More than 24 million cases of dementia have been reported in 2001.

Because of the estimated increase in life expectancy, this number is expected to double every 20 years up to 81 million in 2040. (Ferri *et al.*, 2005).

Besides ageing other genetic risk factors that are possible agents of AD are: AD's family history (Payami *et al.*, 1977), having history of depression (Speck *et al.*, 1995), apolipoprotein E gene-e4 allele presence (Payami *et al.*, 1977; Kukull *et al.*, 1996), race (Schoenberg *et al.*, 1985) and Down's syndrome (Brayne, 1991; Van Duijn *et al.*, 1991). Along with these other possible agents are hypertension (Kokmen *et al.*, 1991), head trauma with loss of consciousness (Chandra *et al.*, 1989; Brayne, 1991), low serum vitamin B12 and vascular disease (McCaddon and Kelly, 1994), lower education (Beard *et al.*, 1992), electromagnetic fields (Sobel *et al.*, 1995), gender (Schoenberg *et al.*, 1985), antacid consumption (Graves *et al.*, 1990a) and aluminum absorption (McLachlan *et al.*, 1996). Finally, some factors arousing debate include maternal age at birth (Van Duijn and Hofman, 1992), diabetes (Leibson *et al.*, 1997) occupational exposure to solvents and glues (Gun *et al.*, 1997), and alcohol consumption (Graves *et al.*, 1991).

Along with risk factors, protective factors have also been studied. Protective factors include cigarette smoking (Brayne, 1991; Graves *et al.*, 1991), non-steroidal anti-inflammatory drugs, arthritis (McGeer *et al.*, 1996), and estrogen intake (Lerner *et al.*, 1997). Other factors such as severe headache, blood transfusion (Brayne, 1991), apolipoprotein E e2 allele (Bickeboller *et al.*, 1997) and physical activity (Yoshitake *et al.*, 1995) are assumed to be the protective factors of AD.

Three clinical stages of AD with functional and cognitive decrease extending over 5 to 8 years have been reported. The early or mild stage mostly lasts for 2 to 3 years and is characterized by short-term memory impairment often along with symptoms of depression and anxiety. The symptoms of depression and anxiety of mild stage appear to abate as neuropsychiatric signs, such as visual delusions, false beliefs and reversal of sleep patterns emerge in the moderate stage. The last and severe stage is distinguished by motor signs, for example motor rigidity and prominent cognitive decline. Throughout the above mentioned stages of AD, the cognitive and functional decrease tend to be linear, while during sever stage caregiver burden increases with the appearance of neuropsychiatric symptoms and decreases to some extent, when the patient is more sedentary (Gauthier, 2002).

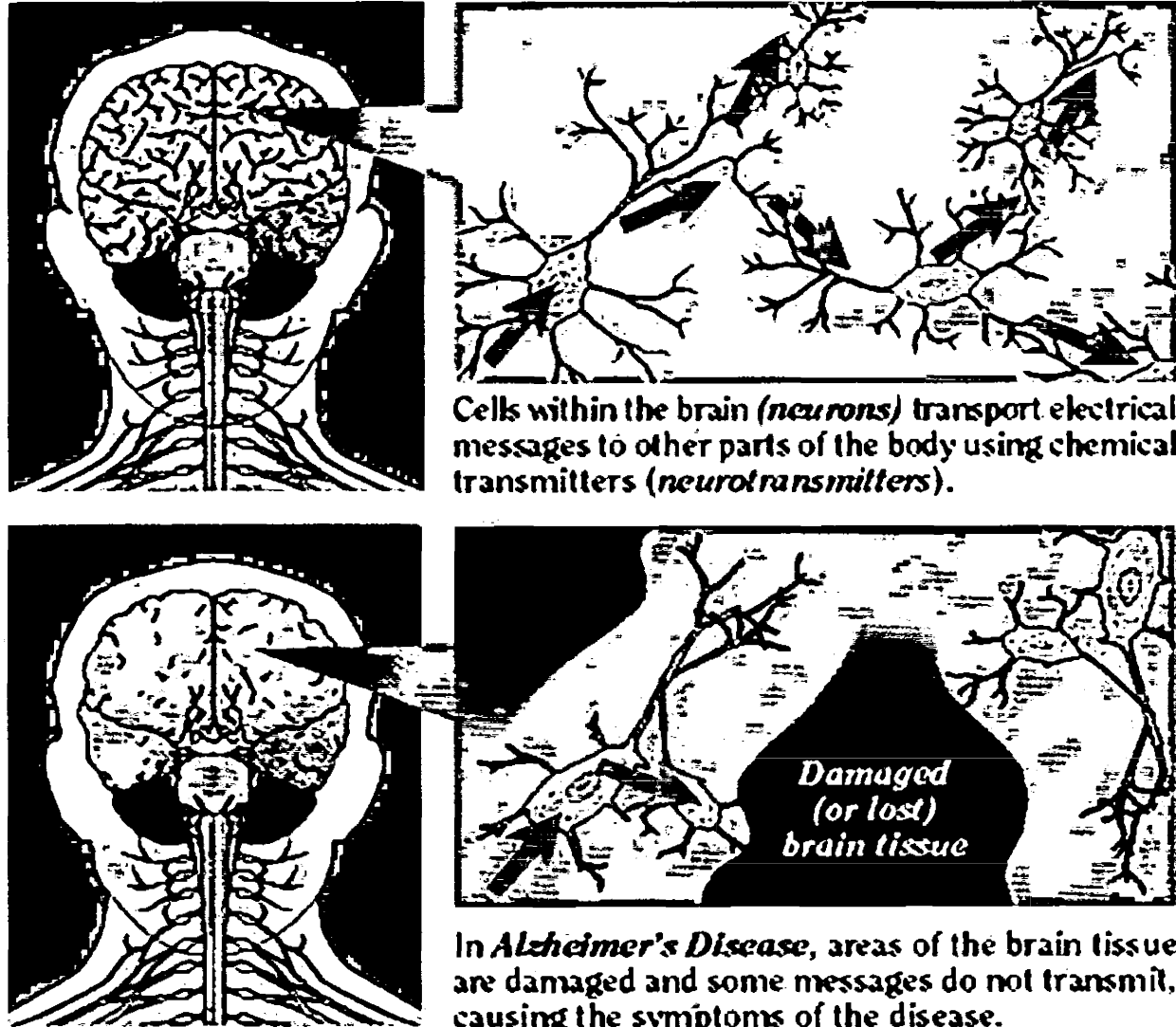


Figure 2.1: Comparison of Normal Brain verse Alzheimer's Patient Brain

For the treatment of different stages of AD, the use of cholinesterase inhibitors (ChEIs) has been documented to be effective (Doody, 2003; Rockwood *et al.*, 2003). In 1993 tacrine was the first ChEI to be approved by the Food and Drug Administration (Davies *et al.*, 1989) which is now rarely used because of toxicity associated with it and the introduction of safer ChEIs (Ritchie *et al.*, 2004). Donepezil, galantamine, and rivastigmine are the commonly used ChEIs. These three ChEI have been proven to lower or stabilize cognitive decline of AD (Ritchie *et al.*, 2004; Briks, 2006; Hansen, 2008). Besides ChEIs, in 2004 the FDA approved an NMDA antagonist named as memantine, for treating dementia symptoms in moderate to severe cases of AD (Lleo *et al.*, 2006).

Table 2.1: List of Drugs Approved by FDA

DRUG NAME	DRUG TYPE & USES	HOW IT WORKS	SIDE EFFECTS
Namenda® (memantine)	N-methyl D-aspartate (NMDA) antagonist approved for treating moderate to severe AD symptoms	By Blocking the toxic effects linked with excess glutamate. It also regulates glutamate activation.	Causes Constipation, dizziness, headache and confusion
Razadyne ® (galantamine)	ChEI approved for treating mild to moderate AD symptoms.	By preventing the breakdown of acetylcholine and simulates the nicotine receptors to release more acetylcholine in brain	Causes Vomiting, Nausea, loss of appetite, weight loss and diarrhea
Exelon ® (rivastigmine)	ChEI approved for treating mild to moderate AD symptoms.	By preventing of acetylcholine and butyrylcholine in brain.	Causes Vomiting, Nausea, loss of appetite, weight loss, diarrhea and muscle weakness
Aricept ® (donepezil)	ChEI approved for treating mild to moderate and moderate to severe AD	By preventing the breakdown of acetylcholine in brain	Causes Vomiting, nausea and diarrhea

The known ChEIs can cause severe hepatic complications (Sequeira *et al.*, 2008). Therefore, the development of new more effective drugs having lesser side effects is still a main preference.

Cholinesterases (ChEs) are family of the most efficient enzymes identified. Based on inhibitor sensitivities and substrate specificities, ChEs are further classified into two types: i) acetylcholinesterase (AChE; EC 3.1.1.7) and ii) butyrylcholinesterase (BChE; EC 3.1.1.8) (Massoulie *et al.*, 1993). Both ChEs shared 65% of sequence homology. Both have catalytic triad for substrate hydrolysis.

A membrane-bound enzyme, AChE is mostly found in the brain, cholinergic neurons, muscles and erythrocytes. AChE hydrolysis the neurotransmitter acetylcholine (ACh) in cholinergic synapses (Massoulie *et al.*, 1993; Silman *et al.*, 2005) and as result plays an important role in the regulation of several physiological actions (Milatovicet *et al.*, 1996; Schetinger *et al.*, 2000).

BChE present in the serum, heart, lung, intestine, liver and kidney plays an important role in the metabolism of ester containing compounds (Dave *et al.*, 2000; Prody, 1987; Ecobicon, 1973).



Figure 2.2: Ribbon Diagram of Human BChE from PDB entry 1P0I.

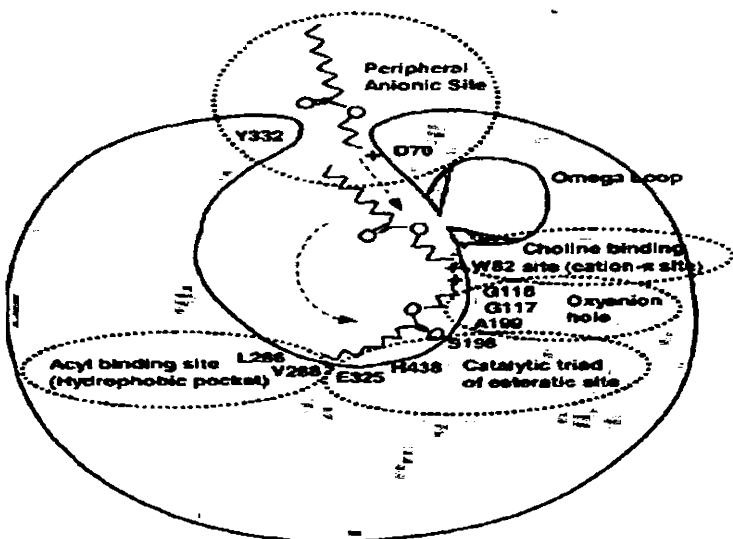


Figure 2.3: Active site of BChE

Even though the accurate role of BChE is not fully known so far, its function in morphogenesis, cytogenesis and tumorigenesis, regulation of cell proliferation and onset of differentiation during early neuronal development, as a scavenger in the detoxification of certain chemicals, and in lipoprotein (VLD) metabolism has been reported (Giacobini, 2003).

Besides this, several neuronal groups solely show the activity of BChE in the human brain (Wright *et al.*, 1993), such as in the inhibition or absence of AChE, BChE can replace AChE in the degradation of acetylcholine Ach (Li B *et al.*, 2000; Chatonnet *et al.*, 2003). Such replacement in Alzheimer's patient brains renders BChE as a more effective drug target than AChE (Carreiras *et al.*, 2004).

BChE involvement in the disruption of cholinergic neurotransmission in AD has been supported by biological facts (Combarros *et al.*, 2005). AD-related neurofibrillary tangles are also linked with the processing of α -amyloid protein to β -amyloid peptide (Carreiras *et al.*, 2004). The disease's etiology is further complicated because of an association between AD and the formation of β -amyloid plaques. It is believed by many researchers that AD is a consequence of increased production or accumulation of α -amyloid in the brain which in turns results nerve cell death. Recently it has been reported that in the AD patient's brains, there is a significant reduction in the level of AChE whereas the level of BChE increases which in turn aggravates the toxicity of β -amyloid peptide. In AD AChE and BChE activity is expressed by neurofibrillary tangles and amyloid plaques (Wright *et al.*, 1993). In AD patient's brain, this abnormal expression has

been detected around the amyloid plaques and neurofibrillary tangles (Small *et al.*, 1996). It has also been documented that AChE and BChE co-localize within the brain in amyloid plaques to form insoluble β -amyloid fibrils (Diamant *et al.*, 2006).

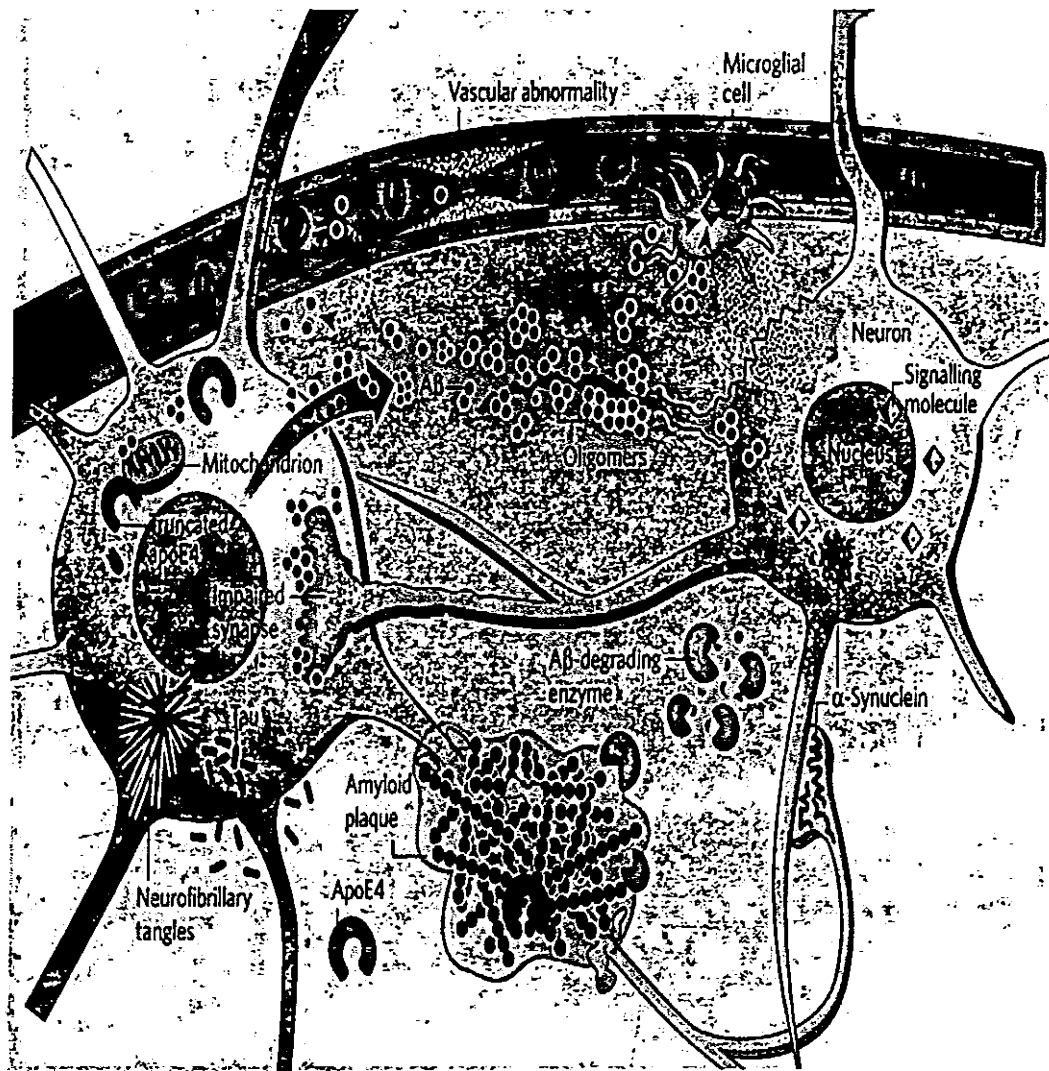


Fig 2.4: Pathogenesis of Alzheimer's disease

AChE inhibition has been proven as effective drug target against Alzheimer's disease but use of BChE as a drug remains a matter of concern in treating Alzheimer's disease. Even though little literature is available on the inhibition of butyrylcholinesterase, studies have revealed that BChE is a genetically authorized drug target and its selective inhibition lessens the beta-amyloid plaques formation (Ul-Haq *et al.*, 2010).

Table 2.2: Similarities and Differences between BChE and AChE

BuChE verse AChE

- In brain represents 20% total ChE activity, mostly glial.
- In human brain is present also in specific neurons.
- 65% amino-acid sequence homology.
- Chromosome 3 (BuChE) vs. chromosome 7 (AChE).
- Catalytic site: valine–leucine replacing phenylalanine.
- No substrate inhibition.
- Most efficient, at high substrate concentration.
- Less substrate specific than AChE.

(Ezio Giacobini., 2004)

In the current studies, BChE would be used as a drug target.

Up till now the only therapeutic agents that consistently proven to be efficacious in treating the cognitive and functional symptoms of AD is cholinesterase inhibitors (Weinstock, 1999). ChEIs are basis of AD therapy. Four ChEIs namely tacrine (an aminoacridine), donepezil (a benzylpiperidine), rivastigmine (a carbamate) and galantamine (a tertiary alkaloid) have been approved for the symptomatic treatment of

mild to moderate AD. As these compounds show likeness in efficacy (Weinstock, 1999; Wilkinson *et al.*, 2002), their clinical differentiation may base on variations in tolerability profiles and ease of use. The variations in the tolerability profiles of ChEIs may occur as a result of selectivity difference for AChE and BChE (Rogers *et al.*, 1998; Rogers and Friedhoff, 1998). AChE and BChE both are linked with cholinergic dysfunction. Central cholinergic systems play a very important part in a wide variety of brain functions such as memory and learning. Thus, the development of AChE and BChE inhibitors for the improvement of cholinergic signalling and overall cognition in patients is very important in the treatment of AD (Rook *et al.*, 2010).

The studies and efforts for the development of a drug are costly, prolonged, risky and comprehensive. It is projected that the development of a drug from an idea to a standard finished product would take 12 years and on an average cost more than US \$800 million (DiMasi *et al.*, 2003). In order to shorten the time consuming research efforts and to lessen the expenses, numerous advance technologies have hence been developed and applied in drug research and development (R&D). Among these technologies, Computer-aided drug design (CADD) is one such revolutionary technology (Jorgensen, 2004).

2.4 Computer-Aided Drug Designing

In the field of drug design, both computational and experimental approaches are used and present complementary approaches. Nowadays, computational techniques are gaining rapid popularity and implementation in drug designing and discovery. Computer-

aided drug design (CADD), computer aided molecular modeling (CAMM), computer-aided molecular design (CAMD), computer-aided rational drug design, computational drug design, *in silico* drug design and rational drug design are the different terms applied to this area (Kapetanovic., 2008)..

Molecular simulations play different roles in different disciplines of science in various research areas. In bioinformatics and drug designing, the focus is on two parallel areas. The first approach focuses on the use of mathematical algorithms currently used in the field of molecular biology examples include simulating protein-protein interactions or protein-ligand interactions. The results are then used for further experimentation. The second approach obviously is the focus on designing new algorithms with much effective outcomes (Huang *et al.*, 2010).

The process of drug development is demanding, time consuming, costly, and requires many aspects to be considered. According to a study, the cost ranges from \$800 million to \$1.8 billion in the drug discovery process (Hileman, 2006). However, depending on the type and nature of the disease being targeted and the drug, considerable variation is seen both in time and cost. Bharath and co-workers summarized the overall drug development process and the cost incurring at each step (Bharath *et al.*, 2011).

Table 2.3: The costs incurring in each step in overall drug development process

	Cost US \$ Million	Cost %	Time in years
Biology			
Target identification	165	18.8	1.0
Target validation	205	23.3	2.0
Chemistry			
Screening	40	4.5	4.5
Optimization	120	13.6	2.7
Development			
Pre-clinical	90	10.2	1.6
Clinical	260	29.5	7.0
Total	880	100.0	14.7

Furthermore, out of 40,000 compounds tested in animals only 5 reach human testing and the number of compounds which is approved for reaching clinical studies is just 1 out of 5. This depicts a huge investment in terms of time, money and other resources (Kapetanovic, 2008). A report suggests that extensive usage of bioinformatics and *in silico* technologies would cause reduction up to 50% in the overall drug development cost (PricewaterhouseCoopers, 2007). Current work is all *in silico* and it suggests a new drug for the treatment of Alzheimer's disease.

Application areas where CADD technologies work are two: structure based drug design and ligand based drug design. In structure-based drug design, we should have complete knowledge of the target protein structure and its active sites for finding the binding pocket, the binding energy and the steric properties of ligand and protein. It includes de novo ligand design and docking among other topics. While in ligand-based drug design, focus is on ligands which interact with the target protein. The technologies include pharmacophore, QSAR and 3D-QSAR. Both the techniques produce lead compound as a final product. CADD process flowchart is given as drawn by Huang and collaborators in their review about CADD.

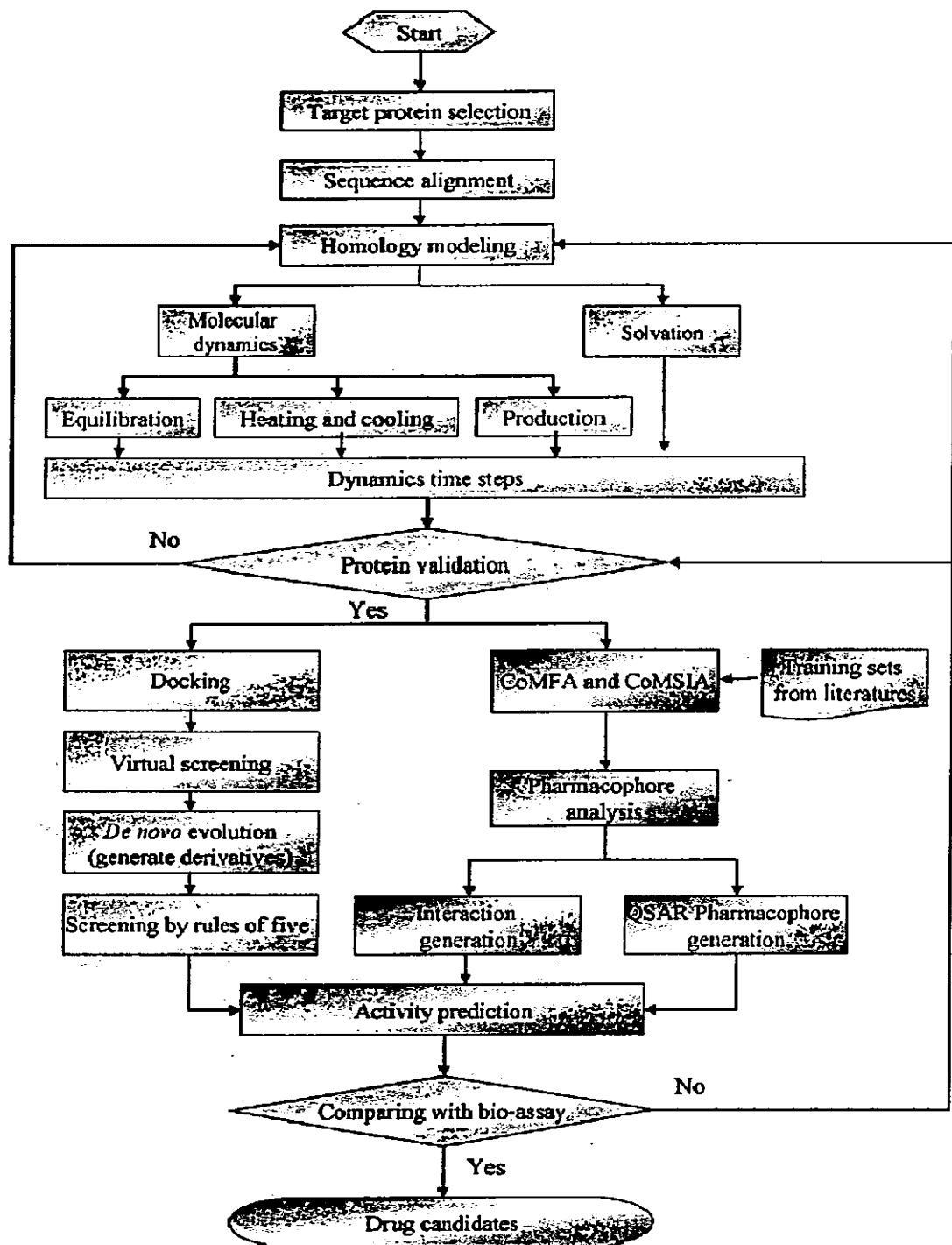


Figure 2.5: Computer Aided Drug Designing flow chart

In structure based drug design, we should have a protein structure at hand. Two physical methods of obtaining structure are NMR spectroscopy and X-ray diffraction. Numerous protein structures are found at RCSB PDB. Those that are not included in the PDB database can be modelled. Homology Modelling is a technique used to predict unknown protein structure by sequence similarity to known protein structure(s). If the protein sequence has 30% similarity with its template (homologous protein) it can be modelled (Marti-Renom *et al.*, 2000). Ab initio modeling and threading are other two methods for protein structure prediction.

In early 1960s the idea of CADD emerged as a quantitative structure-activity relationship (QSAR) analysis but later the concept of CADD has developed very quickly. Along with other CADD technologies, molecular modeling and simulation have proven successful and productive in drug discovery. Usage of computational techniques along with bioinformatics techniques in drug discovery and development process is quickly gaining popularity and appreciation (Kapetanovic., 2008). Using CADD technology, rational design of selective inhibitors of p90 ribosomal protein S6 kinase is designed successfully (Cohen *et al.*, 2005).

In order to considerably reduce time and resource required for drug development and testing, CADD is employed. From 1997 to 2004, the rapid growth of virtual screening is reported as the number of citations increase from 4 to 302 (Pozzan, 2006).

In this study different in silico techniques like molecular docking, QSAR and Pharmacophore modeling are used to design a new novel cholinesterase inhibitor for AD.

Molecular docking is a computational procedure of searching for an appropriate ligand that fits both energetically and geometrically the protein's binding site. In other words, it is a study of how two or more molecules e.g. ligand and protein, fit together. The problem is like solving a 3D puzzle (Aatu *et al.*, 2002).

During past decade for understanding the formation of intermolecular complexes, the application of computational methods in this area has been subjected to intensive research. It is commonly known that molecular binding of one molecule (the ligand) to the pocket of another, usually macromolecule (the receptor), which is commonly a protein is responsible for accurate drug activity. Molecular docking has been proved very efficient tool for novel micro molecule drugs discovery for targeting protein (Wang *et al.*, 1999). Among different fields of docking, protein-ligand docking is of special interest, because of its application in medicinal industry (Muegge *et al.*, 2001). Protein-ligand docking refers to search for the accurate ligand conformations within a targeted protein when the structure of protein is known or can be estimated (Sousa *et al.*, 2006).

Docking procedures are basically the grouping of search algorithms and scoring function. Large number of search algorithms and scoring functions are available. Search algorithms predict the ligand biding orientation and confirmations commonly refer as posing (Sousa *et al.*, 2006). Some common search algorithms are (Aatu *et al.*, 2002):

- Molecular dynamics
- Monte Carlo methods
- Genetic algorithms

- Fragment-based methods
- Point complementary methods
- Distance geometry methods
- Tabu searches
- Systematic searches

In order to differentiate the active and random compounds the scoring functions are employed. The scoring functions predict binding free energies in ligand-protein docking generally in 7- 10 kJ/mol (Bissantz *et al.*, 2000). The three major classes of scoring functions are (Sousa *et al.*, 2006):

- Force field based
- Empirical
- Knowledge based scoring functions.

Numbers of different molecular docking softwares are employed in drug research industry (Aatu *et al.*, 2002). The most popular and commonly use softwares for molecular docking are AutoDock (Morris *et al.*, 1998; Goodsell *et al.*, 1990; Morris *et al.*, 1996) GOLD (Jones *et al.*, 1997; Jones *et al.*, 1995) FlexX (Rarey *et al.*, 1996) along with DOCK (Ewing *et al.*, 1997) and ICM (Abagyan *et al.*, 1994).

In some cases for reproducing crystallographic conformations and orientations of ligand-protein complexes, Autodock has been produced better results than DOCK, FlexX, and GOLD (Park *et al.*, 2006).

For docking purpose, AutoDock pre calculate energy grids on target around a site of interest (Morris *et al.*, 1998). While considering the target energy grids, Lamarkian Genetic Algorithm (LGA) (stochastic search algorithm), for exploring the grid space is employed to perform energy evaluations of the position of the ligand (Morris *et al.*, 1998). LGA investigate all the possible ligand-protein poses relative to the energy grids and returns the lowest energy conformation in the target site (Morris *et al.*, 1998). The LGA is of great importance for modeling systems having maximum numbers of rotatable bonds and possible numbers of conformations (Morris, 1998).

DOCK and FlexX both employed an incremental construction algorithm. Incremental construction algorithm attempts to reconstruct the bound ligand by first placing a rigid anchor in the binding site and later using a greedy algorithm to add fragments and complete the ligand structure.

GOLD (Genetic Optimization for Ligand Docking) considers degrees of freedom in the binding site that correspond to reorientations of hydrogen bond donor and acceptor groups. These degrees of freedom represent only a very small fraction of the total conformational space that is available but should account for a significant difference in binding energy values (Shih- Ching Ou *et al.*, 2005).

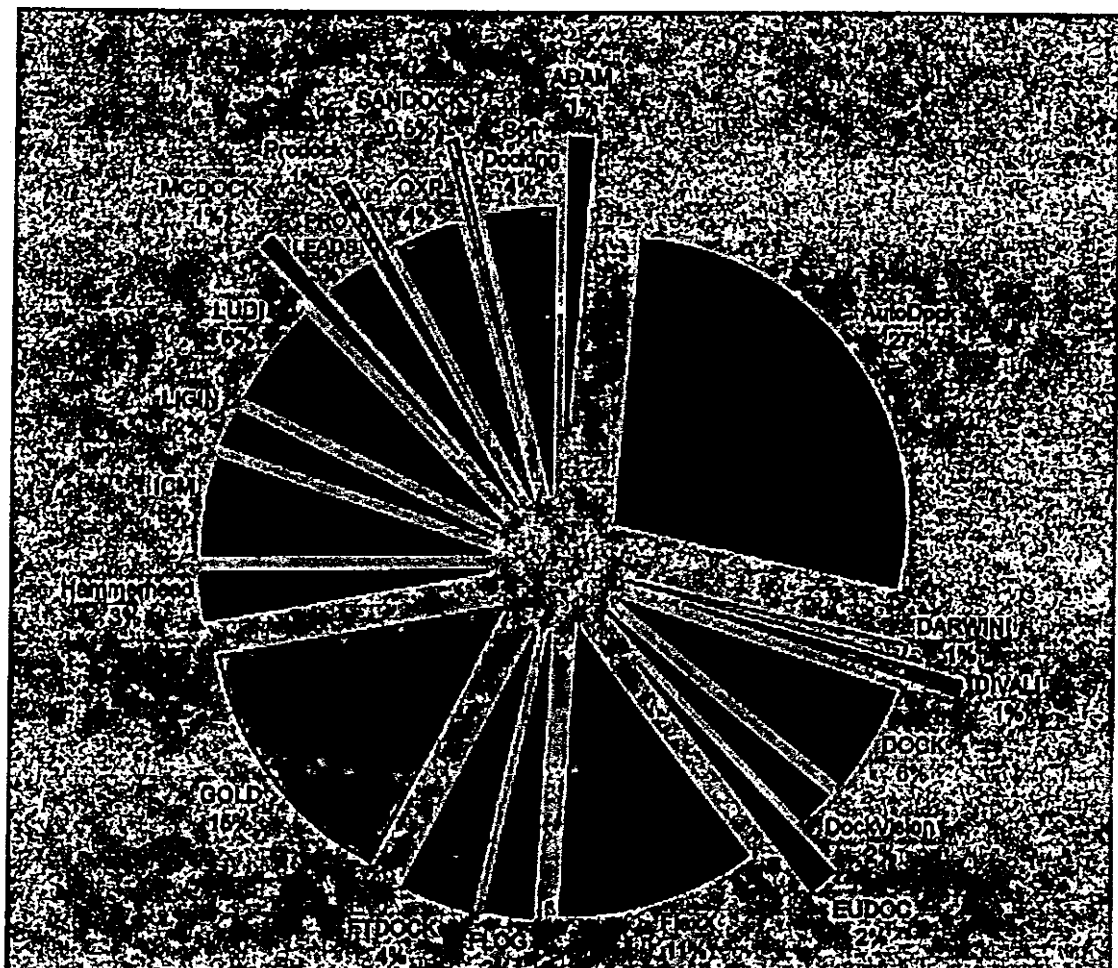


Figure 2.6: Different Softwares for Molecular Docking (Sousa *et al.*, 2006)

AutoDock Vina is an upgraded version of Auto Dock 4 and it is a ligand to protein docking and virtual screening simulator. It is compatible with the Auto Dock PDBQT file format and offers the following advantages over Auto Dock 4; while using AutoDock Vina grid computation is not necessary which was a complex process elsewhere, it gives higher accuracy of binding mode, and it is considerably faster, moreover it is available for each operating system and use iterated local search algorithm (Chang *et al.*, 2010).

Pharmacophore is one of the most lasting ideas of computer-aided drug design. Historically, the concept of a Pharmacophore is presented, from its initial articulation by Kier in 1967 (Kier, 1967) and uses the term in a publication in 1971 (Kier, 1971).

In recent years the term Pharmacophore has been increasingly use in medicinal chemistry. Pharmacophore are often attributed as the structural fragments or functional groups of a chemical compounds. However, the IUPAC gave an accurate definition of Pharmacophore in 1998. According to IUPAC: "Pharmacophore is an ensemble of steric and electronic features that is necessary to ensure the optimal supra molecular interactions with a specific biological target and to trigger (or block) its biological response (Kapetanvoic, 2008).

Pharmacophore does not represent the real association of functional groups but it gives abstract concept about common molecular interaction capacities of a group of compounds towards their target structure. Typical Pharmacophore features include regions where molecule is hydrophobic, aromatic, a hydrogen bond acceptor, a hydrogen

bond donor, a cation, or an anion. These features need to match different chemical groups with similar properties, in order to identify novel ligands. Best pharmacophore model formed must include both hydrophobic volumes and hydrogen bond vectors (Kapetanovic *et al.*, 2008).

In the current era, Pharmacophore modelling has become an integrated part of drug development and designing (Cheng Chang *et al.*, 2005). A Pharmacophore highlights the 3D arrangement of structural features of a compound that are required for a certain biological activity. The Pharmacophore model leads to the generation and identification of the new compounds that shares the same Pharmacophoric features. For limited structure activity data availability for few compounds, the medicinal chemist can easily generate manually a common featured Pharmacophore model. However, an availability of diverse data makes the manual computation of Pharmacophore features difficult. To overcome this difficulty, Computational approaches prove helpful for generating Pharmacophore (Venkatarajan S Mathura *et al.*, 2010).

Steps involved in Pharmacophore identification are to find a number of ligands known to interact with a single target, then finding similarities between the ligands leading to the creation of Pharmacophore and at the end using Pharmacophore for virtual screening.

Numerous softwares are available for the Pharmacophore identification such as: Ligand Scout (Judith *et al.*, 2009) Catalyst, Phase, Sybyl including Galahad, GASP, DISCO tech, UNITY 3D and MOE (Kapetanovic *et al.*, 2008).

Ligand Scout has become an integrated platform for building pharmacophore models either based on a protein structure or ligand (Cambridge MedChem *et al.*, 2009). Ligand Scout is software that allows to rapidly deriving 3D chemical featured Pharmacophore from structural data of macromolecule or ligand in a fully automated and convenient way (Judith *et al.*, 2009). Upon several mouse clicks the entire characteristic features critical for drug activity are determined and along with it Ligand Scout enable user to align several compounds having similar Pharmacophore (Judith *et al.*, 2009; Cambridge Med Chem *et al.*, 2009). Unlike other programs, the alignment is based on Pharmacophore points rather than on atomic contributions and is reflected better the way the small molecule presents itself to the active site of the macromolecule (Judith *et al.*, 2009). From several molecules or Pharmacophore, a shared feature Pharmacophore can be derived to determine common features by setting reference point, thus making Pharmacophore modelling convenient and easy.

Lastly Virtual screening can be done by **Quantitative Structure- Activity Relationship (QSAR)** studies. According to Hansch (1969) Quantitative Structure Activity Relationship (QSAR) is a mathematical technique which links chemical structure and activity of chemical compounds in a quantitative manner. It is commonly used computational method in predicting toxicology (Kapetanovic *et al.*, 2008). Independent variables represent molecular descriptors, e.g. electronic, conformational and thermo-dynamical etc. The aim of QSAR techniques is to develop correlations between biological activity and the physiochemical properties of the set of molecules

related to same class. Softwares such as COMFA and COMSIA (Klebe *et al.*, 1998), Chem Draw (Zielesny *et al.*, 2005), Hyper Chem (Tsuij *et al.*, 2010) and many more are used for finding molecular descriptors.

Chem Draw Ultra, using an add-on, Chem Prop/Draw, calculates predicted values for physical and thermodynamic properties of a selected structure of up to 100 atoms. (Loren *et al.*, 2004) Chem draw software package is a chemical structure drawing tool which enables several features upon the drawing of structure which includes boiling point, melting point, and critical volume, heat of formation, Log P and molar refractivity (MR). Minimization of the energy of the compound is done by using Hyper Chem. Energy minimization alters molecular geometry to lower the energy of the system, and yields a more stable conformation. It generates a log file using computational chemistry techniques such as semi-empirical formula, molecular mechanics etc (hypercube *et al.*, 2002).

Molecular dynamics (MD) simulation is one of the important tools in the theoretical study of biological molecules. Because molecular systems generally contain a large number of particles, it is impossible to analyze such complex systems. By using numerical methods, molecular dynamics simulation can avoid such analytic intractability. During simulation, atoms and molecules are allowed to interact for a period of time. The motion for every atom is calculated and can be played to examine the overall behaviour (Mccammon *et al.*, 1977). Overall, the background algorithm for a MD simulation includes: (1) the determination of the initial positions and velocities of every atom; (2)

the calculation of forces applied on the investigated atom using inter-atomic potentials; (3) the progression of atomic positions and velocities through a short- time period. These new positions and velocities are then turned into new inputs to step 2, and when steps 2 and 3 are repeated, each repetition forms an additional time step.

CHAPTER 3

METHODOLOGY

3. METHODOLOGY

3.1 Protocol for the *Insilco* Drug Designing

The stepwise protocol for Insilco drug designing for the cure of Alzheimer's disease is described in figure 3.1:

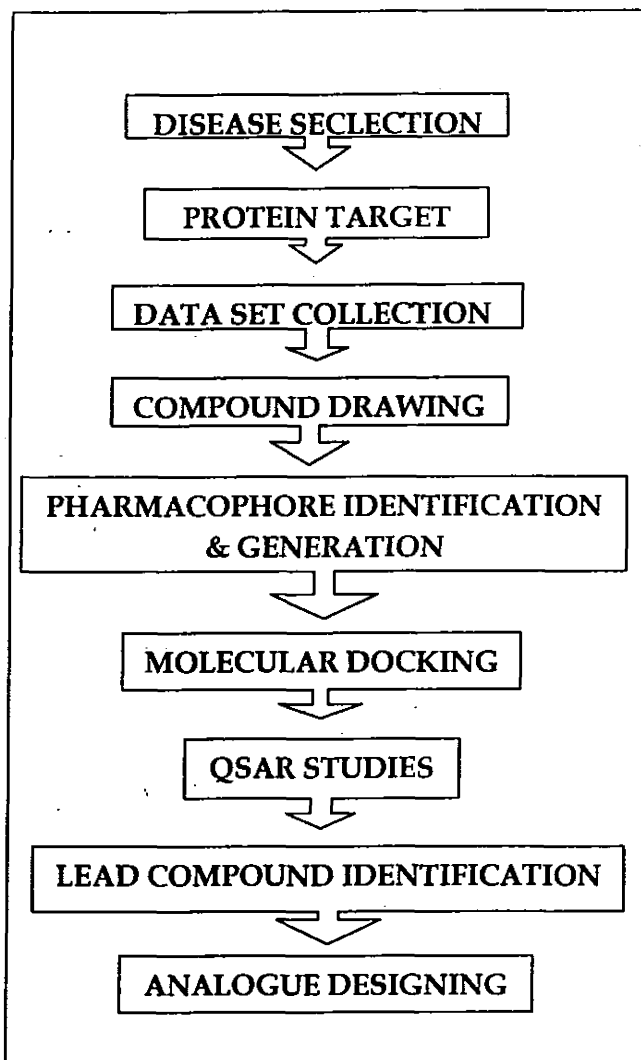


Figure 3.1: Protocol for the *Insilco* drug designing and development

As the pioneer step disease was identified leading to the potential protein target. Further data collection was incorporated; it was followed by drawing of drugs using 2D view. Later Pharmacophore identification and generation was done it led to the docking of compounds which resulted in the lead compound identification and analogues formations after this QSAR analysis was done. Each step of the protocol along with the challenges faced is discussed below.

3.2 Disease Selection

Alzheimer's disease was selected for current study because it is the major reason of dementia and is considered as a major killer that slowly destroys a person's memory until the person dies from forgetting how to perform routine tasks. Approximately 24 million people worldwide have dementia of which the majority (~60%) is due to Alzheimer's. According to Alzheimer's Drug Discovery Foundation more than 5 million patients in the US and more than 35 million individuals worldwide are suffering from Alzheimer's disease. The disease is believed to have an annual impact of \$172 billion on health care in the United States and is projected to increase rapidly in the near future. AD is not only brutal on the person who has this condition, family members suffer as well. In an attempt to combat this major killer and make a novel drug this study is a subsequent contribution.

3.3 Protein Target

There are multiple protein targets that can be considered to cure Alzheimer's disease. Among several targets, BChE is considered and protein structure was taken from Protein Data Bank by PDB ID: 1P0I. BChE is a key acetylcholine hydrolyzing enzyme in the blood (Darvesh *et al.*, 2003). Besides acylcholines, it can degrade a large number of ester containing compounds. Consequently, it plays noteworthy pharmacological and toxicological roles. BChE played an important role in the pathological progression of AD by depleting acetylcholine. It attenuates amyloid fibril formation in vitro (Diamant *et al.*, 2006). As BChEIs enhance ACh availability, they have been used to delay symptoms of AD (Campbell *et al.*, 2007). BChE can exist as monomers, dimers, or tetramers (Darvesh *et al.*, 2003).

3.4 Data Set Formation

Data set was made keeping in mind some considerations such as all the compounds had passed through bioassay and have reported IC_{50} value. The range of IC_{50} value up to 100 μM was only considered. Secondly it was considered that data set must be composed of different classes of compounds having numerous functional groups so that highly active and potent lead is identified from a vast data set lastly all the selected compounds for this study must not be reported earlier than 2005. Various anti-Alzheimer Cholinesterase Inhibitors were studied and selected for this study, these drugs belongs to different classes having distinct functional groups. Along with these compounds some FDA approved anti-Alzheimer ChEIs were also incorporated to be taken as standard

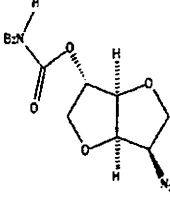
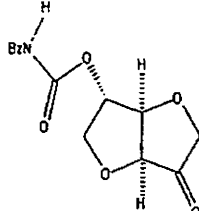
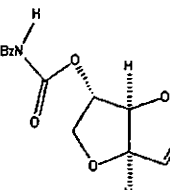
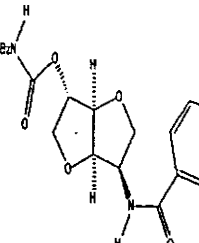
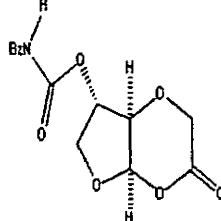
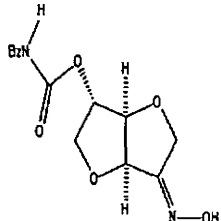
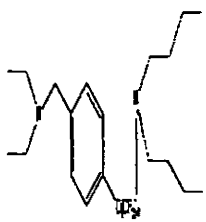
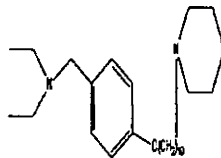
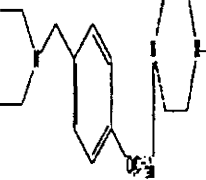
drugs. The data consisting of 26 compounds (Decker *et al.*, 2005; Schott *et al.*, 2006 ; Dillon *et al.*, 2009-10; Liang Yu *et al.*, 2010; Tkakhas *et al.*, 2011) along with two the standard compounds namely Donepezil and Rivastigmine (Isabelle Tomassoli *et al.*, 2010) along with IC₅₀ values are shown in Table3.1.

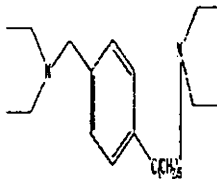
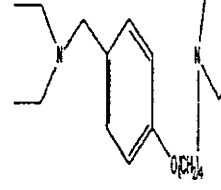
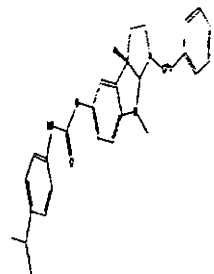
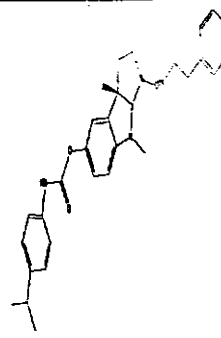
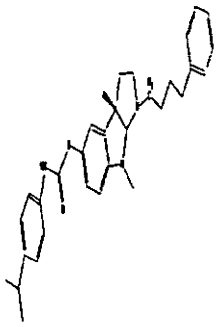
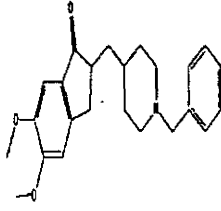
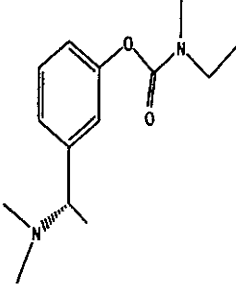
3.5 Compounds Drawing

The compounds were drawn using Chem Draw Ultra Version 8.0 (CambridgeSoft.com) (Loren *et al.*, 2004). ChemDraw is a computational tool for generating and managing drawings of chemical structures. The structures of two standard drugs along with 26 compounds were drawn using it and saved with .cdx extension. Then using Chem3D Ultra the structures of compounds and two standard drugs were modeled in pdb format.

Table 3.1: 2D view of selected Compounds and their IC₅₀ values

S.NO	Structures	IC50 μM	S.NO	Structures	IC50 μM
SW1		>500	SW2		11.9
SW3		>500	SW4		50.1
SW5		17.4	SW6		17.5
SW7		20.9	SW8		1.2
SW9		1.6	SW10		2.7

SW11		0.504	SW 12		0.46
SW 13		10.25	SW 14		0.88
SW 15		0.56	SW 16		0.4
SW 17		2.52	SW 18		0.078
SW 19		0.011	SW 20		2.20

SW 21		4.42	SW 22		1.40
SW 23		0.51	SW 24		0.51
SW 25		0.55	SW 26		0.5
Donepezil		14.8	Rivastigmine		2.0

3.6 2D and 3D Pharmacophore Generation

Pharmacophore model of the data set was generated using Ligand Scout (Wolber *et al.*, 2005). Ligand Scout version 3.02(inteligand.com) was used in the studies. It generates ligand based as well as structure based Pharmacophore models based on sophisticated algorithms for performing alignments and interpreting ligand-macromolecule interactions. It generates customized and highly specific 2D as well as 3D Pharmacophore models. Ligand derived Pharmacophore was generated for the selected data. This approach employs the conformational flexibility of ligands and searches for a common feature pattern that shared in an active ligand set.

For Pharmacophore generation, the pdb files of the data set were provided as an input. PDB files of the data set were obtained from ChemDraw Ultra. A pdb file was opened in a structures based view. The imported ligand was then copied to ligand based view using data exchange widget. This process was repeated for all the ligand from each class and also for the two standard drugs. After loading, all candidate ligands for the Pharmacophore model generation were set to 'training set' by choosing 'Ligand-Set -> Flag Selected Molecules as Training Set'. Different conformations for loaded data set were generated by using 'Apply Best Settings' instead of default. The training set was then was clustered according to 3D Pharmacophore characteristics of the ligands using the 'cluster' button on the bottom of the 3D view. By keeping default parameter in the dialog box, the clustering process started by pressing the 'OK' button. Espresso created a new column in the ligand table called 'Cluster ID'. The ligand table was sorted by using

column header ‘Cluster ID’. After sorting, all ligands with cluster ID ‘1’ were selected as test set by using the table controls. Next, the merged Pharmacophore model was generated by clicking the button ‘Create ligand-based Pharmacophore’ using the default values. Thus a merged feature Pharmacophore was generated and displayed in the 3D view. Same procedure was repeated for getting the shared Pharmacophore. In case of shared feature Pharmacophore, the Pharmacophore model was generated by checking the “shared feature Pharmacophore” while keeping the other parameters same. Based on these Pharmacophores, common and merged features were calculated. At the end unique merged and shared Pharmacophores has been predicted for anti-Alzheimer Cholinesterase.

3.7 Molecular Docking using AutoDock 4.0

Docking phase is meaningless without its two components target protein and ligand. For docking studies a suitable target protein for chosen anti-Alzheimer’s disease cholinesterase inhibitors was recognized (Nicolet et al., 2003). Recently reported Human Butryl cholinesterase (pdb id: 1P0I) was chosen as a target for current study. Pdb file of 1P0I was downloaded from the protein data bank (rscb.org). Docking was done using software AutoDock 4.0 and its patch AutoDock Vina (Chang et al., 2010).

Autodock 4.0 reads the pdb files of the target protein and ligand as an input. The 3D structures of the data set were generated as pdb files with Chem3D Ultra and were placed in the same directory containing installed software.

3.7.1 Steps for Molecular Docking

The complete docking procedure could be stated as follows: first of all the water molecules were eliminated from the protein. After the removal of water molecules the pdb file of the macromolecule 1P0I was provided as an input to the software. Kollman and Gasteiger charges were automatically computed for the macromolecule by AutoDock. Then the macromolecule was checked for the missing atoms and repaired. After repairing missing atoms, the hydrogens were added by keeping all the parameters at default settings. The macromolecule after all these modification was saved as RH.pdb in the same directory. Then the ligand preparation was carried out. Like macromolecule, Kollman and Gasteiger charges were automatically computed for the ligand. Then some of the torsions of the ligands were defined. The root was detected; the rotatable bonds were converted in to non-rotatable bonds and vice versa and the number of active torsions was set to most atoms rather than fewest. A pdbqt file was then created for the modified ligand.

After the preparation of a macromolecule and ligand, rigid residue was prepared using GRID module provided in AutoDock 4.0. Grid module employed RH.pdb file. AutoDock automatically added charges and merged hydrogens for rigid residue. The flexible macromolecule was then saved with .pdbqt extension.

For docking purpose AutoDock Vina (Trott *et al.*, 2010) was used. Vina is an open source program. It employed a conf file referring pdbqt files of

macromolecule and ligands prepared using AutoDock and Grid properties. As an output Vina generated log files and pdbqt files of energy models for selected data set. The output file contained different energy models. Among these models, the lowest energy model against each ligand was selected and appended at the end of original protein file. As a result of this step docked files for the selected set generated.

3.7.2 Ligand-Protein Interaction

The ligand- protein interactions were visualized using Visual Molecular Dynamics (VMD). The docked file prepared using AutoDock Vina was provided as input to the VMD. After this the interactions (ionic, hydrogen and hydrophobic) between the ligand and the active site of the target were drawn selecting atoms within 5 °A.

3.7.3 Lead Identification

Most active or lead compound was identification after finding interactions. Lead identification was done while considering three properties:

- Number of interactions, most importantly Ionic.
- IC-50 values.
- Energy values of the model generated through docking.

3.7.4 Analogue Designing

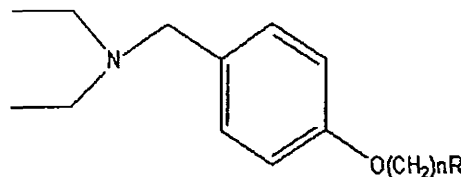
Four structural analogues of the lead were made by introducing or eliminating various functional groups in it, focusing on increasing and decreasing hydrophobicity and hydrophilicity. Docking studies on the analogue were then performed using the same process using Auto Dock Vina.

3.8 Quantity Structure Activity Relationship

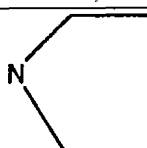
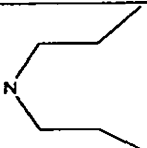
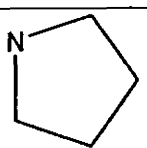
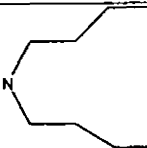
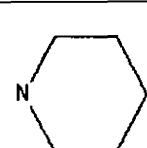
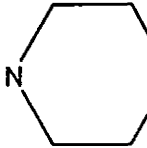
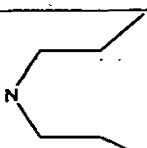
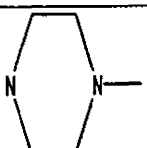
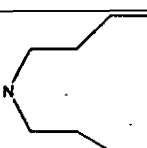
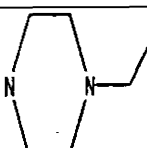
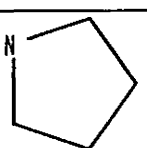
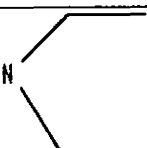
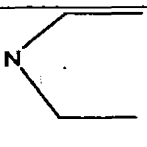
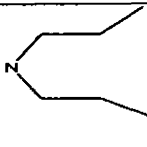
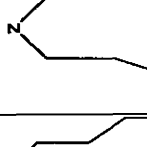
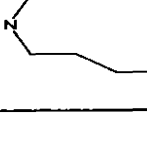
A quantitative structure activity relationship (QSAR) simple linear regression analysis was performed for BChE inhibitors by computing electronic and steric descriptors. Set of selected 27 compounds, drawn using ChemDraw were used for QSAR studies (Liang Yu *et al.*, 2010). Data set is shown in table 3. For computing descriptors Chem Draw and Hyper Chem Professional 8.0 (HyperCube, Inc.) were used. Then QSAR equation was calculated by correlating the descriptors and activity value (IC50). A QSAR generally takes the form of a linear equation:

$$\text{Biological Activity} = \text{Const} + (S1 W1) + (S2 W2) + (S3 W3) + \dots + (S_n W_n)$$

Where the parameters W1 through Wn are computed for each molecule in the series and the coefficients S1 through Sn are calculated by fitting variations in the parameters and the biological activity. After that a graph was generated using GRAPH software.

Table3.2: Chemical Structure and IC₅₀ values of Compounds for QSAR studies.

Compd.	n	R	IC ₅₀ μ M	Compd.	n	R	IC ₅₀ μ M
SA1	2		10.10	SA15	8		0.015
SA2	2		20.27	SA16	8		0.0073
SA3	4		1.40	SA17	8		0.011
SA4	4		0.71	SA18	8		0.014
SA5	4		9.73	SA19	8		0.048

SA6	4		2.74	SA20	8		0.0091
SA7	5		1.54	SA21	8		0.017
SA8	5		0.67	SA22	10		0.078
SA9	6		1.78	SA23	10		0.033
SA10	6		1.90	SA24	10		0.19
SA11	6		1.28	SA25	10		0.027
SA12	6		1.66	SA26	10		0.026
SA13	6		1.34	SA27	10		0.015
SA14	6		0.23				

CHAPTER 4

RESULTS AND DISCUSSION

4. RESULTS AND DISCUSSIONS

Through this work, I aim to identify the lead compound, i.e., the most active compound from our data set and the analogue designing with the help of techniques of computer aided drug designing.

4.1 Rule of Five

Although all the drugs have undergone the bioassay, to counter check the drug-likeness properties, In-Silico techniques i.e. rule of 5 or Lipinski rule was applied to incorporate the pharmacokinetics of the drug. The results are given in Table 4.1.

The results show that all the compounds including data for molecular docking and QSAR follow the HBA, HBD and MW constraints of Lipinski's rule (Rule of Five) but some compounds from QSAR data set deviate from the LogP constraint.

Table 4.1: Lipinski's rule (Rule of Five) applied to data set

Rule of Five for Ligands				
Ligand No.	No more than 5 HBD	No more than 10 HBA	MW(under 500Da)	Log P less than 5
RIV	3	7	250.34	2.36
DO	1	3	379.49	4.01
SW1	0	1	264.32	4.96
SW2	1	0	250.34	3.21
SW3	1	0	252.35	2.69
SW4	2	0	238.33	2.33
SW5	0	1	225.29	3.06
SW6	2	1	213.25	1.40
SW7	1	1	227.28	1.76
SW8	2	1	227.28	1.98
SW9	3	1	213.25	2.05
SW10	2	1	227.28	2.41
SW11	4	4	318.28	4.37
SW12	2	5	291.26	-0.28
SW13	1	4	275.26	4.76
SW14	2	5	396.39	1.53
SW15	2	6	307.26	0.61
SW16	1	6	306.27	0.11
SW17	2	1	362.59	5
SW18	2	1	402.66	5.1
SW19	3	1	398.62	4.05
SW20	3	1	375.59	3.60
SW21	2	1	320.51	3.75
SW22	2	1	304.47	2.99
SW23	2	2	455.59	7.29
SW24	2	2	483.64	7.99
SW25	2	2	497.67	8.41
SW26	2	2	500	8.13
SA1	2	1	290.44	2.88
SA2	2	1	305.46	1.99
SA3	2	1	304.47	2.99
SA4	2	1	318.5	3.39
SA5	3	1	333.51	2.47
SA6	2	1	306.49	3.35
SA7	2	1	318.5	3.39
SA8	2	1	332.52	3.78
SA9	2	1	348.57	4.68
SA10	2	1	376.62	5.48
SA11	2	1	332.52	3.78
SA12	2	1	334.54	4.14

SA13	2	1	362.59	5.08
SA14	2	1	390.65	5.87
SA15	2	1	360.58	4.58
SA16	2	1	374.6	4.97
SA17	3	1	389.62	4.05
SA18	3	1	403.64	4.39
SA19	2	1	362.59	4.94
SA20	2	1	390.65	5.87
SA21	2	1	418.7	6.67
SA22	2	1	402.66	5.76
SA23	3	1	417.67	4.84
SA24	3	1	431.7	5.19
SA25	2	1	390.65	5.73
SA26	2	1	418.7	6.67
SA27	2	1	446.75	7.46

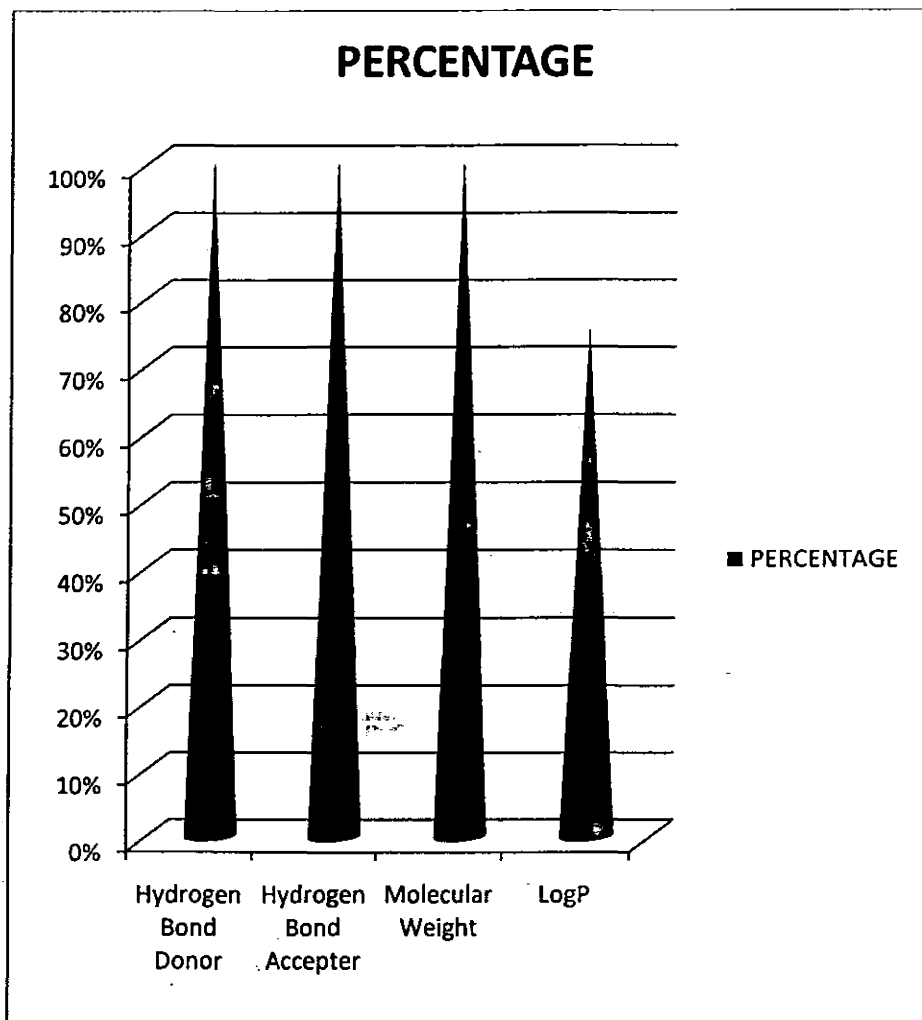


Figure 4.1: Bar Chart showing detailed analysis of Rule of Five in percentage form

4.2 Pharmacophore Modeling

In the current era, Pharmacophore modeling has become an integrated part of drug development and designing (Cohen *et al.*, 2005). A Pharmacophore highlights the 3D arrangement of structural features of a compound that are required for a certain biological activity. Identification of Pharmacophoric features of the ligands, I used in this study, was carried out using Ligandscout. It identified a Merged Feature Pharmacophore as well as the Shared Feature Pharmacophore. For current studies 'Merged Feature Pharmacophore' as well as 'Shared Feature Pharmacophore' has been created.

The methodology for creating the Pharmacophores is explained shortly. After loading the ligands, conformations of the Training-Set are generated. After ranking the molecules according to their number of conformations (flexibility), Pharmacophore features are projected on these molecules and all their conformations. All conformations of the two top ranked (i.e. the least flexible) molecules are then aligned using Inte: Ligand's molecular alignment algorithm. For a configurable number of best alignment solutions common Pharmacophoric features are interpolated and intermediate Pharmacophore models are created and stored for further processing. These intermediate Pharmacophore models are now ranked using several adjustable scoring functions taking into account chemical feature overlap, steric overlap, or both. The intermediate Pharmacophore models are then aligned to all conformations of the third molecule, etc., and a new set of intermediate combined feature Pharmacophores is created until all molecules have been processed. If at any stage no conformation can be found that can be

matched on any intermediate solution, the process is stopped. If at least three common chemical features can be identified throughout the whole alignment and interpolation process, the feature Pharmacophore combination is considered to be successful.

As a result of this, Ligandscout calculates the number of features matched, Pharmacophore fit and 10 Pharmacophore models. Among these models the BChE-1 (model-1) was selected for calculating the merged features present among all the selected ligands. Likewise for Shared Pharmacophore prediction among the 10 generated models 'Model-1' was elected for computing the shared features among the data set. For 'Merged Pharmacophore', the calculated feature patterns, Pharmacophore fit for selected data set and models with scores are shown in figure 4.2a and b and for 'Shared Pharmacophore' all of these calculations are shown in figures 4.3a and b. The common features that are present in all compounds are; Hydrophobic volumes, Hydrogen Bond Acceptors, Hydrogen Bond donors and positive ionizable. The 2D and 3D Pharmacophore of one compound from all the different classes and standard drugs too are shown in figure 4.4 and 4.5.

Line	Item	Name	Type	Specimen	Count	Unit	Quantity	Approximate
1.0	1	1000	1000	1	1	1	1	30000
2.0	1	1000	1000	1	1	1	1	30000
3.0	1	1000	1000	1	1	1	1	30000
4.0	1	1000	1000	1	1	1	1	30000
5.0	1	1000	1000	1	1	1	1	30000

Figure 4.3a: Feature Pattern, best Conformations, Cluster ID and Pharmacophore Fit for Selected Dataset

Figure 4.3b: Feature Pattern, best Conformations, Cluster ID and Pharmacophore Fit for Selected Dataset

Active	Name	Type	Feature Pattern	#Confs	ClusterID	Pharmacophore Fit	
1	■	(150) UNK0	Training ▼	■ ■ ■	265	2	58.5600
2	■	■ UNK0	Training ▼	■ ■ ■	3	2	59.4900
3	■	■ UNK0	Training ▼	■ ■ ■	3	2	58.3700
4	■	UNK0	Training ▼	■ ■ ■	500	2	55.8800
5	■	■ UNK0	Training ▼	■ ■ ■	55	2	55.4600
6	■	■ UNK0	Training ▼	■ ■ ■	500	2	54.6800
7	■	UNK0	Training ▼	■ ■ ■	500	2	54.5600
8	■	■ (150) UNK0	Training ▼	■ ■ ■	2	2	49.5600
9	■	■ UNK0	Test ▼	■ ■ ■	89	1	41.3400
10	■	■ UNK0	Test ▼	■ ■ ■	147	1	35.0800

Figure 4.2a: Feature Pattern, best Conformations, Cluster ID and Pharmacophore Fit for Selected Dataset

name	score
BChE1-1	0.7352
BChE1-2	0.7351
BChE1-3	0.7351
BChE1-4	0.7351
BChE1-5	0.7351
BChE1-6	0.7321
BChE1-7	0.7217
BChE1-8	0.7216
BChE1-9	0.7215
BChE1-10	0.7215

Figure 4.2b: Pharmacophore Models generated for Selected Dataset

Feature Pattern in the table shown in figure 4.2a signifies, which features are met by which ligand. A click on a colored square indicates which feature is linked to the corresponding square. The cluster ID shows the different number of conformations for selected data set. The main purpose of clustering is to select those compounds that are similar in terms of 3D Pharmacophore characteristics and therefore bear a higher chance for delivering a large overlap of chemical features. The 3D clustering algorithms performs fast alignments and clusters based on a similarity value between 0 and 1. Since this algorithm basically performs combinatorial alignments of all conformations of all compounds, a low number of conformations (1-3) is recommended. The Pharmacophore fit signifies the chemical feature overlap, steric overlap, or both score. The higher the value of Pharmacophore fit, better it would be.

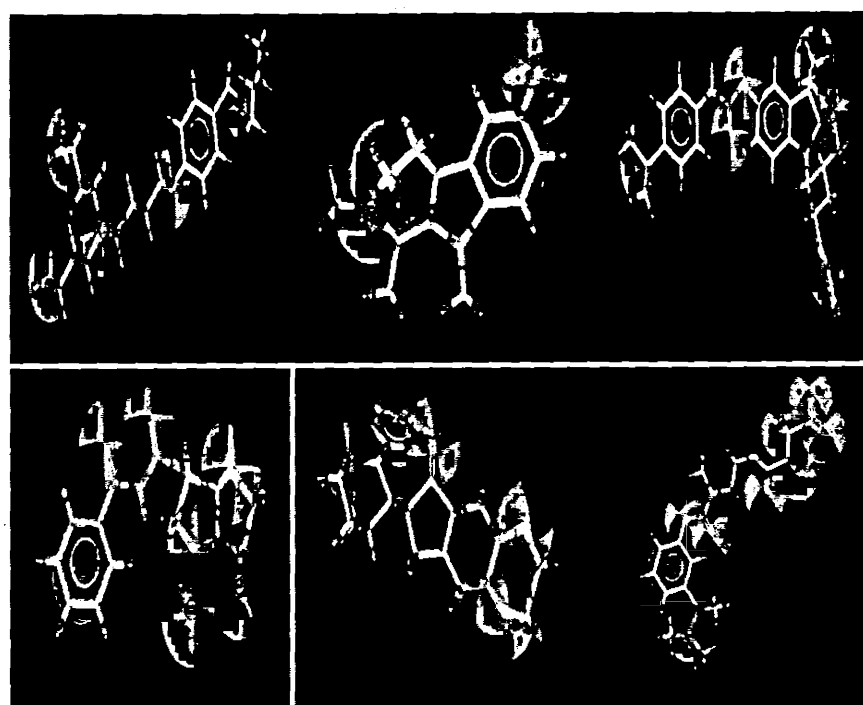


Figure 4.4: 2D Pharmacophore Models of Selected Data along with Standard Drugs

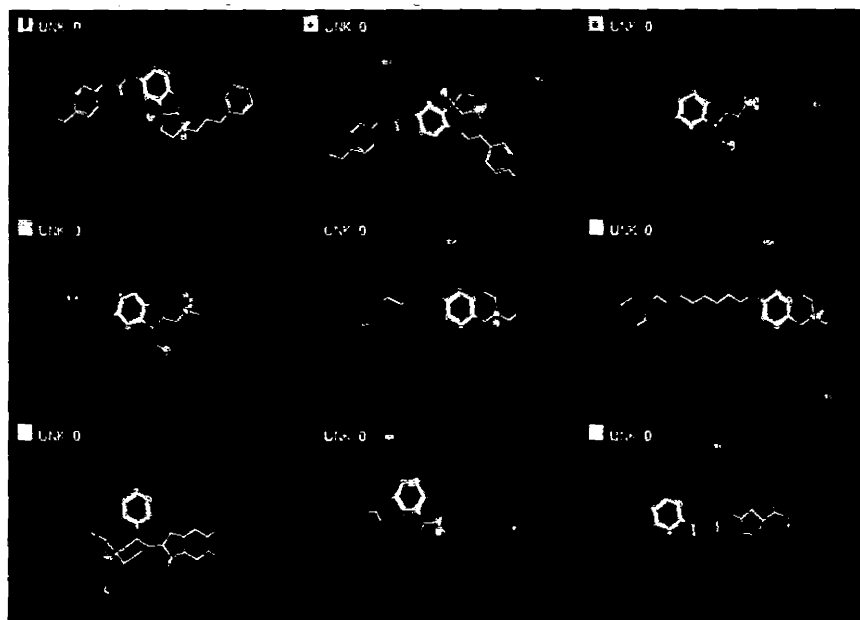


Figure 4.5: 3D Pharmacophore Models of Selected Data along with Standard Drug

The green color in the figures show HBDs, red are HBAs, yellow are hydrophobic and aromatic features and blue star like illustrate positive ionizable. Both 2D and 3D views show consistency. All Pharmacophoric features of each class along with Rivastigmine and Donepezil are summarized in the following table.

Table 4.2: Pharmacophoric Features of Data Set

Compounds	HBDs	HBAs	Ar/HY	Positive ionizable
4-[(diethylamino) methyl]-phenol	Three	One	Four	Two
β -carbolines	Two	One	Three	One
N ¹ -substituted norcymserine	Two	Two	Eight	One
Isosorbide-based	Four	Four	Two	Two
Rivastigmine (Exelon)	Three	Seven	Two	One
Donepezil (Aricept)	One	Three	Two	One

After determining individual Pharmacophore, all the compounds were clustered in 3D and merged and shared Pharmacophores were generated through LigandScout using its ‘Merged Feature Pharmacophore’ and ‘Shared Feature Pharmacophore’ options respectively. The merged Pharmacophore is shown figure 4.6 and shared is shown in 4.7:

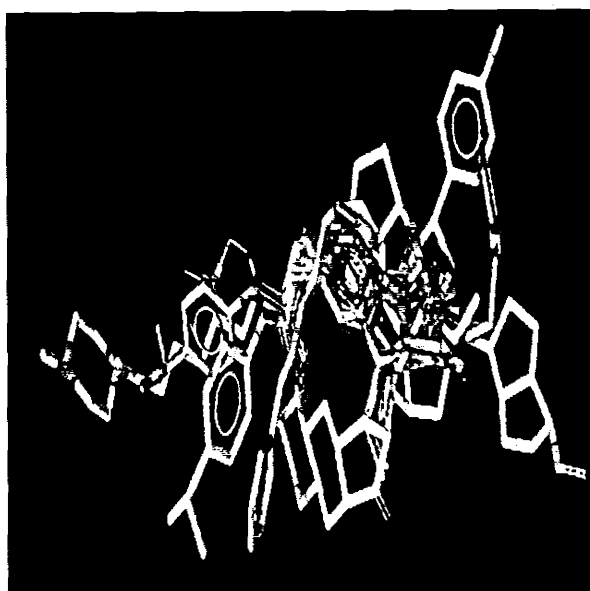


Figure 4.6a: Merged Pharmacophore of selected ligands, Donepezil and Rivastigmine generated by LigandScout

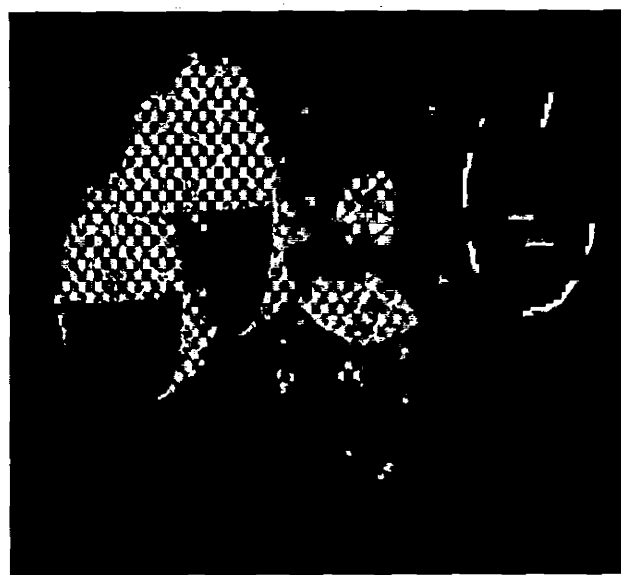


Figure 4.6b: Merged Pharmacophore showing 2 Hydrogen Bond Acceptors, 1 Hydrogen Bond Donor, 1 aromatic ring, 2 hydrophobic volumes and 1 Positive ionizable

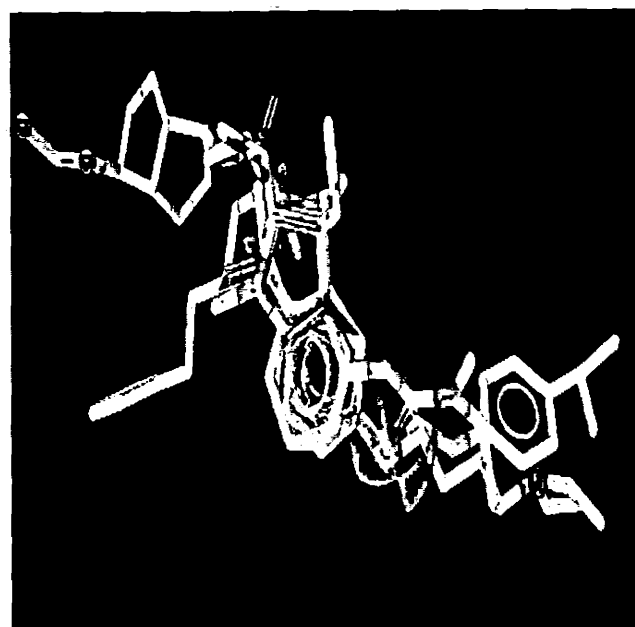


Figure 4.7a: Shared Pharmacophore of selected ligands, Donepezil and Rivastigmine

generated by LigandScout

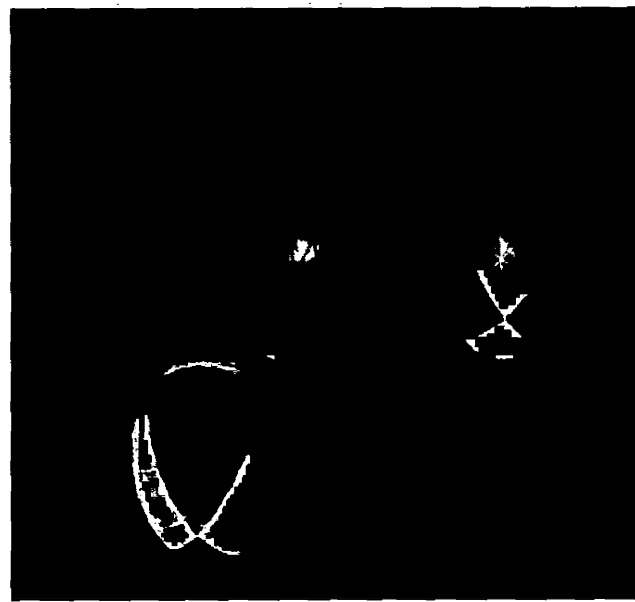


Figure 4.7b: Shared Pharmacophore showing 1 Hydrogen Bond Acceptor, 1 Hydrogen

Bond Donor, 1 aromatic ring, 1 hydrophobic volume and 1 Positive ionizable

The best merged feature Pharmacophore model selected for the four classes of Butyrylcholinesterase inhibitors against the Alzheimer's disease is as; one aromatic ring and two hydrophobic volumes (shown by yellow circles), two Hydrogen Bond Acceptors (shown by red), one Hydrogen Bond donor (shown by green) one positive ionizable (shown by blue) and a set of 30 exclusion volumes. Likewise, the best shared feature Pharmacophore model of selected dataset is as: one aromatic ring and one hydrophobic volume (shown by yellow circles), one Hydrogen Bond Acceptor (shown by red), one Hydrogen Bond donor (shown by green) one positive ionizable (shown by blue) and a set of 30 exclusion volumes. These calculated Pharmacophoric features help in the identification of more active and improved anti-Alzheimer's disease drug.

In order to gain a deep insight of cholinesterase inhibitors, a ligand based 3D QSAR model of dihydropyridine-like compounds using Phase program was indentified and evaluated. The model consists of two hydrogen acceptor vector sites, one hydrogen donor vector, one aromatic ring vector and one hydrophobic group (Davies *et al.*, 1989). Another 3D Pharmacophore model based on eight potent and structurally diverse AChE inhibitors leading to the discovery of dual binding site AChE inhibitors was documented. This Pharmacophores consists of two hydrogen-bond acceptor lipid, one hydrophobe, and two hydrophobic aliphatic features (David *et al.*, 1994). Lastly, using a congeneric carbamate class of AChE inhibitors, scientist's generated quantitative Pharmacophore models. HypoGen program of Catalyst was employed in this study. It has been reported that the best Pharmacophores model comprised of three hydrophobic, one hydrogen bond donor and a set of 34 excluded volumes (Diamant *et al.*, 2006). In our current studies, a 3D Pharmacophore model is developed in order to assist the discovery of type specific

and potent Butyrylcholinesterase inhibitors for the treatment of Alzheimer's disease which has not been reported earlier. Number of previous citations reported the Pharmacophore models employing only AChE inhibitors specific compounds. Current studies involved the Pharmacophore generation of compounds belonging to major groups of BChEIs.

4.2.1 Pharmacophore Triangle

The distance triangle measured between the common Pharmacophoric features of each group of compound using VMD is shown:

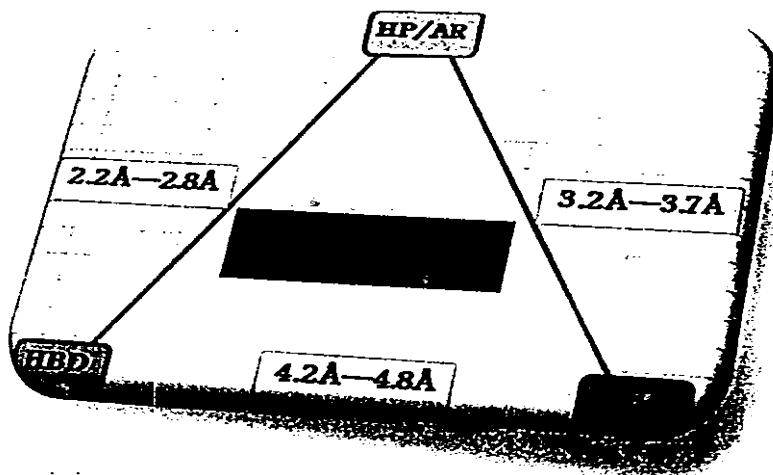


Figure 4.8: Three featured Pharmacophoric Triangle of Butyl Cholinesterase inhibitor
 The distance ranges from minimum to maximum and have been measured between the HBA and HBD, HBA and aromatic ring and HBD and aromatic ring. The distances between hydrophobic and HBD range from 2.2 Å to 2.8 Å, between hydrophobic to HBA range from 3.2 Å to 3.7 Å and between HBA to HBD range from 4.2 Å to 4.8 Å.

4.3 Molecular Docking

Molecular docking studies were carried out using 26 compounds of five different classes of cholinesterase inhibitors along with two standard drugs. Autodock Vina was employed for molecular docking studies. As a result of docking different conformations of the ligands docked into the target protein 1P0I were obtained. For each ligand 10 different conformations have been generated. These conformations were automatically ranked in ascending order on the basis of the binding affinities of the ligand with the target protein. Among these conformations, the most active conformation was chosen based on the binding affinity of the ligand with the target protein.

4.3.1 Active Site of Cholinesterases

Both ChEs have their active sites at the base of enzyme cleft of about 20 Å depth. Complete data set was docked and found to bind at the same active site position. The active site amino acids were identified by looking the 5 Å vicinity. The residues found were TRP82, HIS438, GLY439, ALA328, TYR332, GLU197, PHE329, GLY115, GLY116, GLY117, PHE398, LEU286, TRP231, TRP430, TYR 440, ASP70, GLY121, MET437, TYR128, TRP83, THR120, GLN119, PRO285, ILE69, VAL233 and ASN68. The study revealed that TRP28, HIS438, ALA328, TYR332, GLU197, PHE329, GLY115, GLY116, GLY117, LEU286, TRP231, TRP40, THR120 ASP70 AND PRO285 amino acids are significant for binding interactions.

The docked conformation of two ligands from the selected data of 26 compounds, obtained through Autodock Vina i.e. ligand No.8 and ligand No.16 have been shown in figures 4.9 and 4.10. These figures show the 3D structures of active conformations of the ligands docked into the target protein. The ligands in both figures have been shown as in bonds while target protein has been shown in lines. The active conformations were used for the identification of ligand-protein interaction using VMD.

Table 4.3: Amino acids within 5Å of the target protein where + and – signs indicate the presence and absence of amino acid

Amino Acids	Ligands												
	1	2	3	4	5	6	7	8	9	10	11	12	13
TRP82	+	+	+	+	+	+	+	+	+	+	+	+	+
HIS438	+	+	+	+	+	+	+	-	+	+	-	+	-
GLY439	+	-	-	-	-	+	+	-	-	-	-	-	-
ALA328	+	+	+	-	-	-	+	+	+	+	-	+	-
TYR332	+	+	+	-	+	+	+	+	+	+	-	-	-
GLU197	+	-	-	-	-	-	-	+	+	+	-	-	-
PHE329	+	+	+	-	+	-	-	-	-	-	+	-	+
GLY115	-	+	+	-	-	+	+	+	+	+	-	-	-
GLY116	-	+	+	+	-	-	-	+	+	+	-	+	-
GLY117	-	-	-	+	-	-	-	-	-	-	+	+	+
PHE398	-	-	-	+	-	-	-	-	-	-	+	+	-
LEU286	-	-	-	+	-	-	-	-	-	-	+	+	+
TRP231	-	-	-	+	-	-	-	-	-	-	+	+	+
TRP430	-	-	-	-	+	-	-	+	+	-	-	+	-
TYR440	-	-	-	-	+	-	-	-	-	-	-	-	-
ASP70	-	-	-	-	-	+	+	-	-	-	-	-	-
GLY121	-	-	-	-	-	-	-	+	-	-	-	-	-
MET437	-	-	-	-	-	-	-	+	-	-	-	-	-
TYR128	-	-	-	-	-	-	-	-	+	+	-	-	-

TRP83	-	-	-	-	-	-	-	-	-	-	-	-	+
THR120	-	-	-	-	-	-	-	-	-	-	-	-	-
GLN119	-	-	-	-	-	-	-	-	-	-	-	-	-
ILE69	-	-	-	-	-	-	-	-	-	-	-	-	-
ASN68	-	-	-	-	-	-	-	-	-	-	-	-	-
PRO285	-	-	-	-	-	-	-	-	-	-	-	-	-
TRP238	-	-	-	-	-	-	-	-	-	-	-	-	-
ALA227	-	-	-	-	-	-	-	-	-	-	-	-	-
THR532	-	-	-	-	-	-	-	-	-	-	-	-	-
ASP304	-	-	-	-	-	-	-	-	-	-	-	-	-
VAL233	-	-	-	-	-	-	-	-	-	-	-	-	-
PRO303	-	-	-	-	-	-	-	-	-	-	-	-	-
PHE227	-	-	-	-	-	-	-	-	-	-	-	-	-
LEU307	-	-	-	-	-	-	-	-	-	-	-	-	-
ASN228	-	-	-	-	-	-	-	-	-	-	-	-	-
PRO230	-	-	-	-	-	-	-	-	-	-	-	-	-
TYR396	-	-	-	-	-	-	-	-	-	-	-	-	-
PRO401	-	-	-	-	-	-	-	-	-	-	-	-	-
PRO527	-	-	-	-	-	-	-	-	-	-	-	-	-
THR284	-	-	-	-	-	-	-	-	-	-	-	-	-
ILE356	-	-	-	-	-	-	-	-	-	-	-	-	-
TYR282	-	-	-	-	-	-	-	-	-	-	-	-	-

Amino Acids	Ligands													
	14	15	16	17	18	Inactive	19	20	21	22	23	24	25	26
TRP82	+	+	+	+	-		+	+	-	+	+	+	-	+
HIS438	-	+	+	+	-		+	-	-	-	+	-	+	-
GLY439	-	-	-	-	-		-	-	-	-	-	-	-	-
ALA328	+	-	+	-	-		-	+	-	-	-	+	+	-
TYR332	+	-	+	-	-		-	+	-	+	-	+	-	-
GLU197	-	-	-	+	-		-	-	-	-	-	-	-	-
PHE329	+	+	-	-	-		+	-	+	+	-	+	+	-
GLY115	-	-	-	-	-		-	-	-	-	-	+	-	+
GLY116	+	-	+	+			+	+	+	-	-	-	+	+
GLY117	+	-	+	-	-		+	+	+	-	-	-	-	-
PHE398	-	-	+	-	-		-	-	-	-	-	-	-	-
LEU286	-	-	+	-	-		-	+	-	-	-	-	-	+
TRP231	-	+	+	-	-		-	+	-	-	-	-	-	-
TRP430	+	-	-	-	-		-	+	+	-	-	-	-	-
TYR440	-	-	-	-	-		-	-	+	-	-	-	-	-
ASP70	-	-	-	-	-		-	-	+	-	+	-	-	-
GLY121	-	-	-	-	-		-	-	-	-	-	-	-	-
MET437	-	-	-	-	-		-	-	+	-	-	-	-	-
TYR128	-	-	-	-	-		-	-	-	-	-	-	-	-
TRP83	+	-	-	-	-		-	-	-	-	-	-	-	-
THR120	-	-	-	-	-		-	+	+	-	+	+	+	+

GLN119	-	-	-	-	-	-	+	-	-	-	-	+	-	+
ILE69	-	-	-	-	-	-	-	+	-	+	-	-	-	-
ASN68	-	-	-	-	-	-	-	+	-	+	-	-	-	-
PRO285	-	-	-	-	-	-	-	-	-	-	+	+	+	+
TRP238	+	-	-	-	-	-	-	-	-	-	-	-	-	-
ALA227	-	-	-	+	-	-	-	-	-	-	-	-	-	-
THR532	-	-	-	-	+	-	-	-	-	-	-	-	-	-
ASP304	-	-	-	-	+	-	-	-	-	-	-	-	-	-
VAL233	-	-	-	-	+	-	-	-	-	-	-	-	-	-
PRO303	-	-	-	-	+	-	-	-	-	-	-	-	-	-
PHE227	-	-	-	-	+	-	-	-	-	-	-	-	-	-
LEU307	-	-	-	-	+	-	-	-	-	-	-	-	-	-
ASN228	-	-	-	-	+	-	-	-	-	-	-	-	-	-
PRO230	-	-	-	-	+	-	-	-	-	-	-	-	-	-
TYR396	-	-	-	-	+	-	-	-	-	-	-	-	-	-
PRO401	-	-	-	-	+	-	-	-	-	-	-	-	-	-
PRO527	-	-	-	-	+	-	-	-	-	-	-	-	-	-
THR284	-	-	-	-	-	-	-	-	-	-	-	+	-	-
ILE356	-	-	-	-	-	-	-	-	-	-	-	+	-	-
TYR282	-	-	-	-	-	-	-	-	-	-	-	+	-	-

4.3.2 Docking Of Standard Drugs:

Docking of standard drugs with 1POI was carried out using the AutoDock4 and AutoDock Vina in the same manner. A detailed 3D analysis of the docked site of these drugs indicated that they bind to same active site. Figure 4.11-4.12 shows the hydrogen, hydrophobic and ionic interactions of the standard drugs Donepezil and Rivastigmine.

In case of **Donepezil** there were two types of interactions 3 ionic and 11 hydrophobic. Ionic interactions were between O of GLY116 at a distance of 3.75 with N of Donepezil and N of TRP82 at a distance of 3.67 and of GLY116 at a distance of 3.97 with O of Donepezil. No hydrogen bonds have been identified. Hydrophobic interactions were between C of TYR440, TYR440, TRP430, TRP430, PHE398, PHE329, PHE329, LEU286, LEU286, TRP231, TRP231 and TRP231 at distances of 3.39, 3.74, 3.42, 3.70, 3.74, 3.59, 3.55, 3.92, 3.69, 3.67 and 3.76 with C of Donepezil respectively.

Rivastigmine shows 4 ionic and 15 hydrophobic interactions. No hydrogen bonds have been identified. N of HIS438, of GLY116 and of GLY117 shows ionic interactions with O of Rivastigmine at distances of 3.56, 3.81 and 3.62 respectively. O of SER198 makes ionic bond with N of Rivastigmine at a distance of 3.56. C of TRP231 at distances of 3.82, 3.815, 3.57, 3.77, 3.56 and 3.81, of GLY117 at a distance of 3.40, of VAL288 at a distance of 3.67, of LEU286 at distances of 3.72 and 3.78, of SER198 at distances of 3.73, of HIS438 at a

distance of 3.96 and 3.86 and of TRP82 at distances of 3.96 and 3.81 shows hydrophobic interactions with C of Rivastigmine.

4.3.3 Docking Of Inactive Compound

Docking of inactive compound was done but no active interaction was deduced and the binding site was also slightly different from the rest data set showing that the amino acids in the near vicinity are THR532, ASP304, VAL233, PRO303, PRO230, PHE227, LEU307, ASN228, TYR396, PRO401 AND PRO527 as shown in figure 4.13. These amino acids were not appeared for any other compound or standard drugs.

4.3.4 Interactions of Ligands and Target Protein

The interactions of the active conformations of the ligands of the selected data and the target protein have been identified and marked using VMD and are shown in Table3. VMD provides the facility of labeling and computing distances between atoms. Checking one by one all amino acids in the active site of target and the atoms of the ligands, the interactions were identified. The important identified interactions in a data set and two standard drugs include the ionic, hydrogen and hydrophobic interactions. This exercise of manually selecting one by one all atoms and identifying the interactions, avoiding the mistakes was the most important step of this study.

While checking the amino acids in the target protein pocket one by one, actually the amino acids within 5Å of the pocket has been identified. The amino acids with

in 5Å have been shown in Table 3.5. The amino acids within 5Å of the pocket have been found to be involved in the binding interactions.

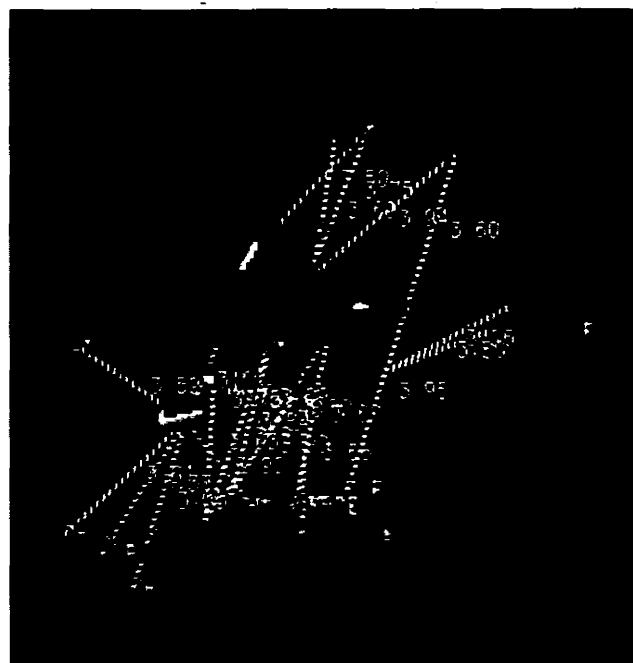


Figure 4.9: Binding Interactions of SW8 with 1P0I

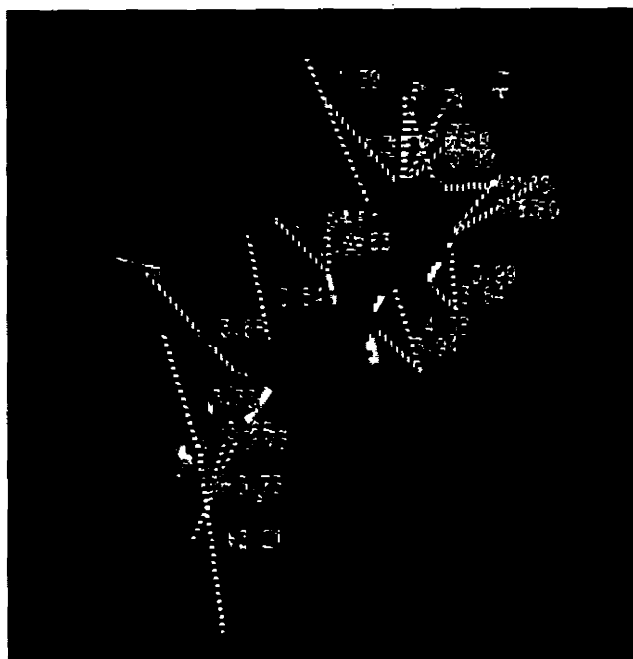


Figure 4.10: Binding Interactions of SW16 with 1P0I

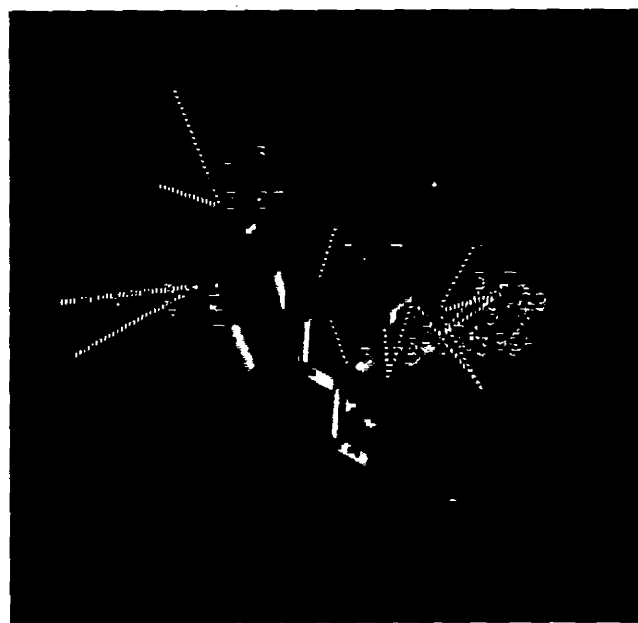


Figure4.11: Binding interactions of Donepezil with 1P0I

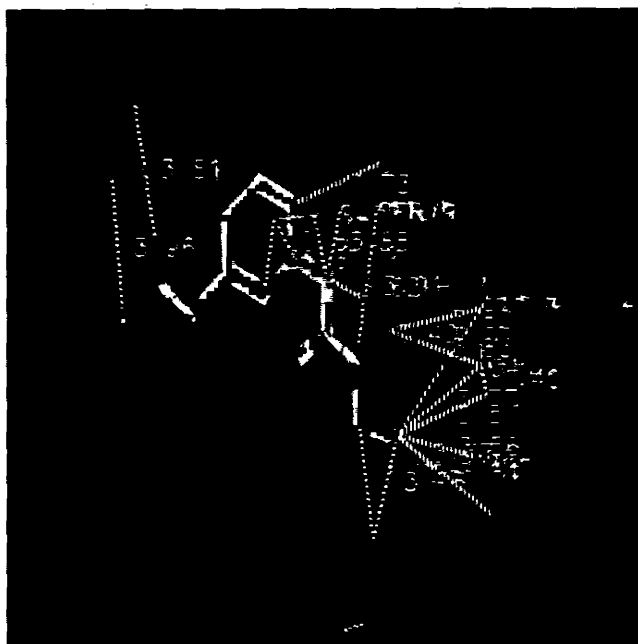


Figure4.12: Binding interactions of Rivastigmine with 1P0I

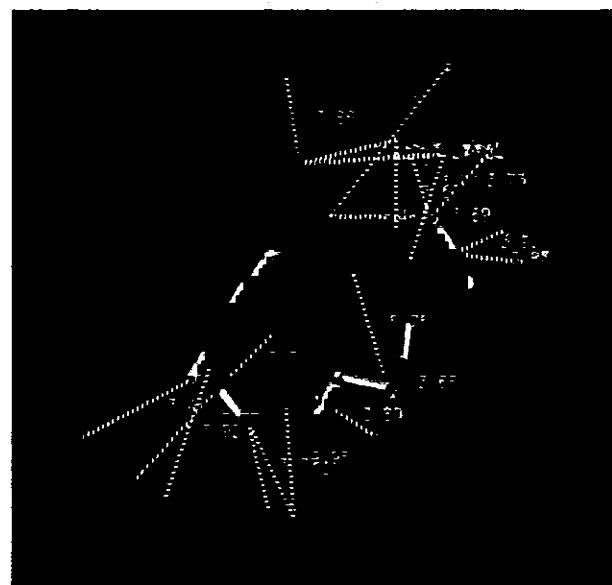


Figure 4.13: Binding Interactions of SW18 (Inactive compound) with 1POI

Table 4.4a: Energies of Ligands and Inhibition Concentration

Compound	Energy value (kcal/mol)	IC ₅₀ (μM)	Compound	Energy value (kcal/mol)	IC ₅₀ (μM)
SW1	-9.5	>500	SW15	-9.8	0.56
SW2	-9.4	11.9	SW16	-8.6	0.4
SW3	-9.4	>500	SW17	-8.8	2.52
SW4	-9.5	50.1	SW18	-6.6	0.078
SW5	-8.0	17.4	SW19	-10.1	0.011
SW6	-7.4	17.5	SW20	-6.6	2.20
SW7	-8.2	20.9	SW21	-9.0	4.42
SW8	-7.4	1.2	SW22	-8.8	1.40
SW9	-8.2	1.6	SW23	-11.4	0.51
SW10	-8.3	2.7	SW24	-9.8	0.51
SW11	-9.6	0.504	SW25	-9.4	0.55
SW12	-8.3	0.46	SW26	-10.5	0.5
SW13	-9.2	10.25	Donepezil	-10.9	14.8
SW14	-9.8	0.88	Rivastigmine	-8.0	2.0

To predict compound activeness IC_{50} value and binding interactions were also incorporated. It is evident from Table 4.4b that compounds SW12, SW16, SW18, SW19 and SW26 had hydrophobic interactions. Among these selected compounds, SW12, SW16 and SW26 had hydrogen bonding while SW18 and SW19 no hydrogen bonding. Standards drugs also showed no hydrogen bonding. Similarly ionic interactions, which observed in both standard drugs, are present in compounds SW12, SW18, SW19 and SW26. All the distances and interactions along with the residues involved in interactions are mentioned in Table 4.4b.

A detailed 3D study of docked files revealed that all the compounds of dataset have the same amino acids with the 5 Å of the ligand and all the interactions were calculated after selecting the best conformation based on energy values.

Table4.4b: Amino Acids within 5Å of the target Protein Pocket

Ligand No.	Hydrogen Bonding		Ionic Interactions		Hydrophobic Interactions		IC ₅₀ μM
	Amino Acids	Distance	Amino Acids	Distance	Amino Acids	Distance	
SW1	None		H-TRP82:NE1	3.72	C-TRP82: CD2 C-HIS438: CD2 C-HIS438:CD2 C-TRP82:CE2 C-TRP82:CE2 C-TRP82:CD2 C-TRP82:CZ3 C-TRP82:CH2 C-TRP82:CZ2 C-TRP82:CZ2 C-TRP82:CE3 C-GLY439: CA C-GLY 439: CA C-ALA328: C C-TYR332:CE1 C-GLU197: CD C-PHE329: CD2 C-PHE329: CD2 C-PHE329: CD2 C-ALA328: CB C-TYR332: CZ C-TYR332:CD2 C-TYR332:CE1 C-TYR332:CD1 C-TYR332: CG	3.69 3.888 3.83 3.66 3.66 3.94 3.63 3.88 3.65 3.98 3.86 3.72 3.75 3.76 3.68 3.40 3.72 3.89 3.63 3.71 3.94 3.95 3.68 3.54 3.69	>500
SW2	None		None		C-PHE329:CE2 C-PHE329:CE2 C-PHE329:CE2 C-PHE329:CD2 C-ALA328: C C-ALA328: CB C-TYR332:CE1 C-TYR332:CE1 C-HIS438:CD2 C-HIS438:CD2 C-TRP82: CE2 C-TRP82: CG C-TRP82: CE3 C-TRP82: CE3 C-TRP82: CZ3 C-TRP82: CB C-TRP82: CB C-TRP82: CE3 C-TRP82: CB C-TRP82: CE3 C-TRP82: CD2 C-GLY115: C C-GLY 116: CA C-GLY116: CA C-TYR332: CD1 C-PHE329: CD2	3.63 3.83 3.78 3.73 3.84 3.355 3.50 3.75 3.73 3.97 3.78 3.92 3.88 3.56 3.92 3.61 3.98 3.42 3.81 3.94 3.87 3.88 3.76 3.86 3.68 3.51	11.9

SW3	None		None		C-TYR332: CE1 C-TYR332: CE1 C-TYR332: CD1 C-TYR332: CD1 C-PHE329: CE2 C-PHE329: CE2 C-PHE329: CE2 C-PHE329: CD2 C-ALA328: CB C-ALA328 : C C-HIS438:CD2 C-HIS438:CD2 C-TRP82: CE2 C-TRP82: CE3 C-TRP82: CE3 C-TRP82: CE3 C-TRP82: CE3 C-TRP82: CB C-TRP82: CB C-TRP82: CB C-TRP82: CG C-GLY 116: CA C-GLY 116: CA C-GLY 115: C C-GLY 115: C	3.52 3.82 3.86 3.96 3.70 3.91 3.77 3.62 3.41 3.92 3.66 3.95 3.87 3.79 3.56 3.50 3.93 3.57 3.76 3.94 3.85 3.86 3.89 3.95	>500
SW4	N-SER198:OG	3.42	H-SER198:OG H-GLY 116: N H-GLY 117: N H-HIS438:NE2	2.92 3.23 3.31 3.98	C-TRP82: CZ3 C-TRP82: CE3 C-TRP82: CD2 C-TRP82: CE2 C-HIS438:CD2 C-HIS438:CD2 C-SER198: CZ C-PHE398:CZ C-PHE398:CZ C-PHE398:CE2 C-PHE398:CE2 C-PHE398:CE2 C-PHE398:CZ C-LEU286: CD2 C-LEU286:CD2 C-LEU286: C C-LEU286: CA C-GLY 117: CA C-GLY 117: CA C-TRP321:CE3 C-TRP321:CD2 C-TRP321:CG C-TRP321:CG C-TRP321:CD2	3.92 3.63 3.52 3.72 3.74 3.84 3.73 3.80 3.78 3.71 3.82 3.92 3.59 3.73 3.83 3.83 3.99 3.39 3.96 3.71 3.73 3.89 3.53	50.1
SW5	None		None		C-TYR 332: CD1 C-TYR 332: CD1 C-TYR 332: CG C-TYR 332: CD2 C-TYR 332: CZ C-PHE 329: CE2 C-PHE 329: CD2 C-PHE 329: CD2 C-HIS 438:CD2 C-HIS 438:CD2 C-TYR 440: CE1 C-TRP 430: CZ2 C-TRP 82:CD1 C-TRP 82: CZ2 C-TRP82:CE2	3.80 3.61 3.81 3.57 3.97 3.66 3.74 3.72 3.86 3.89 3.75 3.86 3.84 3.87 3.76 3.75 3.74 3.61	17.4

					C-TYR 332: CE1	3.90	
SW6	N-TYR332: OH N-ASP70: OD1	3.89 3.21	None		C- GLY 115:C C-TRP82 : CE3 C-TRP82 : CE3 C-TRP82 : CE3 C-TRP82 : CE3 C-TRP82 : CD2 C-TRP82 : CD2 C-TRP82 : CD2 C-TRP82 : CG C-TRP82 : CB C-TRP82 : CG C-TRP82 : CD1 C-TRP82 : CE2 C-TRP82 : CE2 C-TRP82 : CZ2 C-TRP82 : CZ2 C-TRP82 : CH2 C-TRP82 : CZ3 C-TRP82 : CZ3 C-TRP82 : CB C-HIS 438:CD2 C-HIS 438:CD2 C-GLY 439:CA C-TYR 332:CZ C-TYR 332:CE2 C-ASP 70: CG C-ASP70: CB C-ASP70: CB	3.67 3.79 3.60 3.95 3.96 3.77 3.84 3.88 3.99 3.85 3.86 3.95 3.70 3.68 3.64 3.86 3.70 3.79 3.87 3.66 3.84 3.95 3.69 3.76 3.78 3.76 3.96 3.86	17.5
SW7					C- TRP82: CZ3 C-TRP82: CZ3 C-TRP82: CE3 C-TRP82: CD2 C-TRP82: CZ3 C-TRP82: CZ2 C-TRP82: CE2 C-HIS438: CD2 C-HIS438: CD2 C-GLY439: CA C-GLY439: CA C-GLY115:C C-TRP82:CG C-TRP82:CG C-TRP82:CD1 C-TRP82:CB C-TRP82:CB C-TRP82: CH2 C-ASP70: CB C-ASP70: CB C-ASP70: CG C-TYR 332: CZ C-ALA328: CB C-TRP82: CE3 C-TRP82:CE2 C-TRP82:CZ2 C-TRP82:CD2 C-TRP82:CD2	3.80 3.97 3.94 3.81 3.94 3.92 3.70 3.91 3.91 3.69 3.68 3.85 3.85 3.92 3.64 3.82 3.74 3.86 3.87 3.78 3.78 3.71 3.62 3.63 3.59 3.73 3.88	20.9
SW8	N-GLY115: O	3.94	H-GLU197:OE2 H-GLU197:OE1	3.80 3.96	C-ALA328:CB C-ALA 328:C C-ALA 328:CB C-ALA 328:CA C-TRP430:CZ2 C-TRP430:CE2 C-TRP430:CH2 C-TRP82:CD1 C-TRP82:CD1 C-TRP82:CD1 C-TRP82:CD1	3.9 3.92 3.24 3.75 3.37 3.95 3.61 3.63 3.51 3.90 3.84	1.2

					C-TRP82:CG C-TRP82:CG C-TRP82:CG C-TRP82:CD2 C-TRP82:CD2 C-TRP82: CB C-TRP82: CE3 C-TRP82:CD2 C-TRP82:CE2 C-TRP82:CE3 C-TRP82:CE3 C-TRP82:CE1 C-GLY 116: CA C-GLY 116:CA C-GLY 115: C C-GLY121:CA C-MET 437:CE	3.67 3.48 3.80 3.81 3.60 3.73 3.70 3.95 3.66 3.95 3.76 3.60 3.75 3.50 3.60 3.69 3.90		
SW9	None			H-GLU197:OE1 H-GLU197:OE2 H-TYR 128:OH	2.30 3.33 3.72	C- TRP 430: CZ2 C-TYR 332:CE1 C-ALA 328 : CB C-TYR 332: CZ C-TRP 82: CD1 C-TRP 82:CD1 C-TRP 82: CB C-TRP 82: CD2 C-TRP 82: CD2 C-TRP 82:CD2 C-TRP 82:CE3 C-TRP 82:CE3 C-TRP 82:CE3 C-TRP 82:CZ3 C-TRP 82:CZ3 C-TRP 82: CG C-TRP 82:CG C-TRP 82:CG C-TRP 82:CG C-TRP 82: CE3 C-GLY 115: C C-GLY 116:CA C-GLY 116:CA C-HIS 438: CD2 C-HIS 438: CD2	3.70 3.96 3.77 3.68 3.98 3.94 3.71 3.95 3.65 3.77 3.46 3.54 3.59 3.71 3.40 3.82 3.74 3.75 3.68 3.68 3.89 3.75 3.64 3.47	1.6
SW10	None			H-GLU197:OE1 H-GLU197:OE2 H-GLU197: O H-TYR128: OH H-GLY 115: N	1.99 3.71 3.99 3.59 3.76	C- GLY 116:CA C-GLY 116:CA C-GLY 115:C C-HIS 438: CD2 C-HIS 438: CD2 C-TRP82: CZ3 C-TRP82: CZ3 C-TRP82: CE3 C-TRP82: CE3 C-TRP82: CE3 C-TRP82: CE3 C-TRP82: CE3 C-TRP82: CD2 C-TRP82: CD2 C-TRP82: CD2 C-TRP82: CG C-TRP82: CG C-TRP82: CG C-TRP82: CE2 C-TRP82: CD1 C-TRP82: CD1 C-TRP82: CB C-TRP82: CB C-ALA 328: CB C-ALA 328:CB C-TYR 332: CZ	3.76 3.84 3.63 3.44 3.57 3.63 3.67 3.80 3.50 3.52 3.78 2.59 3.86 3.78 3.69 3.90 3.87 3.80 3.99 3.99 3.92 3.79 3.66 3.95 3.74 3.98 3.70	2.7

SW11	None		None		C-TRP231: CG C-TRP231: CD2 C-TRP231: CD2 C-TRP231: CE3 C-TRP231: CE2 C-TRP321: CG C-LEU286: CD2 C-LEU286: CD2 C-LEU286: C C-PHE329: CZ C-PHE329: CE2 C-PHE398: CZ C-PHE398: CZ C-GLY117: CA C-GLY117: CA C-TRP82: CG C-TRP82: CD1	3.70 3.79 3.64 3.88 3.87 3.66 3.61 3.65 3.93 3.80 3.80 3.89 3.67 3.86 3.71 3.90 3.49	0.504
SW12	O-HIS438: NE2 O-GLY117: N O-TRP82: NE1 O-TRP430:NE1 O-GLY116: N	3.91 3.32 3.11 3.82 3.21	H-HIS438: NE2	3.28	C-ALA328: CB C-TRP231: CE2 C-TRP231: CD2 C-TRP321: CG C-TRP321: CG C-LEU286: CD2 C-LEU286: CD2 C-LEU286: CA C-LEU286: CA C-LEU286: CA C-LEU286: C C-LEU286: C C-GLY117: CA C-GLY117: CA C-GLY117: CA C-PHE398: CZ	3.97 3.73 3.48 3.98 3.77 3.52 3.65 3.98 3.86 3.91 3.96 3.97 3.71 3.90 3.94	0.46
SW13	O-TRP82:NE1	3.24	None		C-TRP82: CE2 C-TRP82: CD2 C-TRP82: CD2 C-TRP83: CG C-TRP82: CD1 C-GLY117: CA C-GLY117: CA C-GLY117: CA C-TRP231: CE2 C-TRP231: CD2 C-TRP231: CE3 C-PHE329: CE2 C-LEU286: CD2 C-LEU286: CD2 C-LEU286: CA	3.87 3.81 3.89 3.63 3.72 3.94 3.80 3.96 3.99 3.68 3.76 3.60 3.94 3.61 3.75	10.25
SW14	None		H-GLY117: N	3.76	C-PHE398: CE2 C-PHE398: CZ C-PHE398: CZ C-TRP231: CZ2 C-TRP238: CE3 C-TRP231: CE2 C-TRP231: CE2 C-TRP231: CD2 C-TRP231: CD2 C-TRP231: CZ C-PHE329: CE2 C-PHE329: CE2 C-PHE329: CE2 C-LEU286: CD2 C-LEU286: CD2 C-LEU286: CG C-GLY117: CA C-GLY117: CA C-GLY116: C	3.93 3.84 3.87 3.98 3.98 3.96 3.83 3.74 3.85 3.87 3.87 3.87 6.84 3.94 3.23 3.28 3.87 3.47 3.68 3.98	0.88

					C-TYR332: CE1 C-TYR332: CE1 C-TYR332: CZ C-TRP82: CB C-TRP82: CB C-TRP82: CG C-TRP83: CG C-TRP82: CD1 C-ALA328: CB C-TRP430: CZ2	3.82 3.76 3.80 3.48 3.62 3.56 3.71 3.78 3.47 3.65	
SW15	O-HIS438: NE2 O-TRP82: NE1 O-TRP82: NE 1	3.98 3.16 3.69	None		C-TRP231: CE3 C-TRP231: CD2 C-TRP231: CE2 C-TRP231: CG C-LEU286: CD2 C-LEU286: CD2 C-LEU286: CD2 C-LEU286: CA C-LEU268: C C-PHE329: CE2 C-PHE329: CE2 C-TRP82: CD1 C-TRP82: CG	3.80 3.58 3.81 3.97 3.47 3.91 3.92 3.68 3.87 3.74 3.84 3.88 3.86	0.56
SW16	None		H-ALA328: O H-TYR332: OH H-SER198: OG H-HIS438: NE2	3.33 3.21 2.83 2.58	C-LEU286: CD2 C-LEU286: CD2 C-LEU286: CA C-LEU286: C C-TRP231: CD2 C-TRP231: CD2 C-TRP231: CG C-TRP231: CZ C-PHE398: CZ C-GLY117: CA C-GLY117: CA C-GLT116: C C-GLY116: CA C-HIS438: CD2 C-ALA328: CB C-TRP82: CE2 C-TRP82: CD2 C-TRP82: CD1	3.78 3.45 3.83 3.80 3.71 3.69 3.71 3.75 3.82 3.64 3.94 3.80 3.54 3.68 3.67 3.73 3.74	0.4
SW17	None		None		C-TRP82: CZ3 C-TRP82: CE3 C-TRP82: CD2 C-TRP82: CG C-TRP82: CB C-TRP82: CB C-GLU197: CD C-HIS438: CD2 C-GLY116: CA C-ALA227: CB C-ALA227: CB C-ALA227: CB C-ALA227: CB C-ALA227: CA	3.77 3.48 3.81 3.77 3.47 3.68 3.87 3.80 3.73 3.60 3.77 3.90 3.74 3.90	2.52
SW18	O-THR523: N	3.45	None		C-ASP304: CB C-ASP304: CB C-VAL233: CG2 C-VAL233: CB C-PRO303: CG C-PHE227: CD2 C-PHE227: CE2 C-LEU307: CD2 C-ASN228: CA C-ASN228: CA C-ASN228: CB C-ASP304: CA	3.61 3.69 3.90 3.83 3.73 3.71 3.96 3.86 3.60 3.84 3.74 3.88	0.078

					C-ASP304: CB 3.70 C-PRO230: CA 3.68 C-PRO230: CD 3.32 C-PRO230: CD 3.84 C-PRO230: CG 3.71 C-PRO230: CB 3.83 C-PRO230: CB 3.93 C-TYR396: CD1 3.77 C-TYR396: CE1 3.92 C-TYR396: CE1 3.95 C-TRP522: CB 3.92 C-PRO401: CG 3.71 C-PRO401: CG 3.64 C-PRO527: CG 3.77	
SW19	O-GLY116: N O-GLY116: N O-HIS438: NE2	3.34 3.30 3.89	None		C- PHE329: CZ 3.99 C-HIS438: CD2 3.60 C-HIS438: CD2 3.59 C-HIS438: CD2 3.72 C-HIS438: CD2 3.86 C-HIS438:CD2 3.88 C-HIS348: CD2 3.75 C-GLY116: CA 3.94 C-GLY116: C 3.54 C-GLY116: C 3.85 C-GLY117: CA 3.77 C-GLY117: CA 3.67 C-GLY117: CA 3.65 C-TRP82: CD1 3.97 C-TRP82: CE2 3.80	0.011
SW20	None		None		C- TRP231: CD2 3.72 C-TRP231: CE2 3.92 C-TRP231: CE3 3.91 C-GLY117: CA 3.78 C-GLY116: C 3.96 C-GLY116: C 3.79 C-LUE286: CD2 3.94 C-GLN119: CB 3.99 C-THR120: CG2 3.82 C-THR120: CG2 3.97 C-TYR332: CD1 3.84 C-TYR332: CE1 3.74 C-TYR332: CZ 3.96 C-TYR332: CE1 3.92 C-TYR332: CZ 3.93 C-ALA328: CB 3.65 C-TYR332: CE1 3.58 C-TRP 430: CH2 3.80 C-TRP 430: CZ2 3.46 C-TRP 430: CH2 3.63 C-TRP82: CD2 3.96 C-TRP82: CG 3.79 C-TRP82: CD1 3.79 C-TRP82: CG 3.80	2.20
SW21	None		None		C- TYR440: CE1 3.78 C-TRP430: CE2 3.86 C-TRP430: CZ2 3.73 C-PHE329: CE2 3.92 C-PHE329: CE2 3.61 C-PHE329: CE2 3.61 C-GLY116: C 3.85 C-GLY117: CA 3.87 C-GLY117: CA 3.90 C-THR120: CG2 3.75 C-THR120: CG2 3.87 C-ILE69: C 3.94 C-ILE69: C 3.51 C-ASP70: CB 3.80	4.42

					C-ASN68: C C-MET437: CE	3.85 3.68	
SW22	None		None		C-PHE329: CE2 C-PHE329: CE2 C-PHE329: CD2 C-TRP82: CD2 C-TRP82: CE2 C-TRP82: CE2 C-TRP82: CG C-TRP82: CD1 C-TYR332: CD1 C-TYR332: CE1 C-TYR332: CE1 C-TYR332: CG C-TYR332: CD2 C-TYR332: CE2 C-TYR332: CE2 C-TYR332: CD2 C-TYR332: CD1	3.92 3.89 3.77 3.75 3.77 3.93 3.65 3.60 3.76 3.76 3.91 3.81 3.73 3.86 3.71 3.98 3.98	1.40
SW23	N-THR120: OG	3.40	None		C-TRP82: CG C-TRP82: CE2 C-TRP82: CE2 C-TRP82: CD2 C-TRP82: CD2 C-TRP82: CH2 C-TRP82: CZ2 C-TRP82: CZ2 C-HIS438: CD2 C-THR120: CG2 C-THR120: CG2 C-ASP70: CA C-ASP70: CB C-ILE69: C C-ASN68: CB C-ASN68: CB	3.90 3.60 3.65 3.69 3.55 3.91 3.84 3.81 3.88 3.58 3.70 3.90 3.73 3.93 3.43 3.81	0.51
SW24	N-PRO285: O	3.45	H- TRP82: NE1	3.04	C-TRP82: CE3 C-PHE329: CE2 C-TRP82: CD2 C-TRP82: CE3 C-TYR332: CE1 C-GLN119: CB C-THR120: CG C-GLY115: C C-GLY115: C C-TRP82: CG C-TRP82: CD1 C-TRP82: CD1 C-PHE329: CD2 C-TRP82: CG C-TRP82: CD2 C-TRP82: CD2 C-TRP82: CE2 C-TRP82: CE2 C-TRP82: CZ2 C-ALA328: CB C-TRP82: CD2 C-PHE329: CE2 C-PHE329: CE2 C-PHE329: CE2	3.79 3.98 3.82 3.80 3.56 3.88 3.63 3.83 3.78 3.66 3.63 3.76 3.85 3.57 3.86 3.99 3.98 3.66 3.99 3.89 3.85 3.51 3.78 3.53	0.51
SW25	O-PRO285: N N-GLY116: O NTHR120:OG1	3.84 3.73 3.41	H-THR284: O	3.46	C-ALA328: CB C-ALA328: CB C-ALA328: CB C-ILE356: CD1 C-TYR282: CZ	3.85 3.94 3.43 3.84 3.987	0.55

	N-THR284: O	3.29			C-TYR282: CE2 C-GLY283: C C-PRO285: CA C-PRO285: CA C-THR284: C C-PHE329: CE2 C-HIS438: CD2 C-GLY116: C C-PRO285: C C-THR284: C C-ILE356:CD1	3.63 3.90 3.73 3.73 3.80 3.84 3.63 3.83 3.90 3.93 3.89	
SW26	N-GLY116: O N-PRO285: O	3.75 3.45	H-TRP82:NE1	3.03	C-GLN119: CB C-GLN119: CB C-THR120: CG C-GLY116: CA C-GLY116: C C-GLY115: C C-GLY116: CA C-TRP82:CD2 C-TRP82: CD2 C-TRP82: CD2 C-TRP82: CD2 C-TRP82: CD1 C-TRP82: CE2 C-TRP82: CE2 C-GLN119: CG C-GLN119: CB C-ASN68: CE C-ALA328: CB C-GLY116: C C-TYR332: CZ C-TYR332: CE1 C-TYR332: CD1 C-PHE329: CZ C-PHE329: CE2 C-PHE329: CE2 C-PHE329: CD2 C-PHE329: CD2 C-PHE329: CD2 C-TRP82: CB C-TRP82: CB C-TRP82: CG C-TRP82: CG C-TRP82: CG C-TRP82: CD1 C-TRP82: CE3 C-TRP82:CE3	3.58 3.77 3.61 3.87 3.82 3.78 3.98 3.90 3.80 3.81 3.62 3.68 3.99 3.80 3.82 3.56 3.88 3.64 3.99 3.52 3.74 3.82 3.78 3.92 3.84 3.79 3.98 3.68 3.93 3.61 3.58 3.88 3.55 3.80 3.85	0.5
Donepezil	O-GLY116: N O-TRP82:NE1 O-GLY116:N	3.97 3.75 3.97	None		C-TYR440:CE1 C-TRP430:CE2 C-TRP430:CZ2 C-PHE398:CZ C-PHE329:CE2 C-PHE329:CE2 C-LEU286:CD2 C-LEU286:CD2 C-TRP231:CD2 C-TRP231:CD2 C-TRP231:CE3	3.39 3.74 3.42 3.70 3.74 3.59 3.55 3.92 3.69 3.67 3.76	14.8

Rivastigmine	O-HIS438:NE2 O-GLY116:N O-GLY117:N N-SER198:OG	3.56 3.81 3.62 3.56	None		C-TRP231:CZ3 C-TRP231:CE3 C-GLY117:CA C-TRP231:CD2 C-TRP231:CE3 C-VAL288:CG2 C-TRP231:CG C-TRP231:CB C-LEU286:CD2 C-LEU286:CD2 C-SER198:CB C-HIS438:CD2 C-HIS438:CD2 C-TRP82:CD1 C-TRP82:CE2	3.82 3.815 3.40 3.57 3.77 3.67 3.56 3.81 3.72 3.78 3.73 3.96 3.86 3.96 3.81	2.0
--------------	---	------------------------------	------	--	--	---	-----

4.4 Lead Compound Identification

The binding interactions of all ligands have been analyzed. Five compounds have been identified as the most active from the set of 26 ligands. These ligands are SW12, SW16, SW18, SW19, SW23 and SW26. These ligands have shown strong ionic, hydrogen and hydrophobic interactions with the target protein than the rest of ligands. These five active ligands along with their interactions, binding affinities and IC₅₀ values are shown in Table 4.5. From the table it is clear that the number of ionic bonds in SW12, SW16, SW18, SW19, SW23 and SW26 are 5, 0, 1, 3, 1 and 2 respectively, number of hydrogen bonds in SW12, SW16, SW18, SW19 and SW26 are 1, 4, 0, 0, 0 and 1 respectively and lastly number of hydrophobic bonds in SW12, SW16, SW18, SW19 and SW26 are 15, 17, 26, 15, 16 and 35.

But the binding affinity of the following compounds was least in the data set SW16, SW19, SW23 and SW26 i.e. -8.6, -10.1, -11.4 and -10.5 Kcal/mol respectively reducing the hits to two i.e. SW19 and SW23. Although IC₅₀ value have 30% role in identifying the lead compound but when the IC₅₀ value of SW19 and SW23 were compared and a remarkable difference was observed as the IC₅₀ value of SW19 was 0.011 μ M and that of SW23 is 0.51 μ M.

All these calculations led to the conclusion that SW19 was the lead compound having binding affinity -10.0 Kcal/mol (2nd lowest binding affinity), IC₅₀ value 0.011 μ M (lowest IC₅₀ value) and 3 ionic and 15 hydrophobic interaction as shown in Table 4.4a and Table 4.4b.

The interactions shown in figure 4.15 highlight the important amino acids of the target protein pocket and the atoms of the ligands. Figure as well shows the bonding distances clearly. In case of ionic interactions the O of lead compound form ionic bonds with N of GLY116 at a distance of 3.34Å, of GLY116 at a distance of 3.30Å and of HIS438 at a distance of 3.89Å.

In hydrophobic interactions the C of PHE329 at a distance of 3.99, of HIS438 at distances of 3.60, 3.59, 3.72, 3.86, 3.88 and 3.75, of GLY116 at a distance of 3.94, 3.54 and 3.85, of GLY117 at a distance of 3.77, 3.67 and 3.65, of TRP82 at a distance of 3.97, 3.83 and 3.80, of TRP430 at a distance of 3.83 and 3.34, of MET437 at a distance of 3.96, of TYR332 at a distance of 3.58 and 3.77, of ALA328 at a distance of 3.74 and of PRO285 at a distance of 3.76 n different conformations are identified with the carbons of the lead.

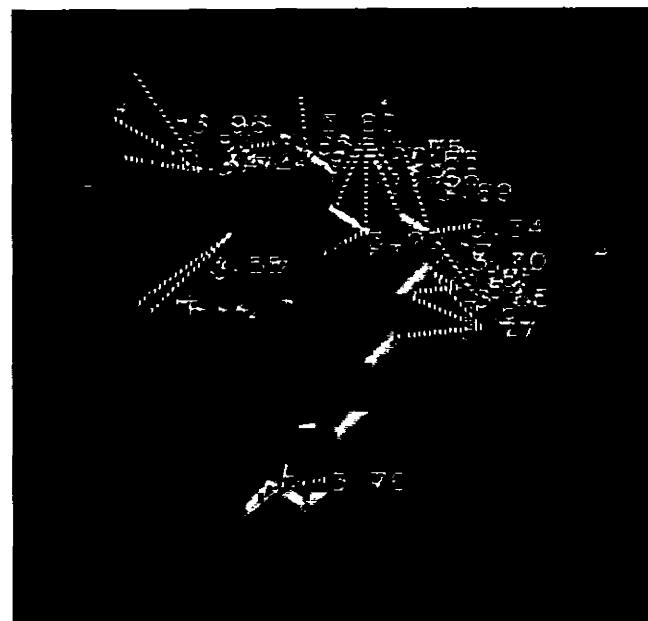
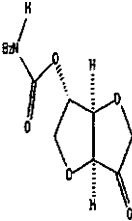
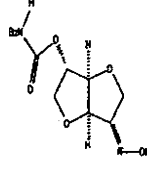
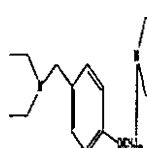


Figure 4.14: Binding interactions of SW19 (Lead Compound) with 1POI

Table4.5: Active Ligands their interactions, IC50 values and Binding Affinity

Ligand	Structure	Ionic Bonding	Hydrogen Bonding	Hydrophobic Interactions	IC ₅₀	Affinity (kcal/mol)
SW12		O-HIS438:NE2(3.91) O-GLY117: N (3.32) O-TRP82:NE1 (3.11) O-TRP430:NE1(3.82) O-GLY116: N (3.21)	H-HIS438:NE2(3.28)	C-ALA328: CB (3.97) C-TRP231: CE2 (3.73) C-TRP231: CD2 (3.48) C-TRP321: CG (3.98) C-TRP321: CG (3.77) C-LEU286: CD2 (3.52) C-LEU286: CD2 (3.65) C-LEU286: CA (3.98) C-LEU286: CA (3.86) C-LEU286: C (3.91) C-LEU286: C (3.96) C-GLY117: CA (3.97) C-GLY117: CA (3.71) C-GLY117: CA (3.90) C-PHE398: CZ (3.94)	0.46	-8.3
SW16		None	H-ALA328: O (3.33) H-TYR332:OH(3.21) H-SER198:OG(2.83) H-HIS438:NE2(3.58)	C-LEU286: CD2 (3.78) C-LEU286:CD2(3.45) C-LEU286: CA(3.83) C-LEU286: C (3.80) C-TRP231: CD2(3.71) C-TRP231: CD2 (3.69) C-TRP231: CG (3.71) C-PHE398: CZ (3.75) C-GLY117: CA (3.82) C-GLY117: CA(3.64) C-GLT116: C (3.94) C-GLY116: CA (3.80) C-HIS438: CD2 (3.54) C-ALA328: CB (3.68) C-TRP82: CE2 (3.67) C-TRP82: CD2(3.73) C-TRP82: CD1 (3.74)	0.4	-8.6
SW18		O-THR532:N(3.45)	None	C-ASP304: CB (3.61) C-ASP304: CB (3.69) C-VAL233: CG2 (3.90) C-VAL233: CB (3.83) C-PRO303: CG (3.73) C-PHE227: CD2 (3.71) C-PHE227: CE2 (3.96) C-LEU307: CD2 (3.86) C-ASN228: CA (3.60) C-ASN228: CA (3.84) C-ASN228: CB (3.74) C-ASP304: CA (3.88) C-ASP304: CB (3.70) C-PRO230: CA (3.68) C-PRO230: CD (3.32) C-PRO230: CD (3.84) C-PRO230: CG (3.71) C-PRO230:CB (3.83) C-PRO230: CB (3.93) C-TYR396: CD1 (3.77) C-TYR396: CE1 (3.92) C-TYR396: CE1 (3.95) C-TRP522: CB (3.92) C-PRO401: CG (3.71)	0.078	-6.6

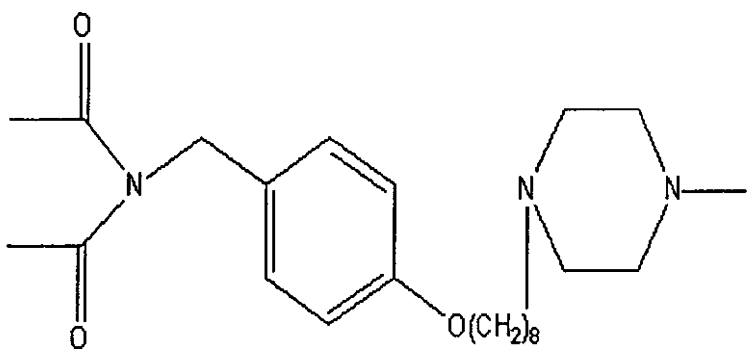
				C-PRO401: CG (3.64) C-PRO527: CG (3.77)		
SW19		O-GLY116:N (3.34) O-GLY116:N (3.30) OHIS438:NE2(3.98)	None	C- PHE329: CZ (3.99) C-HIS438: CD2 (3.60) C-HIS438: CD2 (3.59) C-HIS438: CD2 (3.72) C-HIS438: CD2 (3.86) C-HIS438:CD2 (3.88) C-HIS348: CD2 (3.75) C-GLY116: CA (3.94) C-GLY116: C (3.54) C-GLY116: C (3.85) C-GLY117: CA (3.77) C-GLY117: CA (3.67) C-GLY117: CA (3.65) C-TRP82: CD1 (3.97) C-TRP82: CE2 (3.80) C-TRP430:CE2(3.83) C-TRP82:CD1(3.83) C-MAT437:CE(3.96) C-TYR332:CE1(3.58) C-TYR332:CZ(3.77) C-PRO285:C (3.76) C-TRP430:CZ2(3.34) C-ALA328:CB(3.74)	0.011	-10.1
SW23		N-THR120:OG (3.40)	None	C- TRP82: CG (3.90) C-TRP82: CE2 (3.60) C-TRP82: CE2 (3.65) C-TRP82: CD2 (3.69) C-TRP82: CD2 (3.55) C-TRP82: CH2 (3.91) C-TRP82: CZ2 (3.84) C-TRP82: CZ2 (3.81) C-HIS438: CD2 (3.88) C-THR120: CG2 (3.58) C-THR120: CG2 (3.70) C-ASP70: CA (3.90) C-ASP70: CB (3.73) C-ILE69: C (3.93) C-ASN68: CB (3.43) C-ASN68: CB (3.81)	0.51	-11.4

SW26		N-GLY116: O (3.75) N-PRO285: O (3.45)	H-TRP82:NE1 (3.03)	C-GLN119: CB (3.58) C-GLN119: CB (3.77) C-THR120: CG (3.61) C-GLY116: CA (3.87) C-GLY116: C (3.82) C-GLY115: C (3.78) C-GLY116: CA (3.98) C-TRP82:CD2 (3.90) C-TRP82: CD2 (3.80) C-TRP82: CD2 (3.81) C-TRP82:CD1 (3.62) C-TRP82: CE2 (3.68) C-TRP82: CE2 (3.99) C-GLN119: CG (3.80) C-GLN119: CB (3.82) C-ASN68: CE (3.56) C-ALA328: CB (3.88) C-GLY116:C (3.64) C-TYR332: CZ (3.99) C-TYR332:CE1 (3.52) C-TYR332:CD1(3.74) C-PHE329: CZ (3.82) C-PHE329: CE2(3.78) C-PHE329: CE2(3.92) C-PHE329: CD2(3.84) C-PHE329: CD2(3.79) C-PHE329: CD2(3.98) C-TRP82: CB (3.68) C-TRP82: CB (3.93) C-TRP82: CG (3.61) C-TRP82: CG (3.58) C-TRP82: CG (3.88) C-TRP82: CD1(3.55) C-TRP82: CE3(3.80) C-TRP82: CE3 (3.85)	-9.8	0.5
------	--	--	--------------------	--	------	-----

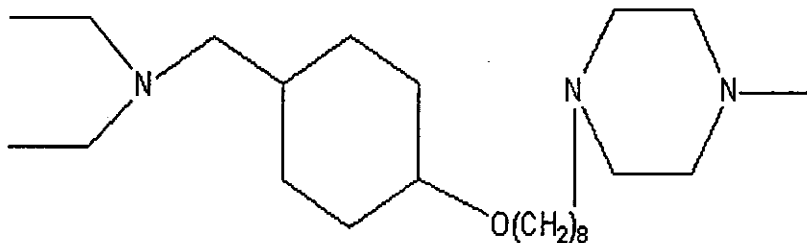
4.5 Analogue Designing

On the basis of binding interactions, binding affinity and IC_{50} value compound SW19 had been considered as the lead compound in this study. Analogues were made of this compound in order to get most active compound to use as BChE inhibitors.

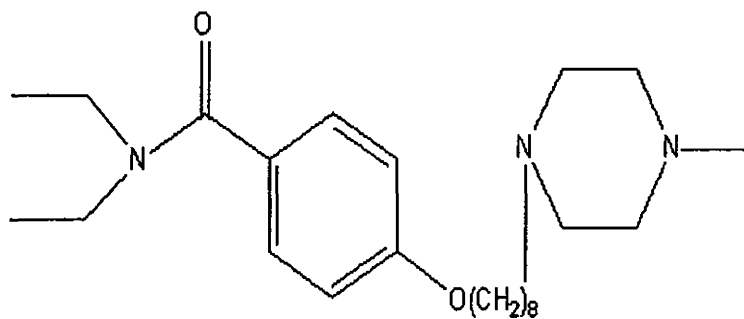
Four analogues of the Lead compound have been designed after detailed study and analysis. Keeping in view the chemical structure of Lead i.e. the hydrophobic features, HBDs, HBAs the analogues have been designed. The analogues of the Lead have been shown in Figure 4.15.

**Analogue 1 (Amide Formation)**

(4-{{8-(3-methyl-1,3-diazinan-1-yl) octyl} oxy} phenyl) methanamine

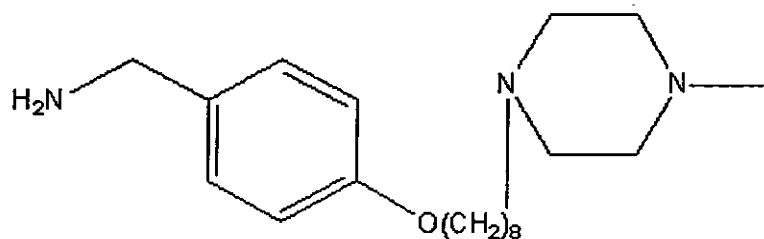
**Analogue 2 (Ring Reduction)**

Diacetyl [(4-{{8-(3-methyl-1,3-diazinan-1-yl) octyl} oxy} cyclohexyl) methyl] amine



Analogue 3 (Oxidation)

N, N-diacetyl- 4-{{8-(3-methyl-1, 3-diazinan-1-yl) octyl} oxy} benzamide



Analogue 4 (Amine Formation)

N-acetyl-N-[(4-{{8-(3-methyl-1, 3-diazinan-1-yl) octyl} oxy} phenyl) methyl] acetamide

Figure 4.15: Analogues of the Lead Compound and their IUPAC names

The analogues have been developed by the introduction or elimination of various functional groups. The first analogue of the lead has been made by replacing NH-CH-CH₂ with NH-CO-CH₂. In this way the hydrophobic character has been decreased in order to observe the impact of decreased hydrophobicity. The hydrophobic character has been increased by replacing the cyclic benzene with cyclo-hexane. In case of third analogue the hydrophobicity has been decreased by the introduction of CO instead of CH₂. With increase in hydrophilicity and hydrophobicity by the introduction of NH₂ instead of CH₃-CH₂-N-CH₂-CH₃, the fourth analogue has been made.

4.6 Docking and Interactions of Analogues with the Target Protein

Docking of the analogues through Autodock Vina has been performed in order to get the active conformations of the analogues. The interactions of the active conformations of each of the analogue bound into the active site of protein have been obtained using VMD.

The important interactions found in the analogue like the Lead are again ionic, hydrogen and hydrophobic interactions. The interactions in the analogue proved to be stronger than the lead due to which they show positive signs towards their being active. The interactions of each analogue and the target protein have been found by taking in account the amino acids with in 5 Å of the active site of target protein. Each amino acid of the active site was noted and the interactions of them with the ligand have been identified. The interactions of the analogue with the protein have been shown in Table

4.6. The binding interactions of each analogue bound in the active site of the protein have been shown in Figures 4.16, 4.17, 4.18 and 4.19.

Figure 4.16 shows the binding interactions of the first analogue within the active site of the target protein. Ionic interactions exist between N of GLY117 at a distance of 3.41 Å, of GLY116 at a distance of 3.80 Å, of HIS438 at a distance of 3.90 Å and of TRP82 at a distance of 3.20 Å with the O of analogue 1. Analogue 1 shows no hydrogen bonding. The hydrophobic interactions have been identified between C of ASN 68 at a distance of 3.76 Å, of PRO285 at a distance of 3.94 Å, of LEU286 at distance of 3.90 Å and 3.85 Å, of SER287 at a distance of 3.94 Å, of ALA328 at distance of 3.85 Å and 3.45 Å, of PHE329 at distance of 3.89 Å and 3.68 Å, of GLY117 at distance of 3.82 Å and 3.72 Å, of TRP82 at a distance of 3.86 Å, of MET437 at a distance of 3.08 Å, of HIS438 at distances of 3.88, 3.83 and 3.97 and of TRP430 at distance of 3.42 Å, 3.93 Å, 3.40 Å and 3.88 Å in different conformations with the C of analogue 1.

The binding interactions of analogue 2 with the target protein are shown in Figure 4.17. Among the interactions, ionic bonding has been identified between the N of GLY116 at a distance of 3.17 Å, of GLY117 at a distance of 3.93 Å, of HIS438 at a distance of 3.88 Å and O of SER287 at a distance of 3.58 Å with the O and N of analogue 2 respectively. No hydrogen interaction has been observed in the closer vicinity of the analogue 2. The hydrophobic interactions include carbon atoms from the amino acids, like TRP430 at a distance of 3.61 Å, of ALA328 at distance of 3.75 Å, 3.70 Å and 3.91 Å, of PHE329 at distance of 3.72 Å, 3.78 Å, 3.87 Å and 3.76 Å, of TRP82 at distance of 3.74 Å, 3.83 Å, 3.74 Å, 3.80 Å, 3.66 Å, 3.87 Å, 3.87 Å, of GLY116 at distance of 3.71 Å and

3.95 Å, of GLY117 at a distance of 3.86 Å, of SER198 at a distance of 3.96 Å, of TRP231 at a distance of 3.78 Å, 3.83 Å, 3.92 Å, 3.83 Å, of GLN119 at distances of 3.91 and 3.91 Å, of LEU286 at distance of 3.68 Å, 3.62 Å, 3.94 Å, 3.72 Å and 3.85 Å in different conformations with the C of analogue 2.

Figure 4.18 depicts the binding interactions of analogue 3 with the target protein. The 2 Ionic interactions have been observed between N of TRP82 at a distance of 3.26 Å and of GLY117 at a distance of 3.23 Å with O of analogue 3. No hydrogen bonding has been identified in case of analogue 3. The 19 closely identified hydrophobic interactions contain carbons belonging to amino acids such as ASN68 at a distance of 3.52 Å, SER287 at distances of 3.86 Å and 3.86 Å, LEU286 at distance of 3.76 Å and 3.92 Å, GLY117 at distances of 3.66 Å and 3.66 Å, GLY116 at a distance of 3.97 Å, TRP82 at a distance of 3.81 Å, TRP430 at a distance of 3.66 Å, TYR332 at a distance of 3.71 Å, HIS438 at distances of 3.83 Å and 3.93 Å, ALA at distances of 3.87 Å, 3.59 Å and 3.50 Å and to PHE329 at distances of 3.38 Å, 3.74 Å and 3.75 Å in different conformations with the C of analogue 3.

Figure 4.19 shows the binding interactions of the ligand fourth analogue and the target protein. The interactions include 3 ionic interactions between O of GLY115 and of TYR128 at a distance of 3.19 Å and 3.10 Å respectively with N and of N of TRP82 at a distance of 3.56 with O of analogue 4. 6 hydrogen bonds between O of GLY115 at distances of 3.13 Å and 2.39 Å, of TYR128 at a distance of 2.78 Å and between N of GLY115 at a distance of 3.56 Å, of GLY116 at distances of 3.56 Å and 3.57 Å with the H of the analogue 4. The hydrophobic interactions exist between C of HIS438 at a distance

of 3.72 Å, of GLY439 at distance of 3.89 Å and 3.59 Å, of TRP82 at a distance of 3.70 Å, 3.86 Å, 3.79 Å, 3.62 Å, 3.98 Å, 3.88 Å, 3.82 Å, 3.88 Å, 3.66 Å, 3.74 Å, 3.98 Å, 3.69 Å, 3.60 Å, 3.76 Å, 3.93 Å, 3.82 Å, 3.88 Å and 3.59 Å, of GLY115 at a distance of 3.63 Å, of GLY116 at distance of 3.57 Å and 3.87 Å, of ALA328 Å at a distance of 3.68 Å, of TYR 332 at a distance of 3.95 Å, 3.84 Å, 3.93 Å, 3.58 Å, 3.65 Å and 3.64 Å and of PHE 329 at a distance of 3.65 Å with the C of analogue 4.

Analogues like lead compound showed the binding interactions which are closer to the standard Rivastigmine, so the designed analogues are also active like the Lead.

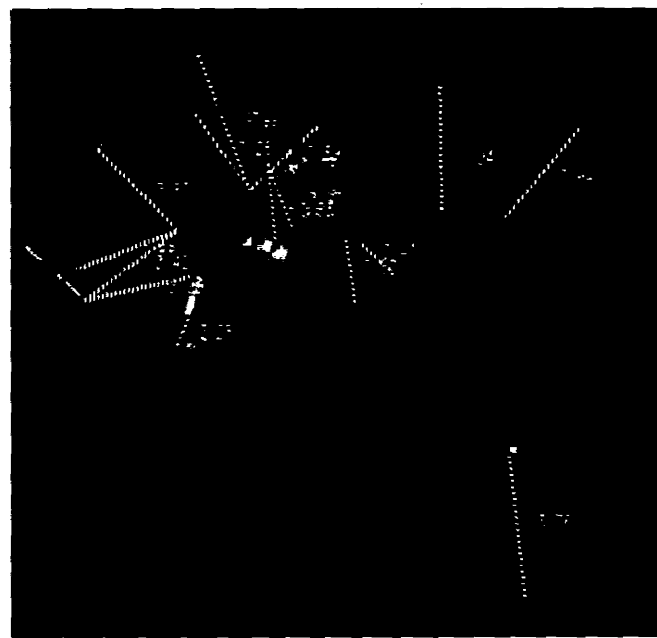


Figure 4.16: Binding interactions of 1st Analogue with 1P0I

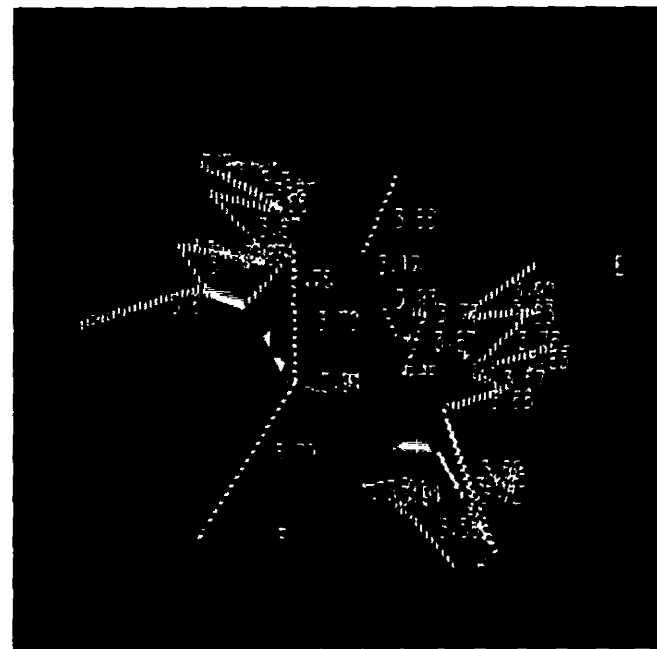


Figure 4.17: Binding interactions of 2nd Analogue with 1P0I

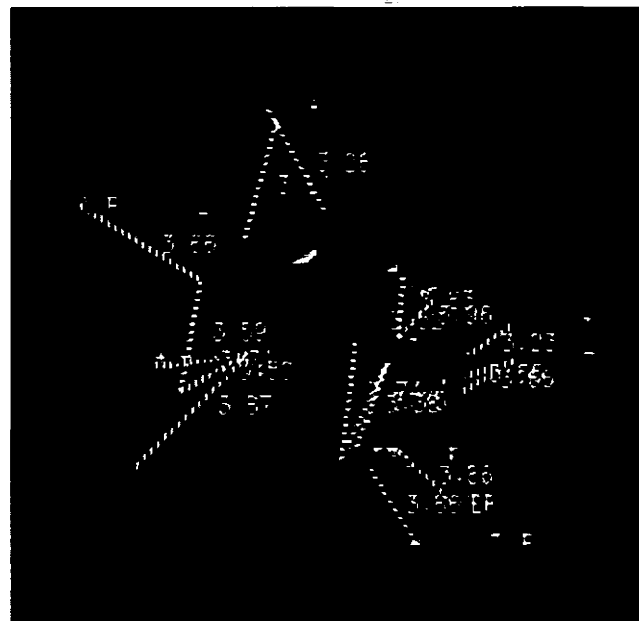


Figure 4.18: Binding interactions of 3rd Analogue with 1P0I

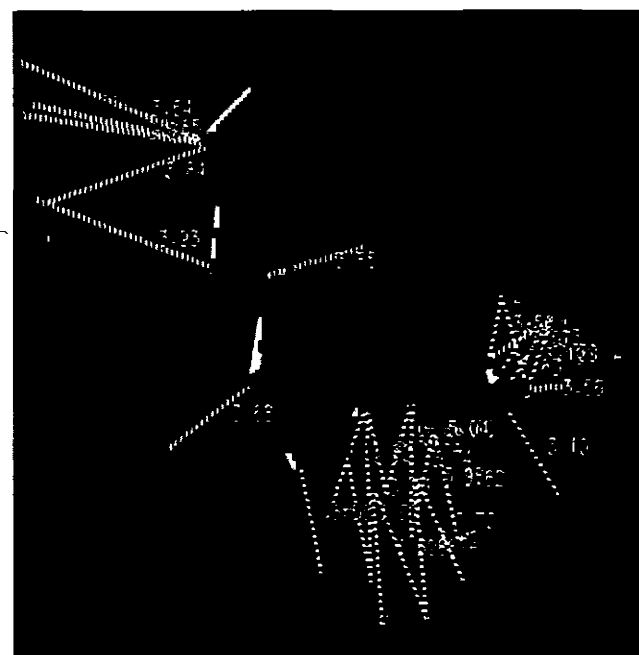
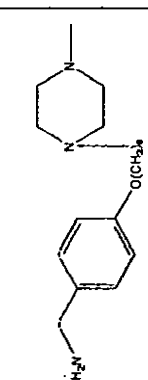


Figure 4.19: Binding interactions of 4th Analogue with 1P0I

Table 4.6: Binding Interactions of Analogue with the target protein.

Comp.	Structure	Ionic Interactions	Hydrogen Bonds	Hydrophobic Interactions	Binding Affinity
Amide Formation		O-GLY117:N(3.41) O-GLY116:N(3.80) O-HIS438:NE2(3.90) O-TRP82:NE(3.20)	None	C-ASN68:CB(3.76) C-PRO285:C(3.94) C-LEU286:CA(3.90) C-LEU286:C(3.85) C-SER287:CB(3.94) C-ALA328:C(3.85) C-ALA328:CB(3.45) C-PHE329:CE2(3.89) C-PHE329:CE3(3.68) C-GLY116:C(3.82) C-GLY117:CA(3.72) C-TRP82:CD1(3.860 C-TRP430:CZ2(3.42) C-TRP430:CZ2(3.93) C-TRP430:CH2(3.40) C-TRP430:CE2(3.88) C-MET437:CE(3.80) C-HIS438:CD2(3.88) C-HIS438:CD2(3.83) C-HIS438:CD2(3.97)	-10.7
Ring Reduction		N-SER287:O(3.58) O-HIS438:NE2(3.88) O-GLY116:N(3.17) O-GLY117:N(3.93)	None	C-TRP430:CZ2(3.61) C-ALA238:CB(3.75) C-ALA238:CB(3.70) C-ALA238:C(3.91) C-PHE329:CE2(3.72) C-PHE329:CD2(3.78) C-PHE329:CE2(3.87) C-PHE329:CZ(3.76) C-TRP82:CD1(3.74) C-TRP82:CD1(3.83) C-TRP82:CG(3.74) C-TRP82:CE2(3.80) C-TRP82:CD2(3.66) C-TRP82:CD2(3.87) C-TRP82:CE3(3.87) C-GLY116:CA(3.71) C-GLY116:CA(3.95) C-GLY117:CA(3.86) C-SER198:CB(3.96) C-PHE398:CZ(3.85) C-TRP231:CD2(3.78) C-TRP231:CD2(3.83) C-TRP231:CE2(3.92) C-TRP231:CG(3.83) C-GLN119:CB(3.91) C-GLN119:CG(3.91) C-LEU286:CD2(3.57) C-LEU286:CD2(3.68) C-LEU286:CA(3.62) C-LEU286:CA(3.94) C-LEU286:C(3.72) C-LEU286:C(3.85) C-TRY332:CE1(3.79)	-7.4

Oxidation	 <p>OTRP82:NE1(3.26) O-GLY117:N(3.23)</p>	None	C-ASN68:CB(3.52) C-SER287:C(3.86) C-SER287:CB(3.86) C-LEU286:C(3.76) C-LEU286:CA(3.92) C-GLY117:CA(3.66) C-GLY117:CA(3.66) C-GLY116:CA(3.97) C-TRP82:CD1(3.81) C-TRP430:CZ2(3.66) C-TYR332:CE1(3.71) C-ALA328:C(3.87) C-ALA328:CB(3.59) C-ALA328:CB(3.50) C-PHE329:CE2(3.38) C-PHE329:CE2(3.74) C-PHE329:CZ(3.75) C-HIS438:CD2(3.96) C-HIS438:CD2(3.93)	-10.2
Amine Formation	 <p>N-GLY115: O(3.19) N-TYR128:OH(3.10) O-TRP82:NE1(3.56)</p>	H-GLY115: O(3.13) H-GLY115: O(2.39) H-GLY116:N(3.56) H-GLY115:N(3.56) H- TYR128:OH(2.78) H-GLY116:N(3.57)	C- HIS438:CD2(3.72) C- GLY439:CA(3.89) C- GLY439:CA(3.59) C- TRP82:CZ3(3.70) C- TRP82:CZ3(3.86) C- TRP82:CE3(3.79) C- TRP83:CE3(3.62) C- TRP82:CE3(3.98) C- TRP82:CH2(3.88) C- TRP82:CH2(3.82) C- TRP82:CD2(3.88) C- TRP82:CD2(3.66) C- TRP82:CD2(3.74) C- TRP82:CD2(3.98) C- TRP82:CZ2(3.69) C- TRP82:CE2(3.60) C- TRP82:CE2(3.76) C- TRP82:CE2(3.93) C- TRP82:CD1(3.82) C- TRP82:CG(3.88) C- TRP82:CG(3.59) C- GLY115:C(3.63) C- GLY116:C(3.57) C- GLY116:C(3.87) C- ALA328:CB(3.68) C- TYR332:CZ(3.95) C- TYR332:CG(3.84) C- TYR332:CE1(3.58) C- TYR332:CD2(3.64) C- TYR332:CE2(3.65) C- TYR332:CD1(3.93) C- PHE329:CE2(3.65)	-7.4

4.7 Quantitative Structure Activity Relationship (QSAR)

QSAR model was built for describing how some descriptors were directly or indirectly related to the biological activity i.e. pharmacokinetics of a compound. A set of descriptor was chosen and this set was then applied to data set. These descriptors were assumed to influence whether a given compound will succeed or fail in binding to the target protein (Barrat et al., 1995). The data of 27 compounds was chosen for QSAR studies. The descriptors chosen for QSAR studies of the data of the ligands include partition coefficient i.e. Log P, Highest occupied molecular orbital (HOMO), Lowest unoccupied molecular orbital (LUMO), Molar refractivity, Total binding energy of the ligand(TE), Heat of formation(HF) and Critical volume (CV). These descriptors were calculated using Hyper Chem and Chem Draw.

Table 4.7: QSAR Descriptors of Ligands

IC50	LogP	E _{Homo}	E _{Lomo}	MR (cm ³ /mol)	ETotal (kcal/mol)	EFormation (kcal/mol)	CV (cm ³ /mol)
10.10	3.26	-1.03918	0.924167	91.27	-70706.86992	3375.40198	746.76
20.27	2.28	-0.29049	0.951345	95.45	-69077.25215	9106.334656	747.69
1.40	3.4	-8.99708	0.158148	95.87	-89336.62128	188.7725522	995.92
0.71	3.82	-8.99794	0.18974	100.47	-89798.85826	169.6575099	1043.33
9.73	2.84	-9.0274	0.124194	104.74	-84866.76925	203.0614264	1059.95
2.74	3.76	-8.93088	0.232264	98.15	-85830.67732	401.8734203	1005.95
1.54	3.82	-8.74162	0.218668	100.47	-90785.35426	183.1615072	1042.12
0.67	4.24	-8.73844	0.221426	105.07	-89230.56846	181.0692503	1075.28
1.78	5.15	-8.68176	0.23022	111.95	-94225.29531	336.6212368	1135.4
1.90	5.99	-8.68176	0.230048	121.15	-95121.89916	326.2612639	1233.12
1.28	4.24	-8.62111	0.309906	105.07	-90228.04406	183.5936399	1088.55
1.66	4.6	-8.70507	0.204516	107.35	-94682.81344	435.9811703	1056.6
1.34	5.57	-8.7098	0.199298	116.55	-96577.33033	427.7081553	1143.36
0.23	6.4	-8.71003	0.198814	125.74	-98474.00664	417.2757165	1240.74
0.015	5.07	-8.96335	0.194380	114.27	-99130.13088	167.7507035	1209.36
0.0073	5.49	-8.95737	0.200304	118.87	-99593.84263	147.1608826	1255.18
0.011	4.51	-8.97695	0.179734	123.13	-98660.1234	182.1950184	1272.54
0.014	4.85	-8.97608	0.180621	127.93	-102106.2852	179.1552059	1318.59
0.048	5.43	-9.00658	0.185247	116.55	-100713.9589	291.0795518	1247.64
0.0091	6.4	-9.00936	0.185253	125.74	-98610.14145	281.140904	1353.53
0.017	7.24	-9.00859	0.185194	134.94	-105506.9998	270.5264662	1451.78
0.078	6.32	-8.9522	0.206553	128.07	-101489.484	137.7633626	1362.23
0.033	5.34	-8.96668	0.190833	132.33	-105556.7599	171.8024408	1379.5
0.19	5.68	-8.96607	0.191460	137.13	-109002.9307	168.7535403	1425.58
0.027	6.27	-9.00303	0.188839	125.74	-98610.33059	280.9517634	1354.35
0.026	7.24	-9.00559	0.188794	134.94	-105506.3291	271.197176	1460.24
1.52	8.01	-9.00542	0.188688	144.14	-112403.181	260.5891417	1559.23

The total binding energy, CV, HOMO, LUMO and heat of formation were calculated using Hyper Chem. The LogP and the molar refractivity were obtained using Chem Draw. The values of the calculated descriptors have been shown in Table 4.7. Calculated descriptor has been plotted against the IC₅₀ values of the ligands in order to check the correlation of the ligand's activity with the chosen descriptor. Based on these, a QSAR equation has been calculated. Figure 4.20 shows the calculated equation for QSAR expressing the multivariate mathematical relationship between the calculated descriptor and the biological activity (IC50).

$$\mathbf{IC50} = 4.731415482255\text{E+001} + -2.732492020898\text{E+000} * (\text{LogP})$$

$$+ -3.065343328435\text{E+000} * (\text{MR}) + 3.778859642465\text{E-004} * (\text{ET})$$

$$+ 1.086962615661\text{E-003} * (\text{HF}) + -1.320725348069\text{E-001} * (\text{CV})$$

$$+ 2.165645682814\text{E+000} * (\text{HOMO}) + -2.285913461484\text{E+001} * (\text{LUMO})$$

$$+ -6.019614673287\text{E-001} * (\text{MolWt})$$

Prakash et al. | *Journal of Molecular Modeling*

The statistical analysis of the calculated equation shows that the RSQ value is 92.22% so it shows that current calculate QSAR is a good QSAR model, hence better predictions it will provide for new test data. The high difference in RSQ and Adjusted RSQ indicates stronger overall prediction. The F statistics show the measure of strength of regression. The higher F statistics than Critical F means more efficient the equation. Table 4.8 shows the statistics of the analysis. The correlation of descriptors with activity and correlation among descriptors shows the trend of relatedness. Based on calculated correlation among descriptors, high correlating descriptor pairs identify. The high correlating descriptor pairs are: ET*MR, CV*LogP, CV*MR, CV*ET, HOMO*HF, LUMO*HOMO Mol.Wt*MR, Mol.Wt*ET, Mol.Wt*CV. Table 4.9 shows the correlation of descriptors with activity and correlation among descriptors.

Table 4.8: Statistics of the Analysis

SS_R	473.93	RSQ	92.22%
SS_E	40.00	Adjusted RSQ	88.76%
SS_T	513.93	F Statistics	26.66

Table 4.9a: Correlation among Descriptors

	LogP	MR	CV	HF	LOMO	HOMO	Mol.Wt	ET
LogP	-	-	-	-	-	-	-	-
MR	0.89	-	-	-	-	-	-	-
CV	0.94	0.99	-	-0.42	-	-	-	-0.91
HF	0.45	-0.39	-	-	-	-	-	0.66
LUMO	-0.47	-0.48	-0.49	0.89	-	0.99	-	0.74
HOMO	-0.48	-0.47	-0.49	0.91	-	-	-	0.74
Mol.Wt	0.86	1.00	0.98	-0.38	-0.47	-0.46	-	-0.90
ET	-0.85	-0.91	-	-	-	-	-	-

Table4.9b: Correlation of Descriptors with Activity

(LogP) = -0.62
(MR) = -0.53
(ET) = 0.78
(HF) = 0.90
(CV) = -0.56
(HOMO) = 0.86
(LOMO) = 0.82
(Mol.Wt) = -0.51

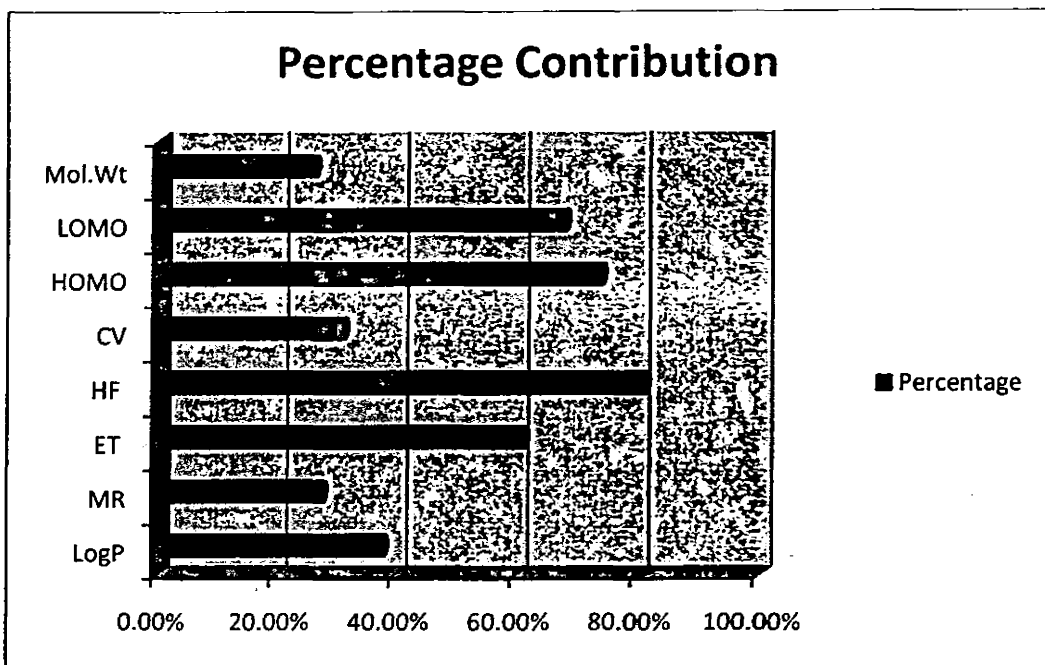


Figure 4.21: Percentage Contribution of Each Descriptor to Activity

Further a plot was generated for the training data that was generated by the QSAR equation. This shows the relationship between the actual IC-50 values and those predicted by the QSAR model. This will prove how much rightly the equation is fitting the data. Table 4.10 shows the actual IC-50 values and the predicted values alongside. Figure 4.22 shows the plot between the actual and predicted values.

Table 4.10: Actual Values and Predicted Values

Comp.	Actual	Predicted	Comp.	Actual	Predicted
SA1	10.1	10.07	SA15	0.01	0.17
SA2	20.27	20.25	SA16	0.01	-0.61
SA3	1.4	2.26	SA17	0.01	2.3
SA4	0.71	0.87	SA18	0.01	1.17
SA5	9.73	6.27	SA19	0.05	-0.33
SA6	2.74	2.11	SA20	0.01	1.3
SA7	1.54	1.46	SA21	0.02	-0.13
SA8	0.67	1.53	SA22	0.08	-0.26
SA9	1.78	0.87	SA23	0.03	0.66
SA10	1.9	1.71	SA24	0.19	-0.46
SA11	1.28	0.44	SA25	0.03	1.59
SA12	1.66	2.62	SA26	0.03	-0.2
SA13	1.34	1.32	SA27	1.52	-1.44
SA14	0.23	1.84			

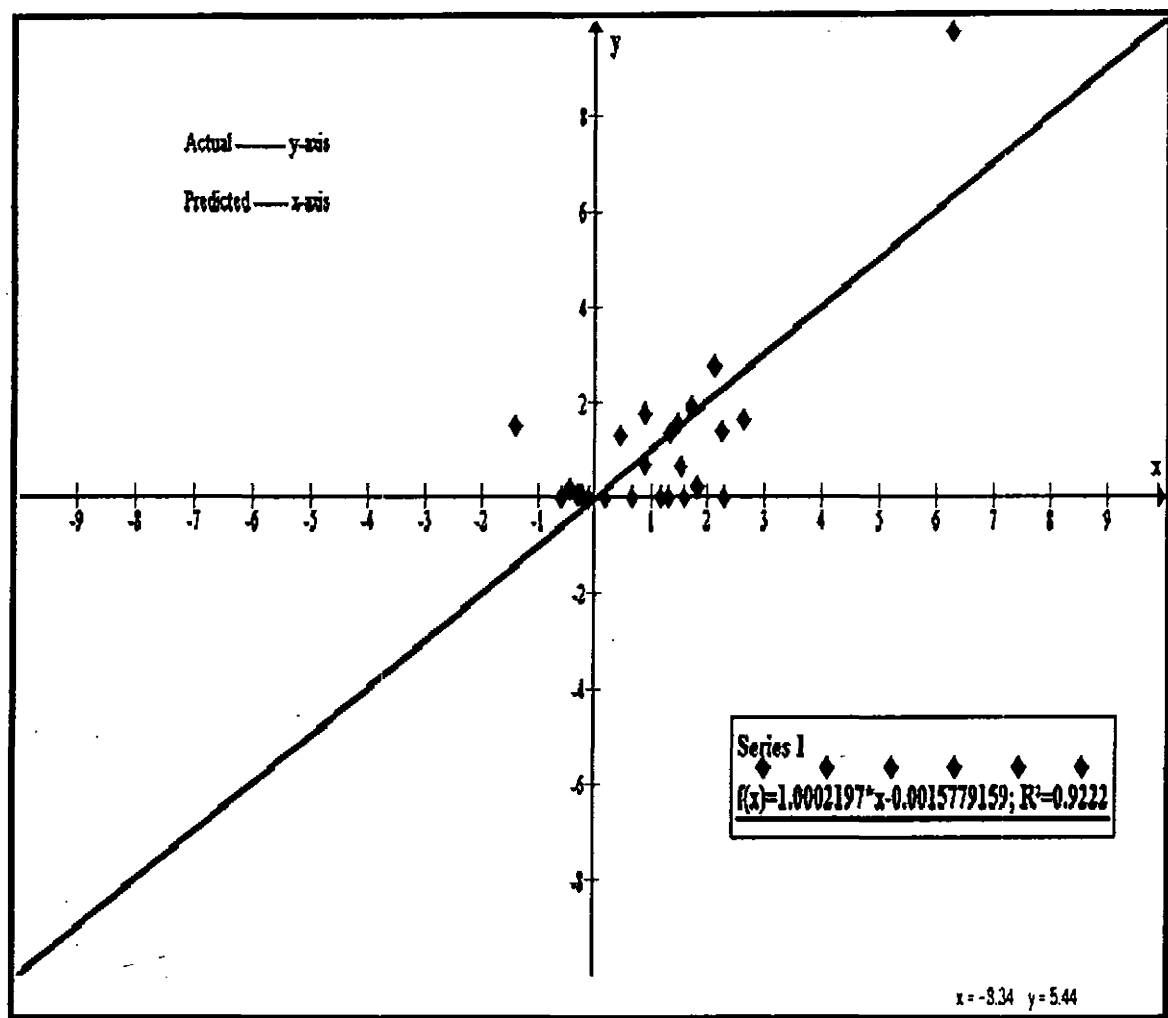


Figure 4.22: Plot of Actual values verses Predicted Value

CONCLUSION

Conclusion

The present study was aimed at finding novel drug for the treatment of Alzheimer's disease that had best Pharmacophore features and reversible binding interaction.

It has been inferred from current studies that for generating a good Pharmacophore model, a set of compounds along with their activities ranging over several orders can be used. The resulted Pharmacophore in turn can be used for effective calculation of the activity of a wide number of chemical scaffolds and as a 3D query in database searches for identifying the compounds that can be effectively use as potent inhibitors. Prior to any further research, Pharmacophore model can also use as a standard for checking the behavior of newly designed compounds by the interpretation of their mapping on Pharmacophore.

Current study showed that the best model of BChE inhibitors were made up of two Hydrogen Bond Acceptors, one Hydrogen Bond Donor and two Hydrophobic/Aromatic features and 1 Positive ionizable. The active compound / lead compound from the selected data perfectly match the resulted Pharmacophore.

Molecular docking has been used as added tools. Docking study resulted in the important interactions between the potent BChE inhibitors and target protein's active site residues.

Current studies showed that 27 4-[(diethylamino) methyl]-phenol derivatives selected for QSAR studies have prominent anti-Alzheimer activity. Moreover, the main

governing physicochemical factors for Alzheimer's disease include LUMO, HOMO, total energy (TE) and heat of formation (HF) and LogP as it has negative co-relation. Such a QSAR evaluation would open future perspectives to use these compounds as new lead compounds in clinical trials.

The combination of different computational techniques like Pharmacophore modeling, QSAR, and molecular docking used in present study lead to the successful identification of putative novel BChE inhibitors, which can be further evaluated by in vitro and in vivo biological tests.

FUTURE ENHANCEMENTS

Future Enhancements

With computational techniques like Molecular Dynamics (MD), the limitations imposed by the availability of crystal structures are overcome and a large number of different conformations can be generated. After docking of our dataset, now it is possible to perform MD simulations on this system. It will validate and optimize the Docked Complexes. QSAR descriptors can be investigated for other classes to propose specific descriptors important as BChEIs.

Furthermore, additional efforts shall be directed to extend the use of docking tools to facilitate a better drug designing approach for the benefits of bioinformatics group. In the future, as even more structural information becomes readily available, the use of the target structure to screen large databases of compounds and virtual libraries will become increasingly important in the drug discovery process. Large virtual libraries will be constructed based on available chemistry or a set of existing combinatorial scaffolds, as well as known drug properties.

REFERENCES

References

1. Aatu Kaapro, Janne Ojanen., (November 27, 2002) Protein docking. <http://www.lce.hut.fi/teaching/S-114.500/k2002/Protdock.pdf>.
2. Abagyan R, Totrov M, Kuznetzov D., (1994) ICM-a new method for protein modelling and design: application to docking and structure prediction from the distorted native conformation, *J Comput Chem*, 15,p.488- 506.
3. Beard C M, Kokmen E, Offord K P, Kurland L T., (1992) Lack of association between Alzheimer's disease and education, occupation, marital status, or living arrangement, *Neurology* 42, p. 2063–2068.
4. Bharath E N, Manjula S N, Vijaychand A.,(2011) In Silico Drug Design tool for Overcoming the Innovation Deficit in The Drug Discovery Process. *International Journal of Pharmacy and Pharmaceutical Sciences*, 3 (2),p.8-12.
5. Bickeboller H, Campion D, Brice A, Amouyel P, Hannequin D, Didierjean O, Penet C, Martin C, Perez-Tur J, Michon A, Dubois B, Ledoze F, Thomas-Anterion C, Pasquier F, Puel M, Demonet J F , Moneaud O, Babron M C, Meulien D, Guez D, Chartier-Harlin M C, Fregourg T, Agid Y, Martinez M, Clerget-Darpoux F., (1997) Apolipoprotein E and Alzheimer's disease: genotype-specific risks by age and sex, *Am. J. Hum. Genet*, 60, p. 439–446.
6. Birks J., (2006) Cholinesterase inhibitors for Alzheimer's disease, *Cochrane Database Syst Rev*.

7. Bissantz C, Flokers G, Rognan D., (2006) Protein-based virtual screening of chemical database.1. Evaluation of different docking/ scoring combinations, *J Med Chem*, 43, p.4759-4767.
8. Blass J P., (1993) Metabolic alterations common to neural and non-neuronal cells in Alzheimer's disease, *Hippocampus*, 3, p.45-53.
9. Brayne C., 1991 The EURODEM collaborative re-analysis of case-control studies of Alzheimer's disease: Implications for public health, *Int. J. Epidemiol.* 20, p.S68-S71.
10. Cambridge MedChem Consulting., (2009) *LigandScout 3.0 Review*.
11. Caroline McNeil., (1997) *Alzheimer's disease unrevealing the Mystery*.
12. Carreiras M C, Marco J.L., (2004) Recent approaches to novel anti-Alzheimertherapy, *Curr Pharm Design*, 25, p.3167-3175.
13. Chandra V, Kokmen E, Schoenberg B S, Beard M., (1989) Head trauma with loss of consciousness as a risk factor for Alzheimer's disease, *Neurology* 39, p.1576-1578.
14. Chang M W, Ayeni C, Breuer S, Torbett B E., (2010), Virtual Screening for HIV Protease Inhibitors: A Comparison of AutoDock 4 and Vina, *PLoS ONE* 5(8), e11955.
15. Chanin Nantasesamat, Chartchalelm Isarankura-Na-Ayudhya, Thanakorn Naenna, Virapong Prachayasittikul., (2009) Review article: A Practical Overview of Quantitative Structure-Activity Relationship, *Excli Journa*, 8, p.74-88.

16. Chatonnet F, Boudinot E, Chatonnet A, Taysse L, Daulon S, Champagnat J, Foutz A.S.,(2003) Respiratory survival mechanism in acetylcholinesterase knockout mouse, *Eur. J. Neurosci.*, 18, p.1419–1427.
17. **Cheng Chang and Peter W Swaan., (2005)** Computational approaches to modelling drug transporters, Elsevier B.V.
18. Cohen M S et al., (2005) Structural bioinformatics-based design of selective, irreversible kinase inhibitors, *Science* 308, p. 1318–1321.
19. Combarros O, Riancho JA, Infante J, Sañudo C, Llorca J, Zarrabeitia MT, Berciano J., (2005) Interaction between CYP19 aromatase and butyrylcholinesterase genes increases Alzheimer's disease risk, *Dement Geriatr Cogn Disord*, 20,p.153–157.
20. Darvesh S, Hopkins D.A, Geula C., (2003) Cholinesterase inhibitors modify the activity of intrinsic cardiac neurons, *Nat. Neurosci.*, 4, p.131–138.
21. Darvesh S, David A. Hopkins., (2003) Differential distribution of butyrylcholinesterase and acetylcholinesterase in the human thalamus, *The Journal of Comparative Neurology*, 463, p. 25–43.
22. Dave K R, Syal A R, Katyare S S., (2000), Tissue cholinesterases. A comparative study of their kinetic properties, *Z. Naturforsch.* 55, p.100–108.
23. David Rogers, A. J. Hopfinger., (1994) Application of genetic function approximation to Quantitative Structure-Activity Relationships and Quantitative Structure-Property Relationships, *J.Chem. Inf. Comput.Sci*, 34, p.854-866.

24. Davies B, Andrewes D, Staggatt R, Ames D, Tuckwell V, Davis S., (1989) Tacrine in Alzheimer's disease, *Lancet*, 2, p.163–4.
25. Diamant S, Podoly E, Friedler A, Ligumsky H, Livnah O, Soreq H., (2006) Butyrylcholinesterase attenuates amyloid fibril formation in vitro, *Proc Natl Acad* , 103, p.8628-8633.
26. Dillon G P , Gaynor J M, Khan D , Carolan C G, Ryder S A , Marquez J F , Reidy S, Gilmer J F., (2010) Isosorbide-based cholinesterase inhibitors; replacement of 5-ester groups leading to increased stability, *Bioorganic & Medicinal Chemistry*, 18,p. 1045–1053.
27. DiMasi J A. et al., (2003) The price of innovation: new estimates of drug development costs, *J. Health Economics* 22, p. 151–185.
28. Doody R S., (2003) Current treatments for Alzheimer's disease: cholinesterase inhibitors, *J Clin Psychiatry*, 64 (9), p.11-7.
29. Ecobicon D J, Corneau A M., (1973) Pseudocholinesterase of mammalian plasma: physiochemical properties and organophosphate inhibition in eleven species, *Toxicol. Appl. Pharmacol.*, 24, p.29–100.
30. Esposito E X, Hopfinger A J, Madura J D., (2004) Chemoinformatics: concepts, methods, and tools for drug discovery. In *Chemoinformatics: Concepts, Methods, and Tools for Drug Discovery*, Bajorath, J., Ed, 275, p. 131–213.
31. Ewing T J A, Kuntz I D., (1997) Critical evaluation of search algorithms for automated molecular docking and database screening, *J Comput Chem*, 18, p.1175-1189.

32. Ezio Giacobini., (2004) Cholinesterase inhibitors: new roles and therapeutic alternatives, *Pharmacological Research*, 50, p.433–440.
33. Ferri C P, Prince M, Brayne C, et al., (2005) Global prevalence of dementia: a Delphi consensus study, *Lancet*, 366, p.2112–17.
34. Gadit A A, vahidy A A, Shafique F.,(1998) Mental Health Morbidity in a Community psychiatric Clinic, *J. Coil. Phys. Surg.*, 8, p.262-264.
35. Gadit A A, Vahidy A A., (1999) Mental health morbidity pattern in Pakistan, *JCPSP*, 9, p.362-365.
36. Garrett M Morris, Ruth Huey, William Lindstrom, Michel F Sanner, Richard K., (2009) Automated Docking with Selective Receptor Flexibility, *Wiley InterScience*.
37. Gauthier S., (2002) Advances in the pharmacotherapy of Alzheimer's disease, *CMAJ*, 166, p.616–623.
38. Giacobini Ezio., (2003) Butyrlcholinesterase: Its structure and function, *Taylor and Francis Group plc*.
39. Godert M, Spillantini MG., (2006) A century of Alzheimer's disease. *Science*, 314, p.777–81.
40. Goodsell D S, Olson A J., (1990) Automated docking of substrates to proteins by simulated annealing, *Proteins*, 8, p.195-202.
41. Graves A B, Van Duijn C M, Chandra V, Fratiglioni L, Heyman A, Jorm A F, Kokmen E, Kondo K , Mortimer J A, RoccaW A, Shalat SL,Soininen H.,

(1991) Alcohol and tobacco consumption as risk factors for Alzheimer's disease: a collaborative re-analysis of case-control studies, *Int. J. Epidemiol.*, 20, p. 48–57.

42. Graves A B, White E, Koepsell T D, Reifler B V, van Belle G, Larson E B., (1990a) The association between aluminum-containing products and Alzheimer's disease, *J. Clin. Epidemiol.* 43, p.35–44.

43. Gun R T, Korten A E, Jorm A F, Henderson A S, Groe G A, Creasey H, McCusker E, Mylvaganam A., (1997) Occupationnal risk factors for Alzheimer's disease—a case-control study, *Alzheimer Dis. Assoc. Disord.* 11, p.21–27.

44. Hajduk P J et al., (2005) Predicting protein druggability., *Drug Discov.*, p.1675–1682.

45. Hansch and A. Leo., (1979) Substituent Constants for Correlation Analysis in Chemistry and Biology, John Wiley & Sons, New York.

46. Hansen R.A, Gartlehner G, Webb A.P, Morgan L.C, Moore C.G, Jonas D.E., (2008) Efficacy and safety of donepezil, galantamine, and rivastigmine for the treatment of Alzheimer's disease: a systematic review and meta-analysis, *Clin Interv Aging*, 3, p.211–25.

47. Hebert, L. E., Scherr, P. A., Bienias, J. L., Bennett, D. A., & Evans, D. A., (2003) Alzheimer disease in the US population: Prevalence estimates using the 2000 census, *Archives of Neurology*, 60(8), p. 1119-1122.

48. Hileman B., (2006) Accounting for R&D, Many doubt the \$800 million pharmaceutical price tag, *Chemical Eng news*, 84, p. 50-51.

49. <http://thcsupport.com/blog/?tag=/medical+medical+doctor>

50. <http://www.chem.qmul.ac.uk/iupac/medchem/ix.html#p7>.
51. http://www.nature.com/nature/journal/v461/n7266/fig_tab/461895a_F1.html
52. <http://www.nia.nih.gov>.
53. <http://www.nmr.sinica.edu>.
54. <http://www.umm.edu/ency/article/003358.htm>.
55. <http://www.vlifesciences.com>.
56. Hugo Kubinyi., (1997) QSAR and 3D QSAR in drug design Part2: applications and problems, DDT 2 (12), p.457-467.
57. Hung-Jin Huang , Hsin Wei Yu, Chien-Yu Chen , Chih-Ho Hsu , Hsin-Yi Chen ,Kuei-Jen Lee , Fuu-Jen Tsai, Calvin Yu-Chian Chen., (2010) Current developments of computer-aided drug design, Journal of the Taiwan Institute of Chemical Engineers ,4,p.623–635.
58. Hypercube, Inc., HyperChem® Release 7 for Windows®, (Jan 2002).
59. Isabelle Tomassoli, Lhassane Ismaili, Marc Pudlo, Cristóbal de los Ríos, Elena Soriano, Inés Colmena , Luis Gandía, Luis Rivas , Abdelouahid Samadi , José Marco-Contelles , Bernard Refouvelet., (2011) Synthesis, biological assessment and molecular modeling of new dihydroquinoline-3-carboxamides and dihydroquinoline-3-carbohydrazide derivatives as cholinesterase inhibitors, and Ca channel antagonists, European Journal of Medicinal Chemistry, 46,p.1-10.
60. Jones G, Willett P, Glen RC, Leach AR, Taylor R., (1997) Development and validation of a genetic algorithm for flexible docking, J Mol Biol, 267, p.727-748.

61. Jones G, Willett P, Glen RC., (1995) Molecular recognition of receptor sites using a genetic algorithm with a description of desolvation, *J Mol Biol*, 245, p. 43-53.

62. Jorgensen W.L. (2004), The many roles of computation in drug discovery. *Science*, 303, p. 1813–1818.

63. Judith M. Rollinge., (2009) Assessing target information by virtual parallel screening—the impact on natural product research, *Phytochemistry Letters*, 2 (2), p.53-58.

64. Kapetanovic I M., (2008) Computer-aided drug discovery and development (CADD): In silico-chemico-biological approach, *Chemico-Biological Interactions*, 171, p.165–176.

65. Katalinic M, Rusak G, Barovic J. D, Goran Sinko G , Jelic D, Antolovic R , Kovarik Z., (2006) Structural aspects of flavonoids as inhibitors of human Butyrylcholinesterase, *European Journal of Medicinal Chemistry* 45,p. 186–192

66. Kier L. B., (1967) Molecular orbital calculation of preferred conformations of acetylcholine, muscarine, and muscarone, *Mol. Pharmacol.*, 3 (5), p.487-94.

67. Kier L. B., (1971) Molecular orbital theory in drug research, Boston: Academic Press, p. 164–169.

68. Kokmen, E., Beard, C.M., Chandra, V., Offord, K.P., Schoenberg, B.S., Ballard, D.J., (1991) Clinical risk factors for Alzheimer's disease: a population based case-control study, *Neurology*, 41, p.1393–1397.

69. Kubinyi, H., (1993) 3D QSAR in Drug Design. Theory, Methods and Applications. Escom: Leiden, The Netherlands, p. 759.

70. Kukull, W.A., Schellenberg, G.D., Bowen, J.D., McCormick, W.C., Yu, C.E., Teri, L., Thompson, J.D., O'Meara, E., Larson, E.B., (1996) Apolipoprotein E in Alzheimer's disease risk and case detection: a case control study, *J. Clin. Epidemiol.* 40, p.1143–1148.

71. Leibson, C.L., Rocca, W.A., Hanson, V.A., Cha, R., Kokmen, E., Obrien, P.C., Palumbo, P.J., (1997) Risk of dementia among persons with diabetes mellitus—a population-base cohort study, *Am. J.Epidemiol.* 145, p.301–308.

72. Lennart Mucke (2009) Neuroscience: Alzheimer's disease, *Nature*, 461, p.895-897.

73. Lerner, A., Koss, E., Debanne, S., Rowland, S., Smyth, K., Friedland, R., (199). Smoking and estrogen-replacement therapy as protective factors for Alzheimer's disease, *Lancet* 349, p.403–404.

74. Li B, Stribley J. A , Ticu A, Xie W, Schopfer L. M, Hammond P, Brimijoin S, Hinrichs S. H, Lockridge O., (2000) Abundant tissue butyrylcholinesterase and its possible function in the acetylcholinesterase knockout mouse, *J. Neurochem*, 75, p.1320–1331.

75. Liang Yu, Rihui Cao, Wei Yi, Qin Yan, Zhiyong Chen, Lin Ma, Wenlie Peng , Huacan Song (2010) Synthesis of 4-[(diethylamino)methyl]-phenol derivatives as novel cholinesterase inhibitors with selectivity towards

Butyrylcholinesterase, Bioorganic & Medicinal Chemistry Letters, 20 p.3254–3258.

76. Li, J.A. Stribley, A. Ticu, W. Xie, L.M. Schopfer, P. Hammond, S. Brimijoin, S.H. Hinrichs, O. Lockridge., (2000) Abundant tissue butyrylcholinesterase and its possible function in the acetylcholinesterase knockout mouse, *J. Neurochem*, 75,p.1320–1331.

77. Lleó, S.M. Greenberg and J.H. Growdon Current Pharmacotherapy for Alzheimer's disease., (2006) *Annual Review of Medicine*, 57,p. 513-533.

78. Loren D. Mendelsohn (2004), ChemDraw 8 Ultra: Windows and Macintosh Versions, *J. Chem. Inf. Comput. Sci.*, 44 (6), p. 2225–2226.

79. M.M. Mesulam, A. Guillozet, P. Shaw, A. Levey, E.G. Duysen, O. Lockridge., (2002) Acetylcholinesterase knockouts establish central cholinergic pathways and can use butyrylcholinesterase to hydrolyze acetylcholine, *Neuroscience* 110 (40), p.627–639.

80. Maja Katalinic , Gordana Rusak , Jelena Domac inovic Barovic, Goran S inko , Dubravko Jelic ,Roberto Antolovic , Zrinka Kovarik., (2010) Structural aspects of flavonoids as inhibitors of human Butyrylcholinesterase, *European Journal of Medicinal Chemistry*, 45, p.186–192.

81. Marti-Renom M A , Stuart A C , Fiser A , Sanchez R, Melo F., Sali A., (2000) Comparative Protein Structure Modeling of Genes and Genomes, *Annu. Rev. Biophys. Biomol. Struct.*, 29, p. 291-325.

82. Massoulie J.L, Pezzementi S, Bom E, Krejci F.M, Vallette, (1993) Molecular and cellular biology of cholinesterases, *Prog. Neurobiol.*, 41, p.31–91.

83. Massoulie, J., Sussman, J., Bon, S., and Silman, I., (1993) Structure and functions of acetylcholinesterase and Butyrylcholinesterase, *Prog Brain Res* 98, p.139–146.

84. McCaddon, A., Kelly, C.L., (1994) Familial Alzheimer's disease and vitamin B12 deficiency, *Age Ageing* 23, p.334–337.

85. McCammon, J. A., Gelin, B. R. & Karplus, M. (1977). Dynamics of folded proteins. *Nature*, 267, 585-590.

86. McGeer, P.L., Schulzer, M., McGeer, E.G., (1996) Arthritis and anti-inflammatory agents as possible protective factors for Alzheimer's disease: a review of 17 epidemiologic studies, *Neurology* 47, p.425–432.

87. McLachlan, D.R., Bergeron, C., Smith, J.E., Boomer, D., Rifat, S.L., (1996) Risk for neuropathologically confirmed Alzheimer's disease and residual aluminum in municipal drinking water employing weighted residential histories, *Neurology* 46, p.401–405.

88. Michael Decker, Fabian Krauth, Jochen Lehmann., (2006) Novel tricyclic quinazolinimines and related tetracyclic nitrogen bridgehead compounds as cholinesterase inhibitors with selectivity towards Butyrylcholinesterase, *Bioorganic & Medicinal Chemistry*, 14 (6), p. 1966-1977.

89. Milatovicet, W.D. Dettbarn., (1996) Modification of acetylcholinesterase during adaptation to chronic, subacute paraoxon application in rat, *Toxicol. Appl. Pharmacol.*, 136, p.20-28.

90. Minino A Xu, J Kochanek KD., (2010) Deaths: Preliminary Data for 2008, *National Vital Statistics Reports*. Hyattsville, Md.; National Center for Health Statistics; 2010, Available at www.cdc.gov/nchs/data/nvsr/nvsr59/nvsr59_02.pdf.

91. Morris G M, Goodsell D S, Halliday R S, Huey R, Hart W E, Below R K, Olson A J., (1998) Automated docking using a Lamarckian genetic algorithm and an empirical binding free energy function, *J Comput Chem*, 19, p.1639-1662.

92. Morris G M, Goodsell D S, Huey R, Olson A J., (1996) Distributed automated docking of flexible ligands to proteins: parallel applications of AutoDock 2.4, *Comput Aided Mol Des*, 10, p.293-304.

93. Muegge I, Rarey M., (2001) Small molecule docking and scoring, *Rev Comput Chem*, 17, p.1-60.

94. Mufson, E J, Mash, D C and Hersh L B., (1988) Neurofibrillary tangles in cholinergic pedonculopontine neurons in Alzheimer's disease, *Ann. Neurol.*, 24, p. 623-629.

95. NH Greig, K Sambamurti, QS Yu, TA Perry, HW Holloway, F Haberman, A Brossi, D.K. Ingram, DK Lahiri., (2003) Butyrylcholinesterase: its selective inhibition and relevance to alzheimer's disease therapy. in: E. Giacobini

(Ed.), Butyrylcholinesterase: Its Function and Inhibitors, first ed. Martin Dunitz, Taylor and Francis Group Plc, United Kingdom, p. 69–90.

96. Neelakantan Suresh, N.S. Vasanthi, (2010) Pharmacophore Modeling and Virtual Screening Studies to Design Potential Protein Tyrosine Phosphatase 1B Inhibitors as New Leads, *JPB* Vol.3.

97. O Trott, A J Olson., (2010) AutoDock Vina: improving the speed and accuracy of docking with a new scoring function, efficient optimization and multithreading, *Journal of Computational Chemistry*, 31, p.455-461.

98. Park H, Lee J, Lee S., (2006) Critical assessment of the automated AutoDock as a new docking tool for virtual screening, *Proteins*, 65, p. 549–554.

99. Payami H, Grimsild H, Oken B, Camicioli R, Sexton G, Dame A, Howieson D, Kaye J., (1977) A prospective study of cognitive health in the elderly (Oregon brain aging study)—effects of family history and apolipoprotein E genotype, *Am. J. Hum. Genet*, 60, p. 948–956.

100. Perkins R, Fang H, Tong W, Welsh WJ., (2003) Quantitative structure-activity relationship methods: perspectives on drug discovery and toxicology, *Environ Toxicol Chem*, 22(8), p.1666-1679.

101. Perry E K, Tomlinson B E, Blessed G, Bergmann K, Gibson P H and Perry R H.,(1987) Correlation of cholinergic abnormalities with senile plaques and mental test scores in senile dementia, *Br. Med. J.*, 2, p.1457–1459.

102. Pozzan A., (2006) Molecular descriptors and methods for ligand based virtual high throughput screening in drug discovery, *Curr. Pharm.Des.* 12, p.2099–2110.

103. Pricewaterhouse Coopers., (2007) *Pharma 2020: The vision – Which path will you take?* Available at <http://www.pwc.com/pharma2020>.

104. Prody C A, Zevin-Sonkin D, Gnatt A, Goldberg O, Soreq H., (1987) Isolation and characterization of full length cDNA clones coding for cholinesterase from fetal human tissues, *Proc. Natl. Acad. Sci. U.S.A.* 84, p.3555–3559.

105. Puranik Purushottamachar, Aakanksha Khandelwal, Pankaj Chopra, Neha Maheshwari, Lalji K Gediya, Tadas S. Vasaitis, Robert Bruno, Omoshile O. Clement, and Vincent C. O. Njar., (2007) First Pharmacophore-Based Identification of Androgen Receptor Down-regulating Agents: Discovery of Potent Anti-Prostate Cancer Agents, *Bioorg Med Chem*, 15(10): p.3413–3421.

106. Rarey M, Kramer B, Lengauer T, Klebe G., (1996) A fast flexible docking method using an incremental construction algorithm, *J Mol Biol.*, 261, p.470-489.

107. Ritchie C W, Ames D, Clayton T, Lai R., (2004) Metaanalysis of randomized trials of the efficacy and safety of donepezil, galantamine, and rivastigmine for the treatment of Alzheimer disease, *Am J Geriatr Psychiatry*, 12, p.358–69.

108. Rockwood K, Darvesh S, (2003), In *Drug Advances*; Gray, J., Ed., p.159–177.

109. Rogers S L, Doody R S, Mohs R C, Friedhoff L T., (1998) Donepezil improves cognition and global function in Alzheimer's disease: a 15- week, double-blind, placebo-controlled study, *Arch. Intern. Med.* 58, p.1021–1031.
110. Rogers S L, Friedhoff L T., (1998) Long-term efficacy and safety of donepezil in the treatment of Alzheimer's disease: an interim analysis of the results of a US multicentre open label extension study, *Eur. Neuropsychopharmacol.*, 8, p.67–75.
111. Rook Y, Schmidtke K U, Gaube F, Schepmann D, Wunsch B, Heilmann J, Lehmann J, Winckler T., (2010) Bivalent β -carbolines as potential multitarget anti Alzheimeragents, *J. Med. Chem.*, 53, p.3611–3617.
112. Rossor M N, Garret N J, Johnson A L, Mountjoy C Q, Roth M and Iversen L L., (1982) A post-mortem study of the cholinergic and GABA systems in senile dementia, *Brain*, 105, p.313–330.
113. Santos-Filho O A, Hopfinger A J, Cherkasov A, de Alencastro R B., (2009) The receptor-dependent QSAR paradigm: an overview of the current state of the art, *Med. Chem.*, 5, p. 359–366.
114. Schetinger R C, Porto N M, Moretto M B, Morsch V M, Rocha J B T, Vieira V, Moro F, Neis R T, Bittencourt S, Bonacorso H G, Zanatta N., (2000) New benzodiazepines alter acetylcholinesterase and ATPase activities, *Neurochem. Res.*, 25, p.949–955.

115. Schoenberg B S, Anderson DW, Haeren A F., (1985) Severe dementia: Prevalence and clinical features in a biracial US population, *Arch. Neurol.*, 42, p.740–743.
116. Schott Y, Decker M, Rommelspacher H and Lehmann J., (2006) 6-Hydroxy- and 6-methoxy- β -carbolines as acetyl- and butyrylcholinesterase inhibitors, *Bioorganic & Medicinal Chemistry Letters*, 16, p.5840–5843.
117. Sequeira R P., (2008) Central nervous system stimulants and drugs that suppress appetite, Aronson JK, Elsevier Science, p. 1-15.
118. Shih- Ching Ou Chun- Yen Chung, Hung-Yuan Chung Wen- Tsai Sung, Chia - Chih Tsai ,Cheng - Chih ,Chien Da -Yu Su ,Shi-Yong Lin., (2005) Molecular Docking for Protein Folding Structure and Drug-likeness Prediction, WSEAS Conferences, Udine, Italy, p. 20-22.
119. Silman J, Sussman L., (2005) Acetylcholinesterase: ‘classical’ and ‘nonclassical’ functions and pharmacology, *Curr. Opin. Pharmacol.*, 5, p.293–302.
120. Small D H, Michaelson S, Sberna G., (1996) Non-classical actions of cholinesterases: Role in cellular differentiation, tumorigenesis and Alzheimer’s disease, *Neurochem Int*, 28, p.453-483.
121. Sobel E, Davanipour Z, Sulkava R, Erkinjuntti T, Wikstrom J, Henderson V W, Buckwalter G, Bowman J D, Lee P J., (1995) Occupations with exposure to electromagnetic fields: a possible risk factor for Alzheimer’s disease, *Am. J. Epidemiol.*, 142, p.515–524.

122. Sousa S F, Fernandes P A, Ramos M J., (2006) Protein-ligand docking: current status and future challenges, *Proteins: Struct Funct Bioinf.*, 65, p.15–26.

123. Speck C E , Kukull W A , Brenner D E, Bowen J D, McCormick W C, Teri L, Pfanschmidt M L, Thompson J D, Larson E R., (1995) History of depression as a risk factor for Alzheimer's disease, *Epidemiology* 6, p.366–369.

124. Taylor J B, Triggle D J., (2007) in vitro studies of drug metabolism, *Comprehensive Medicinal Chemistry II*, Elsevier: Amsterdam, The Netherland, 231–257.

125. Terfloth L., (2003) *Chemoinformatics: A Textbook* ; Gasteiger, J., Engel, T., Eds.; Wiley-VCH: Weinheim, Germany, p. 401–437.

126. Theodora M Steindl, Carolyn E Crump, Frederick G Hayden, and Thierry Langer., (2005) Pharmacophore Modeling, Docking, and Principal Component Analysis Based Clustering: Combined Computer-Assisted Approaches to Identify New Inhibitors of the Human Rhinovirus Coat Protein, *J. Med. Chem.*, 2005, 48 (20), p. 6250–6260.

127. Tsuji M., (2010) Homology Modeling for HyperChem, Revision F1, Saitama, JAPAN.

128. Ul-Haq Z, Khan W, Kalsoom S, Ansari FL., (2010) In silico modeling of the specific inhibitory potential of thiophene-2, 3-dihydro-1, 5-benzothiazepine against BChE in the formation of beta-amyloid plaques associated with Alzheimer's disease, *Theor Biol Med Model*, 7, p. 1742-4682.

129. VA Campbell and A Gowran., (2007) Alzheimer's disease; taking the edge off with cannabinoids, *British Journal of Pharmacology*, 152, p.655–662.

130. Van Duijn C M , Hofman A., (1991). Relation between nicotine intake and Alzheimer's disease, *Br. Med. J.* 302, p.1491–1494.

131. Van Duijn C M, Hofman A , (1992) Risk factors for Alzheimer's disease: The EURODEM collaboration re-analysis of case-control studies, *Neuroepidemiology*, 11, p.106–113.

132. Venkatarajan S Mathura, Nikunj Patel, Corbin Bachmeier, Michael Mullan, Danie Paris., (2010) A 3D-QSAR model based screen for dihydropyridine-like compound library to identify inhibitors of amyloid beta (A β) production, *Bioinformation*, 5 (3), p.122-127.

133. Verma J, Khedkar V M, Coutinho E C., (2010) 3D-QSAR in drug design-- a review, *Curr Top Med Chem.*,10(1),p.95-115.

134. Wang J, Kollman PA, Kuntz ID., (1999) Flexible ligand docking: a multistep strategy approach, *Proteins*, 36(1), p.1-19.

135. Weinstock, M., (1999) Selectivity of cholinesterase inhibition: clinical implications for the treatment of Alzheimer's disease, *CNS Drugs* 12, p.307– 323.

136. Whitehouse P J, Price D L, Clark A W, Coyle J T, DeLong M R.,(1981) Alzheimer disease: evidence for a selective loss of cholinergic neurons in the nucleus basalis, *Ann. Neurol.*, 10, p.122–126.

137. William Thies and Laura Bleiler., (2001) Alzheimer's Association Report, Alzheimer's disease facts and figures Alzheimer's Association.

138. Wilkinson D G, Passmore A P, Bullock R, Hopker S W, Smith R, Potocnik F C, Maud C M, Engelbrecht I, Hock C, leni J R, Bahra R S., (2002) A multinational, randomised, 12-week, comparative study of donepezil and rivastigmine in patients with mild to moderate Alzheimer's disease, *Int. J. Clin. Pract.*, 56, p.441– 446.

139. Wolber G, Langer T., (2005) LigandScout: 3-D pharmacophores derived from protein-bound ligands and their use as virtual screening filters, *J. Chem. Inf. Model.*, 45(1), p.160-169.

140. Wright C I, Geula C, Mesulam M M., (1993) Protease inhibitors and indolamines selectively inhibit cholinesterases in the histopathologic structures of Alzheimer's disease, *Ann N Y Acad Sci*, 695,p.65-68.

141. Wright C I, Geula C, Mesulam M M., (1993) Neurological cholinesterases in normal brain and in Alzheimer's disease: relationship to plaques, tangles and patterns of selective vulnerability, *Ann Neurol.*, 34, p.373–384.

142. Yoshitake T, Kiyahara Y, Kato I, Ohmura T, Iwamoto H, Nakayama K, Ohmori S, Nomiyama K, Kawano H, Ueda K, Sueishi K, Tsuneyoshi M, Fujishima M, (1995) Incidence and risk factors of vascular dementia and Alzheimer's disease in a defined elderly Japanese population: the Hisayama study, *Neurology*,45, p.1161–1168.

143. Yvain Nicole, Oksana Lockridge, Patrick Masson, Juan C. Fontecilla-Camps, and Florian Nachon., (2003) Crystal Structure of Human

Butyrylcholinesterase and of Its Complexes with Substrate and Products, the journal of biological chemistry, 278 (42), p. 41141–41147.

144. Zielesny A., (2005) Chemistry Software Package ChemOffice Ultra 2005, *J. Chem. Inf. Model.*, 45 (5), p. 1474–1477.